Carbon TerraVault III
Class VI Permit Application
Narrative Report

Submitted to:

U.S. Environmental Protection Agency Region 9
San Francisco, CA

Prepared by:

27200 Tourney Road, Suite 200
Santa Clarita, CA 91355
(888) 848-4754

ATTACHMENT A: NARRATIVE REPORT
[40 CFR 146.82(a)]
CTV III

Table of Contents

Document Version History

Version	Revision Date	File Name	Description of Change
1	5/3/2022	Attachment A - CTV III Narrative -final	Original submission
2	8/4/2022	Att A - Narrative_CTV III V2	
3	11/30/2022	Att A - Narrative_CTV III V3	
3.1	12/21/2022	Att A - CTV III Narrative_V3.1	
4	1/23/2023	Att A - CTV III Narrative_V4	
5	5/24/2024	Att A – CTV III Narrative_V5_RtC	Response to February 20, 2024 EPA Comments
6	2/14/2025	Att A – CTV III Narrative_V6_RtC	Response to October 31, 2024 EPA Comments

1. Project Background and Contact Information

Carbon TerraVault Holdings LLC (CTV), a wholly owned subsidiary of California Resources Corporation (CRC), proposes to construct and operate six carbon dioxide (CO_2) geologic sequestration wells at CTV III located in San Joaquin County, California. This application was prepared in accordance with the U.S. Environmental Protection Agency's (EPA's) Class VI, in Title 40 of the Code of Federal Regulations (40 CFR 146.81) under the Safe Drinking Water Act (SDWA). CTV is not requesting an injection depth waiver or aquifer exemption expansion.

CTV will obtain the required authorizations from applicable local and state agencies, including the associated environmental review process under the California Environmental Quality Act. Appendix A1 outlines potential local, state and federal permits and authorizations. Federal act considerations and additional consultation, which includes the Endangered Species Act, the National Historic Preservation Act and consultations with Tribes in the area of review, are presented in the Federal Acts and Consultation attachment.

CTV forecasts the potential CO_2 stored in the Mokelumne River Formation at an average rate of 2.5 million tonnes annually for 28 years. CO_2 will be sourced from a blue hydrogen and ammonia plant (up to 377,000 tonnes per annum) that will be located in proximity to the storage site, direct air capture and other CO_2 sources in the project area.

The Carbon TerraVault III (CTV III) storage site is located in the Sacramento Valley, 15 miles southeast of the Rio Vista Field near Stockton, California (**Figure A-1**) within the southern Sacramento Basin. The project will consist of six injectors, surface facilities, and monitoring wells. This supporting documentation applies to the six injection wells.

CTV will actively communicate project details and submitted regulatory documents to County and State agencies:

- Geologic Energy Management Division (CalGEM)
  District Deputy
  Mark Ghann-Amoah: (661) 322-4031
- CA Assembly District 13
  Assemblyman Carlos Villapudua
  31 East Channel Street – Suite 306
  Stockton, CA 95202
  (209) 948-7479
- San Joaquin County
  District 3 Supervisor –Tom Patti
  (209) 468-3113
  tpatti@sjgov.org
- San Joaquin County Community Development
  Director – David Kwong
  1810 East Hazelton Avenue

Stockton, CA 95205
(209) 468-3121

- San Joaquin Council of Governments
  Executive Director – Diane Nguyen
  555 East Weber Avenue
  Stockton, CA 95202
  (209) 235-0600
- Region 9 Environmental Protection Agency
  75 Hawthorne Street
  San Francisco, CA 94105
  (415) 947-8000

2. Site Characterization

2.1 Regional Geology, Hydrogeology, and Local Structural Geology [40 CFR 146.82(a)(3)(vi)]

2.1.1 Geologic History

The CTV III storage site is located 15 miles southeast of major gas field Rio Vista. Two smaller gas fields lie closer to the project area: McDonald Island to the north and the Union Island Gas Field to the east. The McDonald Island Gas Field was discovered first in June 1936 and the Union Island Gas Field was later discovered in 1972, both by Union Oil Company of California. The McDonald Island Field produced 184 billion cubic feet of gas (BCFG) from the Mokelumne River Formation (Downey, 2010). Although located in a region of prolific gas production, Victoria Island only contains a few exploration type wells and no hydrocarbon accumulations have been discovered in the project area (**Figure A-1**). The Mokelumne River Formation is the target reservoir.

2.1.2 Site Geology Overview

The CTV III project area lies within the Sacramento Basin in northern California (**Figure A-2**). The Sacramento Basin is the northern, asymmetric sub-basin of the larger Great Valley Forearc. This portion of the basin, which contains a steep western flank and a broad, shallow eastern flank, spans approximately 240 miles in length and 60 miles wide (Magoon, 1995).

Basin Structure

The Great Valley was developed during mid to late Mesozoic time. The advent of this development occurred under convergent-margin conditions via eastward, Farallon Plate subduction, of oceanic crust beneath the western edge of North America (Beyer, 1988). The convergent, continental margin that characterized central California during the Late Jurassic through Oligocene time was later replaced by a transform-margin tectonic system. This occurred as a result of the northward migration of the Mendocino Triple Junction (from Baja California to its present location off the coast of Oregon), located along California's coast (**Figure A-3**). Following this migrational event was the progressive cessation of both subduction and arc

volcanism as the progradation of a transform fault system moved in as the primary tectonic environment (Graham, 1984). The major current day fault, the San Andreas, intersects most of the Franciscan subduction complex, which consists of the exterior region of the extinct convergent-margin system (Graham, 1984).

Basin Stratigraphy

The structural trough that developed subsequent to these tectonic events, which became named the Great Valley, became a depocenter for eroded sediment, and thereby currently contains a thick infilled sequence of sedimentary rocks. These sedimentary formations range in age from Jurassic to Holocene. The first deposits occurred as an ancient seaway and, through time, were built up by the erosion of the surrounding structures. The basin is constrained on the west by the Coast Range Thrust, on the north by the Klamath Mountains, on the east by the Cascade Range and Sierra Nevada, and the south by the Stockton Arch Fault (**Figure A-2**). To the west, the Coastal Range boundary was created by uplifted rocks of the Franciscan Assemblage (**Figure A-4**). The Sierra Nevada, which make up the eastern boundary, are a result of a chain of ancient volcanos.

Basin development is broken out into evolutionary stages at the end of each time-period of the arc-trench system, from Jurassic to Neogene, in **Figure A-5**. As previously stated, sediment infill began as an ancient seaway and was later sourced from the erosion of the surrounding structures. Sedimentary infill consists of Cretaceous-Paleogene fluvial, deltaic, shelf, and slope sediments. Due to the southward tilt of the basin, sedimentation thickens toward the southern end near the Stockton Arch fault which lies approximately 5 miles southeast of the CTV III Area of Review (AoR), shown in red on **Figure A-1**, creating sequestration quality sandstones. The AoR boundary also signifies the CO_2 plume extent 100 years after the cessation of injection. The AoR was determined based on a risk based approach developed during the project by the methodology described in Attachment B.

In the southern Sacramento Basin, the Mokelumne River Formation is a thick-bedded sandstone that creates the principal reservoir facies in the CTV III area. This area is a minor structural trap with a slight dip of about 2.8 degrees to the west, leaving the area mostly flat.

Submarine Canyons

Falling sea levels and tectonics caused the Paleogene Markley, Martinez, and Meganos submarine canyons to form throughout the Sacramento Basin (**Figure A-2**). The erosional events caused by these canyons played a large part in the current distribution and continuity of Upper Cretaceous and early Tertiary formations within the basin (Downey, 2010). The Late Paleocene/Early Eocene Meganos canyon lies northwest of the AoR. Trending in a northeast-southwest direction and cutting deeply into the Mokelumne River Formation sediments this erosional event spans approximately 25 to 30 miles from southern Sacramento County through northwestern San Joaquin County, and then westward into Contra Costa County. This event caused erosional troughs that were later filled in with fine-grained submarine fan deposits and transgressive deep-water shale due to renewed rising sea levels. This infilled sequence can be seen outcropping on the flanks of Mount Diablo, where it has a minimum thickness of 2,200 feet and serves as the primary trapping mechanism for the Brentwood Oil Field (Downey, 2010).

2.1.3 Geological Sequence

Figure A-6 is a schematic representing the local stratigraphy CTV III, highlighting the area east of the Midland Fault and west of the Stockton Arch fault. The injection zone is shown in red as the Mokelumne River Formation. The six chosen injection wells will inject CO_2 into the Cretaceous-aged Mokelumne River Formation, east of the Meganos Canyon. The average injection depth is approximately -6,975 feet true vertical depth below sea level (TVDSS).

Following its deposition, the Mokelumne River Formation was buried under the Capay Shale, which carries throughout most of its distribution. This formation serves as the upper confining zone for the Mokelumne River reservoir due to its low permeability, thickness, and regional continuity that spans beyond the AoR (**Figure A-7**). Above the Capay Shale are the Domengine Sandstone and Nortonville Shale.

2.2 Maps and Cross Sections of the AoR [40 CFR 146.82(a)(2), 146.82(a)(3)(i)]

As required by 40 CFR 146.82(a)(2), **Figure A-8** is a summary map of the oil and gas wells, water wells, State- or EPA-approved subsurface cleanup sites, and surface features in the project area and the project AoR. AoR delineation is presented in **Attachment B: AoR and Corrective Action Plan**. **Tables A-1**, **A-2**, **and A-3** list the oil and gas wells, California Department of Water Resources (DWR) Well Completion Report (WCR) water wells, and California State Water Resources Control Board Groundwater Ambient Monitoring Assessment Program (GAMA) water wells shown in **Figure A-8**, respectively.

2.2.1 Data

To date, 46 wells have been drilled to various depths within the vicinity of the project AoR. Along with an extensive database of wells in this field, seismic coverage, core and reservoir performance data such as production and pressure give an adequate description of the reservoir (**Figure A-9**).

Well data are used in conjunction with three-dimensional (3D) and two-dimensional (2D) seismic to define the structure and stratigraphy of the injection zone and confining layers (**Figure A-10**). **Figure A-11** shows outlines of the seismic data used and the area for the structural framework that was built from these seismic surveys. The 3D data in this area were merged using industry standard pre-stack time migration in 2013, allowing for a seamless interpretation across the seismic datasets. The 2D data used for this model were tied to this 3D merge in both phase and time to create a standardized datum for mapping purposes. The following layers were mapped across the 2D and 3D data:

- A shallow marker to aid in controlling the structure of the velocity field
- The approximate base of the Valley Springs Formation, which is unconformable with the Eocene strata below
- Domengine
- Mokelumne River

- H&T Shale
- Winters
- Forbes

The top of the Cretaceous Forbes Formation was used as the base of this structural model due to the depth and imaging of Basement not being sufficient to create a reliable and accurate surface. Interpretation of these layers began with a series of well ties at well locations shown in **Figure A-11**. These well ties create an accurate relationship between well data, which are in depth, and the seismic data, which are in time. The layers listed above were then mapped in time and gridded on a 550- by 550-foot cell basis. Alongside this mapping was the interpretation of any faulting in the area, which is discussed further in the Faults and Fracture section of this document.

The gridded time maps and a subset of the highest quality well ties and associated velocity data are then used to create a 3D velocity model. This model is guided between well control by the time horizons and is iterated to create an accurate and smooth function. The velocity model is used to convert both the gridded time horizons and interpreted faults into the depth domain. The result is a series of depth grids of the layers listed above which are then used in the next step of this process.

The depth horizons are the basis of a framework which uses conformance relationships to create a series of depth grids that are controlled by formation well tops picked on well logs. The grids are used as structural control between these well tops to incorporate the detailed mapping of the seismic data. These grids incorporate the thickness of zones from well control and the formation strike, dip, and any fault offset from the seismic interpretation. The framework is set up to create the following depth grids for input in to the geologic and plume growth models:

- Nortonville Shale
- Domengine
- Domengine Top Sand
- Capay Shale
- Mokelumne River Formation
- H&T Shale
- Winters
- Delta Shale
- Delta Shale Base

2.2.2 Site Stratigraphy

Major stratigraphic intervals within the field, from oldest to youngest, include the H&T Shale (L. Cretaceous), Mokelumne River Formation (L. Cretaceous-E. Paleocene), Capay Shale

(E. Eocene), Domengine Sandstone (L. Eocene), and Nortonville Shale (L. Eocene) (**Figure A-12**). Of these formations, the regional upper seal rock that partitions the reservoir consists of the Capay Shale. Also shown in **Figure A-12** is the basin-wide unconformity separating overlying Paleocene and younger beds from Cretaceous rocks. This unconformity resides above the Mokelumne River Formation at the base of the Capay Shale, creating a seal between reservoir and underground source of drinking water (USDW). During Paleogene time, marine and deltaic deposits continued in the basin until the activity of the Stockton Arch began to separate Sacramento Basin from the San Joaquin basin in late Paleogene time (Downey, 2010).

H&T Shale

The H&T Shale acts as a conformable contact to the Mokelumne River Formation. Moving southwest, the H&T thickens and contains a facies change with the upper marine shale as the Starkey section progressively adds, creating a thicker shale (Downey, 2010).

Mokelumne River Formation

The Mokelumne River Formation sandstones are great reservoir quality sands with trap types that include fault truncations, stratigraphic traps and unconformity traps sealed by intervening shales, as well as overlying Meganos submarine canyon mudstone infill (Downey, 2006). Deposited as a fluvial-deltaic sequence, this sandstone was sourced by the Sierra Nevada terrain to the east and prograded west-southwestward into the forearch basin. This formation truncates to the north by the post-Cretaceous angular unconformity until it pinches out in southern Yolo and Sutter counties (Downey, 2006). These large sands can be locally eroded or completely absent due to the downcutting by the Meganos submarine canyons, which are located along the west side of the AoR. In the northwestern portion of Sacramento County, the sandstone is as shallow as 2,000 feet and deepens to over 10,500 feet moving to south-central Solano County. Thickness in this area ranges from hundreds of feet thick, separated by thin shales, to 2,500 feet thick (Downey, 2010). Within the vicinity of the project AoR, thickness ranges from 316 to 1,336 feet and varies in depth from 5,044 to 7,395 feet true vertical depth (TVD) (**Figure A-13).**

Six injectors were chosen to inject into the Mokelumne River sandstone. Injectors for this project are shown in **Figure A-14**.

Capay Shale (Upper Confining Zone)

The Capay Shale provides upper confinement to the Mokelumne River Formation as it spans across the basin as a major regional flooding surface. This Eocene-aged formation was deposited as a transgressive surface blanketing the shelf with shales. East of the Midland fault zone, the Martinez Shale has been stripped by erosion, and the Mokelumne River Formation is unconformable overlain by the Capay Shale. Due to its low permeability, this formation acts as a seal to the Mokelumne River Formation injection zone and is a vertical barrier to any CO_2, from reaching the USDW, if any migration were to occur.

Domengine Sandstone (Monitoring Zone)

The Domengine Formation is approximately 800 to 1,200 feet thick on the north flank of Mt. Diablo (Nilsen, 1975). Prograding across the Capay Shelf in early-middle Eocene, this formation is characterized by interbedded sandstones, shales, and coals. This sand ranges from medium- to coarse-grained silty mudstone and fine sandstone, and onlaps the Capay Shale. It is separated from the Capay by a regional unconformity that progressively truncates older units until the Domengine rests on Cretaceous rocks, moving west. The Domengine consists of an upper and lower portion. The lower member is made up of fluvial and estuarine sandstones. Regionally the lower member is separated from the upper member by an extensive surface of transgression and change in depositional style. This formation acts as a monitoring zone for injection into the Mokelumne River Formation.

Nortonville Shale

Above the Domengine Sandstone is the Nortonville Shale, which is separated by a widespread surface of transgression. The Nortonville Shale is a mudstone member of the Kreyenhagen Formation. It is approximately 500 feet on the north flank of Mt. Diablo and is considered the upper portion of the Domengine Sandstone (Nilsen, 1975). Overlying the Domengine Sandstone, this shale acts as a seal throughout most of the southern Sacramento and northern San Joaquin Basins.

Marine Strata (Markley to Valley Springs)

The upper Paleogene and Neogene sequence begin with the Valley Springs Formation, which represents fluvial deposits that blanket the entire southern Sacramento Basin. The unconformity at the base of the Valley Springs marks a widespread Oligocene regression and separates the more deformed Mesozoic and lower Paleogene strata below from the less deformed uppermost Paleogene and Neogene strata above. The Upper Markley Formation contains water with total dissolved solids (TDS) concentrations of approximately 3,000 to 10,000 milligrams per liter (mg/L), and is the lowermost USDW in the AoR (**Figure A-12**). The USDWs are discussed in Section 2.7 of this document.

2.2.3 Map of the Area of Review

As required by 40 CFR 146.82(a)(2), **Figure A-15** shows surface bodies of water, surface features, transportation infrastructure, political boundaries, and cities. Major water bodies in the area are Discovery Bay, Clifton Court Forebay, Victoria Canals, Grant Line Canal, and the Indian Slough. The project area is in San Joaquin, Contra Costa, and Alameda Counties. This figure does not show the surface trace of known and suspected faults because there are no known surface faults in the AoR. There are also no known mines or quarries in the AoR. **Figure A-16** indicates the locations of State- or EPA-approved subsurface cleanup sites. This cleanup site information was obtained from the State Water Resources Control Board's GeoTracker database, which contains records for sites that impact, or have the potential to impact, groundwater quality. Water wells within and adjacent to the AoR are discussed in Section 2.7.7 of this document.

2.3 Faults and Fractures [40 CFR 146.82(a)(3)(ii)]

2.3.1 Overview

A combination of 3D and 2D seismic, along with well control and published data, were used to define faulting within the area (**Figure A-11**). The project area is bound on the east, south, and west sides by faulting, with the boundaries to the north and northeast open (**Figure A-17**). There is one normal fault within the CO_2 plume boundary that transects the injection zone.

2.3.2 Fault Sealing

An Allan diagram, shale gouge ratio (SGR), and shale smear factor (SSF) analysis were completed for each fault to demonstrate the sealing nature of the project area faults. Allan diagrams display across fault juxtaposition along a mapped fault plane, SGR is a fault seal algorithm used to estimate the sealing potential of a fault-zone, and SSF calculates the likelihood of intact shale smears within the fault plane (Yielding et al, 2010).

The SGR calculation takes stratigraphic thickness, throw, and clay volume into consideration using the following equation:

$$SGR = \frac{\sum(Vcl \times \Delta z)}{throw} \times 100\% \quad \text{(Eq-1)}$$

where Vcl is the clay volume content, Δz is the stratigraphic layer thickness, and $throw$ is the offset of the layer of interest. SGR values can vary vertically and laterally along a fault as stratigraphic changes occur (Freeman et al., 1998). SGR values greater than 20 percent imply there is a high chance of fault zone seal (Yielding et al, 2010).

The SSF calculation takes shale layer throw and thickness into consideration using the following equation:

$$SSF = \frac{throw}{thickness} \quad \text{(Eq-2)}$$

Where $throw$ is the offset of a single shale bed and $thickness$ is the thickness of the shale bed. SSF values can vary laterally along a fault as stratigraphic thickness or changes in offset occur. Small values of SSF, generally less than 4-5, imply a high probability of continuous smear. (Yielding et al, 2010).

Normal Fault within CO_2 Boundary

As discussed in Section 2.2.1, the normal fault within the CO_2 boundary was characterized using 3D seismic data. In the nearby Victoria Islands Farms 1 (04077206780000) well, the thickness of the upper confining zone (Capay Shale) is approximately 220 feet. The geologic model shows an average Capay Shale thickness of 210 feet within the CO_2 plume boundary. The normal fault within this boundary is interpreted as having 100 feet of offset in the uppermost Mokelumne River Formation. This offset is not large enough to completely offset the Capay Shale against

another formation. **Figure A-18** shows a schematic cross-section across this fault based upon the seismic interpretation.

An Allan diagram, SGR, and shale smear factor (SSF) analysis were completed to demonstrate the sealing nature of the Capay Shale. The Allan diagram is shown in **Figure A-19a**. The Allan diagram was generated using 7 different cross section locations along the length of the fault, each approximately 0.25 mile from the other. As shown in the figure, the Capay Shale has an overlap ranging from 98 to 198 feet along the length of the fault. This overlap shows there is adequate thickness of the confining zone within the area of the CO_2 plume.

As displayed and mentioned above, the fault does not have a large enough offset to completely offset the Capay against another formation, therefore the SGR only varies vertically and not laterally as only a portion of a single layer has moved past a given reference point. **Figure A-19b** displays an example of the SGR calculation for the top and bottom of the Capay at Cross Section location D-D', which is the same as cross section location A-A' in **Figure A-18**. The stratigraphic thickness and throw values were calculated using the Allan diagram. The Vcl values were averaged from 6 wells within the vicinity of the normal fault; WOODWARD_ISLAND_UNIT_20-1 (040130027400), SALYER_A_1 (040770042300), BORDEN_1 (040770042500), VICTORIA_ISLAND_FARMS_1 (040772067800), TURNER_1 (040770030700), and CALPAK_10-3 (040770030500). The well locations and Vcl values are displayed in **Figures A-19b**. **Figure A-19c** displays an example of the SSF calculation for the Capay Shale at cross section location D-D'. Since the Capay Shale maintains overlap across the length of the normal fault there is only a single SSF value for the Normal fault.

The SGR analysis results in values of 29 percent for the top of Capay Shale and 47 percent for the bottom of Capay Shale. Both of these values are larger than the 20 percent threshold which shows a high likelihood of fault sealing capability. The SSF analysis results in a value of 1 across the length of the fault, which supports a continuous shale smear along the fault. Both SGR and SSF values support that the fault through the Capay Shale is sealing (Yielding et al., 2010).

As discussed in Section 2.4, mineralogy data for the Capay Shale shows the confining zone to be clay rich and therefore should provide a vertical seal to the Mokelumne River Formation within the fault zone. Additionally, site-specific mineralogy data for the Capay Shale will be collected during preoperational testing to confirm the clay rich nature of the zone. Furthermore, the Domengine sands above the Capay Shale will be monitored as part of the monitoring and testing plan.

Midland Fault

The Midland Fault is located to the west of the AoR. The Midland Fault is a west-side-down normal fault that strikes northwest and dips towards the west. This fault was active in the late Cretaceous-Eocene time (Unruh et al., 2009). This movement created the Rio Vista sub-basin, which has become a developed natural gas field, approximately 12 to 15 miles north of the CTV III area. At Rio Vista, there is gas production on either side of the Midland Fault, with the Midland acting as a seal for trapped hydrocarbons in structural closures. On the eastern side of the Midland Fault at Rio Vista, natural gas has been trapped in three-way closures against the fault at two levels within the Mokelumne River Formation. These Mokelumne River Formation

sands include the Midland Sand, which had an initial pressure gradient of approximately 0.46 pounds per square inch per foot (psi/ft), and the M-5 Sand with an initial pressure gradient around 0.44 psi/ft, both at 4,500 feet or greater. The deeper Winters Formation produces from both sides of the Midland Fault at Rio Vista, with pressure gradients ranging from 0.49 to 0.53 psi/ft. Unruh et al. (2009) interpret that the southern end of the Midland fault was later reactivated as a reverse fault in the late Cenozoic modern transpressional tectonic setting. The trace of the fault was created using the work of Downey and Clinkenbeard (2010) and confirmed on 2D seismic data licensed by CRC/CTV.

An Allan diagram, SGR, and SSF analysis were completed to demonstrate the sealing nature of the Midland Fault. The Allan diagram is shown in **Figure A-20a**. The Allan diagram displays the fault plane within the 'representative fault surfaces boundary' shown in the figure, and is based on a well cross-section centered on well PAGANO_2-4 (040130022700), where stratigraphic data is considered to be reliable. North of the of the representative Allan diagram, along the Midland Fault, the Mokelumne sands thin due to erosion from the Meganos Canyon (**Figure A-13**). This erosion acts to increase the volume of shale in the area due to shale infill of the canyon, thus increasing the sealing capacity of the Midland Fault north of the Allan Diagram. Structural offset along the fault is expected to be consistent in the area west of the Plume Boundary. This consistent offset is displayed in the Allan diagram (**Figure A-20a)**. The Mokelumne Formation on the hanging wall side of the fault (injection zone) is partially juxtaposed against the H&T Shale on the footwall side of the fault. Since the fault does not have a large enough offset to completely offset the Mokelumne Formation against another formation, the SGR values only vary vertically. **Figure A-20b** displays the SGR calculation for the top and bottom of the Mokelumne Formation (injection zone) using the Δz of the layer that moved past a given point, and the Vcl of the layer to which it is juxtaposed. $throw$ was calculated using the offset for both the top and bottom of the Mokelumne Formation. These stratigraphic thickness and throw values were calculated using the Allan diagram. The Vcl values were averaged from 3 wells; PAGANO_2-4 (040130022700), PERRY_1 (040132002500), and NGC_PHILLIPS_CHRISTENSEN_1 (040132023100). The well locations and Vcl values are displayed in **Figure A-20b**. **Figure A-20c** displays the SSF calculation for the Capay offset which demonstrates the vertical sealing nature of the Midland Fault above the Mokelumne injection zone.

The SGR analysis results in values of 30 percent for the top of the Mokelumne Formation and 43 percent for the bottom of Mokelumne Formation. Both of these values are larger than the 20 percent threshold which shows a high likelihood of fault sealing capability. The SSF analysis results in a value of 2, which supports a continuous shale smear along the fault zone above the Mokelumne injection zone. Both the SGR and SSF values, along with the sealing nature of the fault to the north at Rio Vista, support that the fault is sealing, therefore the Midland fault is considered a closed and sealing boundary in the model.

Stockton Fault

The Stockton Fault is located to the east of the AoR. The trace and offset of this fault are well defined and characterized by the 3D seismic data and well control in the nearby Union Island Gas Field. This thrust fault is associated with Post-Eocene/Pre-Miocene movement and

production from the Union Island Gas Field is from a fault-related trap in the footwall. The trace of the Stockton Fault interpreted from the 3D seismic data agrees with the Fault Activity Map from the California Geologic Survey (https://maps.conservation.ca.gov/cgs/fam/).

An Allan diagram, SGR, and SSF analysis were completed to demonstrate the sealing nature of this fault. The Stockton Fault Allan diagram is shown in **Figure A-21a** and was generated from four cross sections, A-A' through D-D'. The Allan diagram is expected to be representative of the Stockton Fault along the entire length of the southeastern model boundary as shown in the figure. As seen in the Allan diagram, the Mokelumne Formation on the footwall side of the fault (injection zone) is partially juxtaposed against the H&T Shale on the hanging wall side of the fault. Since the fault does not have a large enough offset to completely offset the Moke against another formation, the SGR values only vary vertically along the length of the fault. **Figure A-21b** displays example SGR calculations for the top and bottom of the Mokelumne Formation (injection zone) at cross sections B-B' and C-C' using the Δz of the layer that moved past a given point, and the Vcl of the layer to which it is juxtaposed. $throw$ was calculated using the offset for both the top and bottom of the Mokelumne Formation. These stratigraphic thicknesses and throw values were calculated using the Allan diagram. The Vcl value for the Mokelumne Formation and H&T Shale were averaged from 4 wells; Yamada_Brothers_2, Ohlendorf_Unit_1_1, Marchini_M-1, and Phillip_Bronich_A_1. Well locations are displayed in **Figure A-21a**, and Vcl values are displayed in **Figure A-21b**. **Figure A-21c** displays the example SSF calculations for the Capay Shale (confining zone) offset for cross sections B-B' and C-C'.

The SGR analysis results in values of 27 percent for the top of the Mokelumne Formation and 40 percent for the bottom of the Mokelumne Formation which shows a high likelihood of fault sealing capability. The SSF calculation results in values ranging from 1 to 7.5 along the length of the fault as the throw of the Capay varies. Some values are above the threshold of 4-5, however, the likelihood of intact clay smear is still present. The SSF values are calculated using the Capay Shale as the main shale layer however interbedded shales within the Mokelumne River Formation also add additional shale smearing along the fault plane. The SGR and SSF values, along with the known sealing nature of the fault based on production at the nearby Union Island Gas Field, support that the fault is sealing, therefore the Stockton fault is considered a closed and sealing boundary in the model.

West Tracy Fault

The West Tracy Thrust Fault is located to the south of the AoR. This fault is drawn through a mix of 3D and 2D seismic data and is interpreted to connect to the Midland and Stockton Faults through the review of published work. Unruh and Hitchcock (2015) reviewed additional 2D seismic data along with other ancillary data and concluded that the West Tracy Fault was probably active between the Eocene and Miocene with later reactivation during late Cenozoic transpression. This blind reverse fault has steeply dipping strata in the south-west hanging wall and may have ruptured the surface near Byron, CA. Their interpretation also connects the West Tracy Fault to the Midland fault at its western junction. Their work was a more detailed description following that of Unruh and Krug (2007). In both publications, the eastern end of the West Tracy Fault is somewhat connected to the Vernalis Fault that runs east-west to the east of

the project area. Our analysis suggests the West Tracy Fault is better connected to the trace of the Stockton Fault given the strike of the faults in the region. This would agree with the fault trace drawn by Downey and Clinkenbeard (2010). There are no established hydrocarbon fields along the West Tracy Fault that demonstrate fault seal. Due to the sealing nature of the other sub-regional faults in the area, including the Vernalis Fault to the east that seals hydrocarbons at the Vernalis Gas Field, the West Tracy Fault is considered to be sealing.

An Allan diagram, SGR, and SSF analysis were completed to demonstrate the sealing nature of this fault. The West Tracy fault Allan diagram is shown in **Figure A-22a.** The Allan diagram is based on a single well cross section centered between wells WICO_BANKHEAD_1 (04077003130000) and SOUZA_1 (04077205500000), where stratigraphic data is considered to be reliable. The offset displayed in the Allan diagram is based on the seismic interpretation and Mokelumne Formation identified in well SOUZA_1 on the hanging wall (southwest side) of the fault for additional constraint. The Allan diagram is expected to be representative of the West Tracy Fault along the entire length of the southwestern model boundary as shown in the figure. Where covered by the 3D seismic and supported by the available 2D seismic data the fault shows consistently large offset upon which the Allan diagram is based. As seen in the Allan diagram, the Mokelumne Formation on the footwall side of the fault (injection zone) is fully juxtaposed against the H&T Shale on the hanging wall side of the fault. **Figure A-22b** displays the SGR calculations for the top and bottom of the Mokelumne Formation (injection zone) using the Δz of the layer that moved past a given point, and the Vcl of the layer to which it is juxtaposed. $throw$ was calculated using the offset for both the top and bottom of the Moke Formation. The stratigraphic thickness and throw values were calculated using the Allan diagram. The Vcl value for the Mokelumne Formation and H&T Shale were averaged from 2 wells; WICO_BANKHEAD_1 and SOUZA_1. Well locations and Vcl values are displayed in **Figure A-22b**. **Figure A-22c** displays the SSF calculation for the H&T Shale offset. The H&T Shale was used for the SSF calculation since the Mokelumne Formation (injection zone) is juxtaposed against and below the top of the hanging wall H&T Shale.

The SGR analysis results in values of 31 percent for the top of the Mokelumne Formation and 42 percent for the bottom of Mokelumne Formation. Both of these values are larger than the 20 percent threshold which shows a high likelihood of fault sealing capability. The SSF analysis results in a value of 1, which supports a continuous shale smear along the fault zone next to and above the Mokelumne injection zone. The SGR and SSF values, along with the sealing nature of the other sub-regional faults in the area provides evidence that the West Tracy fault is sealing, therefore, it is considered a closed and sealing boundary in the model.

Fault Pressure

None of the three bounding faults in the vicinity of the project area come in contact with the CO_2 plume boundary; therefore, only the pressure front is considered. Our modeling has the Mokelumne River Formation under-pressured across the AoR relative to hydrostatic. In this case, the pressure increase associated with CO_2 injection is seen to increase pressure of the Mokelumne River Formation back to pressures that are documented at other locations along these fault traces within the project area. **Figure A-23** shows the locations of four pseudo wells where pressures are extracted from the model to calculate the pressures that will be seen across

the injection life of this project. The locations for the pseudo wells were chosen to match the highest predicted pressure relative to the fault trace within the pressure front. **Table A-4** shows the average initial, maximum (28 years after initial injection), and 100 years post injection pressure at these locations. An average pressure increase is provided, and these numbers are averages across the Mokelumne River Formation. Given that other formations around these faults, including equivalent Mokelumne River units, have held back hydrocarbons at similar as well as higher pressures above hydrostatic, we believe this to be a safe standard for fault stability. Additional analysis and discussion around the stability of these faults in relation to the modeled pressure increases are provided in Section 2.5.3 Fault Reactivation. The natural seismic history of this area is discussed in the Section 2.6 Seismic History section of this document, and Attachments C and I of this application detail the seismicity monitoring plan for this injection site. The Mokelumne River Formation pressure will be confirmed in pre-operational testing.

2.4 Injection and Confining Zone Details [40 CFR 146.82(a)(3)(iii)]

2.4.1 Mineralogy

No quantitative mineralogy information exists within the AoR boundary. Mineralogy data will be acquired across all the zones of interest as part of pre-operational testing. Several wells outside the AoR have mineralogy over the respective formations of interest, and those data are presented below.

Mokelumne River Formation

The Speckman_Decarli_1 well and Citizen_Green_1 well located outside of the AoR in Roberts Island and King Island gas fields, respectively, have x-ray diffraction (XRD) data for the Mokelumne River Formation (see **Figure A-24** for well locations). Reservoir sand from nine samples within these wells average 33.6% quartz, 47.6% plagioclase and potassium feldspar, and 18% total clay (see **Table A-5**). The primary clay minerals are kaolinite and mixed layer illite/smectite. Calcite and dolomite were not detected in any of the samples.

Capay Shale

Mineralogy data are available for the Capay Shale from three wells in the Rio Vista Field (RVGU_209, RVGU_248, and Wilcox_20). RVGU_209 has FTIR data, while the other two wells have XRD data. Nine samples show an average of 29% total clay, with mixed layer illite/smectite being the dominant species, with kaolinite and chlorite still prevalent. They also contain 32% quartz, 39% plagioclase and potassium feldspar, minimal pyrite, and less than 1% calcite and dolomite.

H&T Shale

Mineralogy data are available for the H&T Shale from the Speckman_Decarli_1 well. Nine samples show an average of 46% total clay, with mixed layer illite/smectite being the dominant species, with kaolinite and chlorite still prevalent. They also contain 23% quartz, 29% plagioclase and potassium feldspar, 2% pyrite, and 1% calcite and dolomite.

2.4.2 Porosity and Permeability

Mokelumne River Formation

Wireline log data were acquired with measurements that include but are not limited to spontaneous potential, natural gamma ray, borehole caliper, compressional sonic, resistivity, neutron porosity, and bulk density.

Formation porosity is determined one of two ways: from bulk density using 2.65 grams per cubic centimeter (g/cc) matrix density as calibrated from core grain density and core porosity data, or from compressional sonic using 55.5 microsecond per foot (µsec/ft) matrix slowness and the Raymer-Hunt equation.

Volume of clay is determined by spontaneous potential and is calibrated to core data.

Log-derived permeability is determined by applying a core-based transform that uses capillary pressure porosity and permeability along with clay values from XRD or FTIR data. A total of 13 core data points from two wells, RVGU_209 and RVGU_248 (see **Figure A-24** for well locations), were used to develop a permeability transform. An example of the transform from core data is illustrated in **Figure A-25**.

Comparison of the permeability transform to log generated permeability (Timur-Coates method) from a nuclear magnetic resonance (NMR) log in the Citizen_Green_1 well in King Island Gas Field is almost 1:1 and matches rotary sidewall core permeability over the Capay-Mokelumne River Formation interval (**Figure A-26**). See **Figure A-24** for location of Citizen_Green_1 well.

In the well Ohlendorf_Unit_1_1, for the Mokelumne River Formation, the porosity ranges from 1.5% to 34% with a mean of 26.5% (**Figure A-27**). The permeability ranges from 0.003 to 697 millidarcies (mD) with a log mean of 68 mD (**Figure A-28**).

A log plot for the Ohlendorf_Unit_1_1 is included in **Figure A-29**.

The average porosity for the Mokelumne River Formation is 27.0%, based on 18 wells with porosity logs and 30,487 individual logging data points. See **Figure A-30** for locations of wells used for porosity and permeability averaging.

The geometric average permeability for the Mokelumne River Formation is 75.4 mD, based on 18 wells with porosity logs and 30,073 individual logging data points. A total of 50 core data points from 5 wells (Citizen_Green_1, Enea_Capital_3, PG&E_Test_Injection_Withdrawl_Well_1, Speckman_Decarli_1, and Whiskey_Slough_1A-E (see **Figure A-30** for well locations) are from the Mokelumne Formation. Porosity and permeability from these core data agree with the log averages (see **Table A-6**).

Capay Shale

The average porosity of the upper confining zone (Capay Shale) is 29.3%, based on 17 wells with porosity logs and 10,044 individual logging data points.

The geometric average permeability of the upper confining zone (Capay Shale) is 0.34 mD, based on the Citizen_Green_1 well NMR permeability from the Timur-Coates method (see **Figure A-24** for well location).

H&T Shale

The average porosity of the lower confining zone (H&T Shale) is 21.4%, based on 16 wells with porosity logs and 31,279 individual logging data points.

The geometric average permeability of the lower confining zone (H&T Shale) is 0.49 mD, based on 16 wells with porosity logs and 30,853 individual logging data points.

2.4.3 Injection Zone and Confining Zone Capillary Pressure

Capillary pressure is the difference across the interface of two immiscible fluids. Capillary entry pressure is the minimum pressure required for an injected phase to overcome capillary and interfacial forces and enter the pore space containing the wetting phase.

No capillary pressure data were available for the Capay Shale. These data will be acquired as part of pre-operational testing.

Capillary pressure data were available for the Mokelumne River Formation (injection zone) from the Citizen_Green_1 well outside the project area in the King Island Gas Field. Two sidewall core samples were collected from the injection zone using mercury-injection capillary pressure (MICP). The raw data was downloaded from the NETL EDX server, and required a closure correction (Shafer & Neasham, 2000). Using the XRD data (**Table A-5**), the mercury injection pressures and saturations were then corrected for clay bound water using the methodology prescribed in Juhasz, 1979. The corrected air-mercury capillary pressure was then converted to reservoir conditions of CO_2-brine using the equation below (Lohr & Hackley, 2018).

$$P_{CO_2-Brine} = P_{Hg-Air} \frac{\sigma_{CO_2-Brine} \cos\theta_{CO_2-Brine}}{\sigma_{Hg-Air} \cos\theta_{Hg-Air}} \quad (1)$$

An interfacial tension (IFT) of 480 dynes per centimeter (dynes/cm) was used for air-mercury and 30 dynes/cm was used for CO_2-brine. The cosine of contact angles of 0.766 and 0.875 degrees were also used for air-mercury and CO_2-brine, respectively. The values of IFT and contact angles for CO_2-brine were based on published studies (Chiquet et al., 2009; Haeri et al., 2020). Refer to **Figure A-31** for final CO_2-brine corrected curves for the two samples.

For computational modeling purposes, capillary pressure data obtained in the similar geologic age and setting Winters Formation in the nearby Union Island Gas field were used in addition to the Citizen_Green_1 data. As discussed in Attachment B: Area of Review and Corrective Action Plan, Section 2.2.2, a sensitivity analysis (Case 11) was run using the Citizen_Green_1 capillary pressure data. Results indicated negligible changes to the AoR, CO_2 plume, and pressure field. Therefore, the Winters Formation data from Sonol_Securities_5 are adequate for modeling purposes until site- and zone-specific data can be obtained as part of the pre-

operational testing program. **Figure A-32** shows the capillary pressure data used for the computational modeling.

The report DOE-PGE-00194-4 cites caprock threshold pressure tests that were performed on samples from the upper confining zone in the King Island gas field. A delta pressure was held across three separate core samples, none of which showed any brine production at the highest delta pressure of 2,000 psi. As stated in the report, "These results support a conclusion that the upper confining zone is an impermeable seal at reservoir conditions" (Medeiros, et al., 2018).

2.4.4 Depth and Thickness

Depths and thickness of the Mokelumne River Formation reservoir and Capay confining zone (**Table A-7**) are determined by structural and isopach maps (**Figure A-33**) based on well data (wireline logs). Variability of the thickness and depth measurements is due to:

- Structural variability within the Mokelumne River and Capay Formations is caused by the Meganos submarine canyon erosional event.
- The Capay Shale remains consistent throughout the AoR both structurally and stratigraphically.
- Thickness variability within the Mokelumne River Formation is due to the Meganos submarine canyon erosion.

2.4.5 Structure Maps

Structure maps are provided to indicate a depth to reservoir adequate for supercritical-state injection.

2.4.6 Isopach Maps

Spontaneous potential (SP) logs from surrounding gas wells were used to identify sandstones. Negative millivolt (mV) deflections on these logs, relative to a baseline response in the enclosing shales, define the sandstones. These logs were baseline shifted to 0 mV. Due to the log vintage variability, there is an effect on quality which creates a degree of subjectivity within the gross sand; however, this will not have a material impact on the maps.

In addition to well log data, site specific depth and thickness information for the Mokelumne River Formation reservoir and Capay confining zone are also available from seismic data (**Figure A-11**). The coverage of the 3D and 2D seismic data and the well control in the structural model area provide confidence in the thickness and continuity of the injection and confining zones. Based on the computational modeling results discussed in Attachment B, the structural variability in the thickness and depth of either the Capay Shale or the Mokelumne River Formation sandstone resulting from the Meganos submarine canyon erosional event, do not impact confinement. CTV will use thickness and depth shown when determining operating parameters and assessing project geomechanics.

2.5 Geomechanical and Petrophysical Information [40 CFR 146.82(a)(3)(iv)]

2.5.1 Caprock Ductility

Ductility and the unconfined compressive strength (UCS) of shale are two properties used to describe geomechanical behavior. Ductility refers to how much a rock can be distorted before it fractures, while the UCS is a reference to the resistance of a rock to distortion or fracture. Ductility generally decreases as compressive strength increases.

Ductility and rock strength calculations were performed based on the methodology and equations from Ingram & Urai (1999) and Ingram et al. (1997). Brittleness is determined by comparing the log derived UCS vs. an empirically derived UCS for a normally consolidated rock (UCS_{NC}).

$$\log UCS = -6.36 + 2.45 \log\left(0.86V_p - 1172\right) \quad (1)$$

$$\sigma' = OB_{pres} - P_p \quad (2)$$

$$UCS_{NC} = 0.5\sigma' \quad (3)$$

$$BRI = \frac{UCS}{UCS_{NC}} \quad (4)$$

Units for the UCS equation are UCS in megapascals (MPa) and V_p (compressional velocity) in meters per second (m/s). OB_{pres} is overburden pressure, P_p is pore pressure, σ' is effective overburden stress, and *BRI* is brittleness index.

If the value of BRI is less than 2, empirical observation shows that the risk of embrittlement is lessened, and the confining zone is sufficiently ductile to accommodate large amounts of strain without undergoing brittle failure. However, if BRI is greater than 2, the "risk of development of an open fracture network cutting the whole seal depends on more factors than local seal strength and therefore the BRI criterion is likely to be conservative, so that a seal classified as brittle may still retain hydrocarbons" (Ingram & Urai, 1999).

Capay Shale

Within the project area, six wells had compressional sonic and bulk density data over the Capay Shale to calculate ductility, comprising 3,769 individual logging data points (see pink squares in **Figure A-24**). A total of 15 wells had compressional sonic data over the Capay Shale to calculate UCS, comprising 9,413 individual logging data points (see black circles in **Figure A-24**). The average ductility of the confining zone based on the mean value is 1.50. The average rock strength of the confining zone, as determined by the log derived UCS equation above, is 2,091 psi.

An example calculation for the well Ohlendorf_Unit_1_1 is shown below (**Figure A-34**). UCS_CCS_VP is the UCS based on the compressional velocity, UCS_NC is the UCS for a normally consolidated rock, and BRI is the calculated brittleness using this method. Brittleness less than 2 (representing ductile rock) is shaded red.

Within the Capay Shale, the brittleness calculation drops to a value less than 2. Additionally, the Nortonville Shale above the Capay Shale has a brittleness value less than 2. As a result of the Capay Shale ductility, there are no fractures that will act as conduits for fluid migration from the Mokelumne River Formation.

2.5.2 Stress Field

The stress of a rock can be expressed as three principal stresses. Formation fracturing will occur when the pore pressure exceeds the least of the stresses. In this circumstance, fractures will propagate in the direction perpendicular to the least principal stress (**Figure A-35**).

Stress orientations in the Sacramento Basin have been studied using both earthquake focal mechanisms and borehole breakouts (Snee and Zoback, 2020; Mount and Suppe, 1992). The azimuth of maximum principal horizontal stress (S_{Hmax}) was estimated at N40ºE ± 10º by Mount and Suppe (1992). Data from the World Stress Map 2016 release (Heidbach et al., 2016) show an average S_{Hmax} azimuth of N37.4ºE once several far field earthquakes with radically different S_{Hmax} orientations are removed (**Figure A-36**), which is consistent with Mount and Suppe (1992). The earthquakes in the area indicate a strike-slip/reverse faulting regime.

In the project AoR, there are no site-specific Mokelumne River Formation fracture pressure or fracture gradient data. A Mokelumne River Formation step rate test will be conducted per the pre-operational testing plan. However, several wells in the project vicinity have formation integrity tests (FITs), step-rate tests (SRTs), and leak off tests (LOTs) for the Mokelumne River Formation and H&T Shale. Two wells recorded minimum fracture gradients of 0.75-0.76 psi/ft based on FIT in the Mokelumne River Formation (Galli_1 and Yamada_Line_Well_1, see **Figure A-37** for well locations and **Table A-8** for well data), and one well recorded a fracture gradient of 0.822 psi/ft based on an SRT in the King Island field. For the computational simulation modeling and well performance modeling, a frac gradient of 0.76 psi/ft was assumed for now.

In the project AoR, there are no site-specific Capay Shale fracture pressure or fracture gradient data. A Capay Shale mini-frac will be conducted per the pre-operational testing plan. In the interim, CTV is assuming that the Capay Shale will have a similar fracture gradient as the Mokelumne River Formation.

The overburden stress gradient in the reservoir and confining zone is 0.91 psi/ft. The overburden gradient was calculated by integrating density logs from seven wells. The method for calculating the overburden gradient integrates the density logs using methodology laid out in Fjaer et al. (2008):

$$\sigma_v = \int_0^D \rho(z) g \, \mathrm{d}z \tag{5}$$

where ρ is the density of the sediments, g is the acceleration due to gravity, D is the depth of interest, z is the vertical depth interval, and σ_v is the vertical stress. This calculation was completed using the "Overburden Gradient Calculation" module in the software Interactive

Petrophysics 5.1.0. **Figure A-38** displays the overburden gradient calculation inputs and outputs from the software. See **Table A-9** for a list of the wells used for overburden stress gradient calculations.

No data currently exist for the pore pressure of the confining zone. This will be determined as part of the pre-operational testing plan.

2.5.3 Fault Reactivation

The stability of the faults within and bounding the CTV III project area were analyzed using Mohr coulomb criteria. Four faults were studied: The Stockton Arch Fault on the eastern boundary of the project area, the West Tracy Fault on the southern boundary of the project area, the Midland Fault on the western boundary of the project area, and the normal fault within the CO_2 plume. The input parameters for the Mohr Circle are shown in **Table A-10** and can be referenced in Sections 2.3.1 and 2.5.2. The reference depth for all calculations was set to 6,900 feet TVD. The maximum horizontal stress gradient was determined using data from Lund-Snee and Zoback (2020). The maximum horizontal stress direction is 37.4º as stated in Section 2.5.2. Fault strike and dip were averaged over each fault's contact with the project area in the vicinity of the AoR. The coefficient of friction was assumed to be 0.6 and the faults were prescribed a cohesive strength of 0 psi. Based on Mohr circle analysis, all of the faults are currently far from failure and will continue to be stable even after CO_2 injection has ceased (**Figure A-39**). Analysis by Mohr circle shows that the required pore pressure increase to reactivate any of the faults is over 1,800 psi above present day conditions (**Figure A-40** and **Table A-11**). This equates to a reservoir pressure of over 4,700 psi (equivalent to 0.68 psi/ft at the reference depth of 6,900 feet TVD), far above the expected final pressure gradients after CO_2 injection has ceased. Pressure gradients in the CTV III project area along the three bounding faults (West Tracy, Midland, and Stockton Arch) are only expected to increase to approximately 0.45 psi/ft, and to 0.464 psi/ft for the normal fault in the plume (**Table A-4**). This pressure gradient is very similar to the discovery pressure of the Mokelumne River Formation in Rio Vista Gas Field, where the Mokelumne River gas reservoir is trapped against the Midland Fault (Section 2.3.1). In deeper reservoirs in direct contact with both the Midland and Stockton Arch faults in the project vicinity, discovery pressures approached 0.49 to 0.53 psi/ft (Section 2.3.1). The fact that these faults held natural gas reservoirs with these pressure gradients for long periods of geologic time helps to reinforce the Mohr circle explanation of these faults being stable at higher reservoir pressures.

2.6 Seismic History [40 CFR 146.82(a)(3)(v)]

2.6.1 Seismic Data

As discussed in prior sections, 3D seismic, along with 2D seismic and well data, were used to create depth surfaces for the major faults within the project area. The traces of these faults agree with published work—for example, the Fault Activity Map created by the California Geologic Survey (CGS) shown in **Figure A-41**. CGS categorizes the Midland Fault as a Quarternary Fault of undifferentiated age, and the Stockton Fault as Pre-Quaternary. CGS does not display a trace for the West Tracy Fault, likely due to the limited public information available to document its

presence. As discussed in Unruh and Hitchcock (2015), seismic reflection data from the hydrocarbon industry are needed to map this fault. Further discussion on the timing on each of the faults is provided in the Faults and Fractures section of this document.

The U.S. Geological Survey (USGS) provides an earthquake catalog tool (https://earthquake.usgs.gov/earthquakes/search/) that can be used to search for recent seismicity that could be associated with faults in the area for movement. A search was made for earthquakes in the greater vicinity of the project area from 1850 to modern day with events of a magnitude greater than three. **Figure A-42** shows the results of this search. **Table A-12** summarizes some of the data taken from them. Events were cut down to include those only in the vicinity of the faults mapped for this project and events associated with the Marsh Creek Fault system to the west are removed from the data table.

Figure A-43 combines the events from the USGS catalog with the mapped faults in the project area including the West Tracy Fault. Events 17, 11 and 10 were likely associated with the Black Butte–Midway Fault system southwest of the project area. Events 5 and 10 are substantially deeper than the sedimentary section and coincide with the trace of the Vernalis Fault; both faults are shown on the CGS Fault Activity Map (**Figure A-41**). Events 6 and 7 have no clear relationship to any mapped fault system, were one day apart, and relatively deep (both greater than 7.5 km as estimated by the USGS catalog). Event 2, west of the AoR occurring in 2018, is close to the Davis Fault on the west side of Brentwood. There are no mapped faults nearby event 16, significantly away from the AoR.

Event 9 appears to be isolated from the fault zones at a depth of 6 km. Reviewing the 3D seismic data in that area there may be a structural feature at the level of seismic basement, but it is not well imaged. The event does not continue into the shallower sediments that are thousands of feet deeper than the proposed injection zone. Similar can be said for event 14, another deep (6 km) event that is outside of the AoR.

For the Stockton Fault, event numbers 3 and 8 are clearly related to the fault trace. Event 8 was a significant distance from the AoR and event 3 was significantly deeper (14.55 km) than the proposed injection zone. Finally, events 1, 4, 13, and 15 are in closest proximity to the Midland Fault. Event 15 appears to align with the Rio Vista Fault, a mapped fault by the CGS that may be a splay of the Midland Fault and to the north of the CTV III AoR. Event 13 is interpreted to be at a significant depth (14.95 km) away from the injection zone and far beneath the sedimentary section of the basin. Event 1 and 4 are likely the most concerning; event 1 happened in 2024, around 7,200 feet (2.2 km), at the approximate level of the Injection zone, and event 4 happened in 2002, at the approximate seismic basement level, which is interpreted to be around 16,000 feet (4.88 km). The average depth of prior seismic events in the region based on these data (**Table A-12**) is approximately 9.3 km, far deeper than the proposed injection zone and sedimentary section.

Given the history of seismicity in the region, minimizing pressure on the mapped faults is a key part of CTV III. Our modeling shows the Mokelumne River Formation to be under-pressured across the AoR, which will be confirmed in pre-operational testing. The Faults and Fractures section of this document provides further information on the expected pressures seen at these

faults and discusses the gradients relative to other geologic zones along them. As stated previously, given that other formations around these faults have held back hydrocarbons at pressures above hydrostatic, we believe this to be a safe standard for fault stability. This is presented along with Mohr coulomb failure criteria analysis in Section 2.5.3 Fault Reactivation.

Lund-Snee and Zoback (2020) published updated maps for crustal stress estimates across North America. **Figure A-44** shows a modified image from that work highlighting the CTV III area. This work agrees with previous estimates of maximum horizontal stress in the region of approximately N40°E in a strike-slip to reverse stress regime (Mount and Suppe, 1992) and is consistent with World Stress map data for the area (Heidbach et al., 2016). Attachments C and I of this application discuss the seismicity monitoring plan for this injection site.

2.6.2 Seismic Hazard Mitigation

CTV III is in an area of historical seismicity, but no events have impacted surrounding oil and gas reservoirs and infrastructure, such as at the nearby Union Island Gas Field. This document defines the confining zone, beginning with the Capay Shale, that separates the Mokelumne River Formation injection interval from USDW.

The following is a summary of CTVs seismic hazard mitigation for CTV III:

The project has a geologic system capable of receiving and containing the volumes of CO_2 proposed to be injected

- Extensive historical operations in the area across multiple geologic formations, including Mokelumne River Formation at Rio Vista, provide valuable experience to understand operating conditions such as injection volumes and reservoir containment. The strategy to limit the injected CO_2 to keep the maximum pressures seen at faults to at or below levels they have been exposed to from other and equivalent zones will mitigate the potential for induced seismic events and endangerment of the USDW.
- There are no faults or fractures identified in the AoR that will impact the confinement of CO_2 injectate. The bounding faults of the project area are not reached by the AoR/CO_2 plume and the small normal fault within the plume is not vertically transmissive, and therefore does not diminish the sealing effectiveness of the Capay Shale Upper Confining Zone.

Will be operated and monitored in a manner that will limit risk of endangerment to USDWs, including risks associated with induced seismic events

- Injection pressure will be lower than the fracture gradient of the sequestration reservoir with a safety factor (90% of the fracture gradient).
- Injection and monitoring well pressure monitoring will ensure that pressures are beneath the fracture pressure of the sequestration reservoir and confining zone. Injection pressure will be lower than the fracture gradients of the sequestration reservoir and confining zone with a safety factor (90% of the fracture gradients)

- A seismic monitoring program will be designed to detect events lower than seismic events that can be felt. This will ensure that operations can be modified with early warning events, before a felt seismic event.

Will be operated and monitored in a way that in the unlikely event of an induced event, risks will be quickly addressed and mitigated

- Via monitoring and surveillance practices (pressure and seismic monitoring program), CTV personnel will be notified of events that are considered an early warning sign. Early warning signs will be addressed to ensure that more significant events do not occur.
- CTV will establish a central control center to ensure that personnel have access to the continuous data being acquired during operations.

Minimizing potential for induced seismicity and separating any events from natural to induced

- Pressure will be monitored in each injector and sequestration monitoring well to ensure that pressure does not exceed the fracture pressure of the reservoir or confining zone.
- Seismic monitoring program will be installed pre-injection for a period to monitor for any baseline seismicity that is not being resolved by current monitoring programs.
- Average depth of prior seismic hazard in the region based on reviewed historical seismicity has been approximately 9.3 km, significantly deeper than the proposed injection zone.

2.7 Hydrologic and Hydrogeologic Information [40 CFR 146.82(a)(3)(vi), 146.82(a)(5)]

The California Department of Water Resources has defined 515 groundwater basins and subbasins with the state. The AoR is primarily within the Tracy Subbasin (Subbasin No. 5-22.15), which lies in the northwestern portion of the San Joaquin Valley Groundwater Basin. **Figure A-45** shows the AoR, Tracy Subbasin, and the surrounding areas. The Subbasin encompasses an area of about 238,429 acres (370 square miles) in San Joaquin and Alameda Counties (DWR, 2006).

2.7.1 Hydrologic Information

Major surface water bodies within the Tracy Subbasin consist of the San Joaquin, Old, and Middle Rivers. **Figure A-45** shows the locations of these surface water bodies. The San Joaquin River makes up almost the entire eastern boundary of the Subbasin and it feeds water into the SWP Clifton Court Forebay, which is located just west of the Subbasin.

Two major pump stations pump water out of the Old River from the Clifton Court Forebay into two large canals: the California Aqueduct and the Delta-Mendota Canal. These large canals traverse the southwestern portion of the Subbasin, and transport water from the Delta to other agricultural and urban water suppliers in the San Joaquin Valley and southern California. In addition to the major natural waterways there is a large network of irrigation canals, which convey surface water to agricultural properties.

2.7.2 Base of Fresh Water and Base of USDWs

The owner or operator of a proposed Class VI injection well must define the general vertical and lateral limits of all USDWs and their positions relative to the injection zone and confining zones. The intent of this information is to demonstrate the relationship between the proposed injection formation and any USDWs, and it will support an understanding of the water resources near the proposed injection wells. A USDW is defined as an aquifer or its portion that supplies any public water system; or that contains a sufficient quantity of ground water to supply a public water system; and currently supplies drinking water for human consumption; or contains less than 10,000 mg/L TDS; and is not an exempted aquifer.

Base of Fresh Water

The base of fresh water (BFW) helps define the aquifers that are used for public water supply. Local water agencies in the Tracy Subbasin have participated in various studies to comply with the 2014 Sustainable Groundwater Management Act (SGMA). Luhdorff & Scalmanini (2016) performed a study that focused on the geologic history of freshwater sediments from which groundwater is extracted for beneficial uses as defined and regulated under SGMA.

Few groundwater wells exist in the Tracy Subbasin because surface water is the source for irrigation use within delta islands. Groundwater usage is limited to eastern Contra Costa County and the Tracy area to the south. In most of western San Joaquin County in the Delta the fresh groundwater aquifers are limited to relatively shallow depths of 500 to 700 feet below ground surface (bgs) in the Contra Costa County area, and to 1,600 feet bgs in the Tracy area (Luhdorff & Scalmanini, 2016).

Luhdorff & Scalmanini (1999) performed a study of over 500 well logs in eastern Contra Costa County groundwater for five water agencies. The focus of this study was the uppermost 500 feet, where most water wells were completed. Subsequently Luhdorff & Scalmanini (2016) used logs also examined for the nature of geologic units at greater depths to better define the BFW. The top of the geophysical logs tended to be at 800 feet or greater depths. These logs generally show fine-grained geologic units with few sand beds. The depth to BFW was difficult to discern in available geophysical logs because of the lack of sand beds. The elevation of the BFW determined from logs were plotted on a base map (see **Figure A-46**). Contour lines of one hundred feet were drawn, but are variable based on well control.

Calculation of Base of Fresh Water and USDW

CRC has used geophysical logs to investigate the USDWs and the base of the USDWs. The calculation of salinity from 41 wells used by CRC is a four-step process (see **Table A-13** for list of wells and **Figure A-47** for well locations):

1. Convert measured density or sonic to formation porosity, using the following equation:

$$POR = \frac{(Rhom - RHOB)}{(Rhom - Rhof)} \quad (6)$$

where POR = formation porosity

Rhom = formation matrix density, g/cc; 2.65 g/cc is used for sandstones

RHOB = calibrated bulk density taken from well log measurements (g/cc)

Rhof = fluid density (g/cc); 1.00 g/cc is used for water-filled porosity

The equation to convert measured sonic slowness to porosity is:

$$POR = -1\left(\frac{\Delta tma}{2\Delta tf} - 1\right) - \sqrt{\left(\frac{\Delta tma}{2\Delta tf} - 1\right)^2 + \frac{\Delta tma}{\Delta tlog} - 1} \quad (7)$$

where POR = formation porosity

Δtma = formation matrix slowness (μs/ft); 55.5 μs/ft is used for sandstones

Δtf = fluid slowness (μs/ft); 189 μs/ft is used for water-filled porosity

Δtlog = formation compressional slowness from well log measurements (μs/ft)

2. Calculate apparent water resistivity using the Archie equation:

$$Rwah = \frac{POR^m R_t}{a} \quad (8)$$

where Rwah = apparent water resistivity (ohm-m)

POR = formation porosity

m = the cementation factor; 2 is the standard value

R_t = deep reading resistivity taken from well log measurements (ohm-m)

a = the archie constant; 1 is the standard value

3. Correct apparent water resistivity to a standard temperature of 75°F:

$$Rwahc = Rwah\frac{TEMP+6.77}{75+6.77} \quad (9)$$

where Rwahc = apparent water resistivity (ohm-m), corrected to surface temperature

TEMP = downhole temperature based on temperature gradient (°F)

4. Convert temperature-corrected apparent water resistivity to salinity (Davis 1988):

$$SAL\_a\_EPA = \frac{5500}{Rwahc} \quad (10)$$

where SALa_EPA = salinity from corrected Rwahc (parts per million [ppm])

The BFW and the USDW are shown on the geologic Cross Section A-A' (**Figure A-12**). **Figure A-48** displays a plan-view map of the base USDW elevation. The BFW and base of the lowermost USDW are at measure depths of approximately 1,100 feet and 2,500 feet, respectively.

2.7.3 Formations with USDWs

Formations with USDWs, from youngest to oldest, include alluvium, flood basin and intertidal deposits, alluvial fan deposits, older alluvium, Modesto Formation, Los Banos Alluvium, Tulare Formation, and fanglomerates. These formations, except for the Tulare Formation, are shown on **Figure A-45**. The Tulare Formation is not exposed at ground surface. The cumulative thickness of these formations increases from about 330 feet near the Coast Range foothills to about 2,000 feet just north of Tracy. Information regarding the water-bearing units and groundwater conditions was taken from several sources (Hotchkiss and Balding, 1971; Bertoldi et al., 1991; Davis et al., 1959) and sorted to agree with more recent geologic map compilation (Wagner et al., 1991).

Alluvium

The Alluvium (Q) includes sediments deposited in the channels of active streams as well as overbank deposits and terraces of those streams. They consist of unconsolidated silt, sand, and gravel. Sand and gravel zones in the younger alluvium are highly permeable and yield significant quantities of water to wells. The thickness of the younger alluvium in the Tracy Subbasin is less than 100 feet (DWR, 2006).

Flood Basin and Intertidal Deposits

The flood basin deposits (Dos Palos Alluvium [Qdp]) and intertidal deposits (Qi) are in the Delta portions of the Subbasin. These sediments consist of peaty mud, clay, silt, sand, and organic materials. Stream-channel deposits of coarse sand and gravel are also included in this unit. The flood basin deposits have low permeability and generally yield low quantities of water to wells due to their fine-grained nature. Flood basin deposits generally contain poor quality groundwater with occasional zones of fresh water. The maximum thickness of the unit is about 1,400 feet (DWR, 2006).

Alluvial Fan Deposits

Along the southern margin of the Subbasin, in the non-Delta uplands areas of the Subbasin are fan deposits (Qf) from the Coast Ranges. These deposits consist of loosely to moderately compacted sand, silt, and gravel deposited in alluvial fans during the Pliocene and Pleistocene ages. The fan deposits likely interfinger with the flood basin deposits. The thickness of these fans is about 150 feet (DWR, 2006).

Modesto Formation

The Modesto Formation (Qm) is located along the east side of the San Joaquin River and is slightly older that the alluvial fan deposits. The formation consists of granitic sands over stratified silts and sands. Near the southern margin of the Tracy Subbasin, there are small occurrences of Los Banos Alluvium (Qlb) and Older Alluvium (Qo) that are of similar age as the Modesto Formation (GEI, 2021).

Tulare Formation

The Tulare Formation is Pleistocene in age and consists of semi-consolidated, poorly sorted, discontinuous deposits of clay, silt, sand, and gravel. The Tulare Formation is not exposed at ground surface in the Tracy Subbasin. The Tulare Formation sand and gravel deposits are moderately permeable, and most of the larger agricultural, municipal, and industrial supply wells extract water from this formation. Wells completed in the Tulare Formation can produce up to 3,000 gallons per minute (gpm). The thickness of the Tulare Formation is about 1,400 feet (GEI 2021).

Within the Tulare Formation is the Corcoran Clay, one of the largest lakebed deposits in the San Joaquin Valley. The clay is about 60 to 100 feet thick. **Figure A-49** shows the lateral extent and structure of the Corcoran Clay. Near the southern edge of the Subbasin, the Corcoran Clay is apparently absent. The extent of the Corcoran Clay is not fully characterized to the west and north (Page, 1986) due to the lack of deep wells. Geologic sections indicate that the clay likely continues to the west, into the East Contra Costa Subbasin (GEI, 2007).

Marine Strata (Upper Markley Formation)

The upper Paleogene and Neogene sequence begin with the Valley Springs Formation, which represents fluvial deposits that blanket the entire southern Sacramento Basin. The unconformity at the base of the Valley Springs marks a widespread Oligocene regression and separates the more deformed Mesozoic and lower Paleogene strata below from the less deformed uppermost Paleogene and Neogene strata above. The Upper Markley Formation contains approximately 3,000 to 10,000 mg/L TDS water and is the lowermost USDW in the AoR (**Figure A-12**).

2.7.4 Geologic Cross Sections Illustrating Formations with USDWs

Geologic sections, as shown on **Figure A-45**, span the length of the Subbasin to illustrate the relationship of the geologic units. The geologic sections were originally prepared for the Tracy Subbasin Groundwater Management Plan (GEI, 2007) and were modified for the Tracy Subbasin GSP (GEI, 2021) to reflect additional information obtained since 2007. Lithologic information from well logs was normalized and digitized to generally conform with the Unified Soil Classification System (USCS). Lithology and well screens from groundwater monitoring wells constructed since the sections were created were also added to the geologic sections. The soil profiles show the subsurface relationships and location of the formations and coarse-grained sediments that comprise the principal aquifers. The cross sections show the sediment types, the approximate base of freshwater, and the estimated contact between the Tulare Formation sediments and younger formations. The cross sections also illustrate the location and extent of the Corcoran Clay (GEI, 2021).

Geologic cross section B-B' (**Figure A-50)** runs northwest-southeast through the non-Delta and Delta portions of the Tracy Subbasin. The Subbasin generally has low-permeability clays and silts (shown in brown color) near surface and permeable sediments (sands and gravels shown in light blue) scattered throughout the profile. Continuous layers of sand and gravels, other than one at the top of the Corcoran Clay have not been identified. The lack of continuous layers of sand and gravels is likely due to the nature of the river channels, and flood deposits associated

with these types of sediments. The Corcoran Clay (or its equivalent) seems to extend to the west and into the East Contra Costa Subbasin. In the southern non-Delta portion of the Subbasin, fine-grained sediments are more prevalent. Based upon groundwater levels and water quality information, the shallow aquifer is likely unconfined and separated from the deeper confined aquifer (GEI 2021).

Geologic cross section C-C' (**Figure A-51**) runs a northeast-southwest orientation across the Delta area. This geologic section illustrates the types of sediments, the estimated BFW, and the possible location of the Corcoran Clay (or its equivalent). Where the clay location is uncertain, no wells were present that penetrated deep enough to confirm its presence or absence. The BFW varies throughout the Subbasin and is shown on the sections. It is as shallow as -400 feet mean sea level (msl) to as much as -2,000 feet msl (GEI, 2021).

2.7.5 Principal Aquifers

The Tracy Subbasin has two principal aquifers that are separated by the Corcoran Clay. Where the clay is absent, which is the condition within most of the Delta area, only the Upper Aquifer is present. The Upper and Lower Aquifers combine where the Corcoran Clay is absent, near the southwestern portion of the subbasin adjacent to the foothills. In this area, the aquifers would be unconfined and are the Upper Aquifer. The Upper and Lower Aquifers also merge north of the Old River in the northern part of the Subbasin (GEI 2021).

Upper Aquifer

The Upper Aquifer is used by domestic, community water systems and for agriculture. The Upper aquifer also supports native vegetation where groundwater levels are less than 30 feet bgs (GEI, 2021). The Upper Aquifer is an unconfined to semi-confined aquifer. It is present above the Corcoran Clay and where the clay is absent. The Upper aquifer exists in the alluvial fan deposits, intertidal deposits, Modesto Formation, flood basin deposits, and the upper portions of the Tulare Formation.

There are multiple coarse-grained sediment layers that make up the unconfined aquifer; however, the water levels are generally similar. Generally, the aquifer confinement tends increase with depth becoming semi-confined conditions. There is also typically a downward gradient in the aquifers (Hotchkiss and Balding, 1971) in the non-Delta areas; the gradient ranges from a few feet bgs to as much as 70 feet bgs. The groundwater levels in the Upper Aquifer are usually 10 to 30 feet higher than in the Lower Aquifer. The groundwater levels In the Delta are typically at sea level and artesian flowing wells are common in the center of the islands (Hydrofocus, 2015).

The hydraulic characteristics of the unconfined aquifer are highly variable. USGS estimated horizontal hydraulic conductivity values for organic sediments ranging from 0.0098 feet per day (ft/d) to 133.86 ft/d (Hydrofocus, 2015). Wells in the unconfined aquifer produce 6 to 5,300 gpm. The transmissivity of the unconfined aquifers ranges from 600 gallons per day per foot (gpd/ft) to more than 2,300 gpd/ft. The storativity is about 0.05 (GEI, 2021).

Water quality in the Upper Aquifer is mostly transitional, with no single predominant anion. Most waters are characterized as sulfate bicarbonate and chloride bicarbonate type (Hotchkiss and Balding, 1971). The TDS of these transitional water ranges from 400 to 4,200 mg/L. Nitrate is generally high in the Upper aquifer in the non-Delta portions of the Subbasin. Nitrate is generally low in the Delta portions of the Subbasin (GEI, 2021).

Lower Aquifer

The Lower Aquifer is typically used by community water systems (City of Tracy) and agriculture. The Lower Aquifer is mainly comprised of the lower portions of the Tulare Formation below the Corcoran Clay and extends to the BFW. The clay is present in the southern third of the Subbasin; the clay's extent to the west and north is uncertain and has been estimated to have a vertical permeability ranging from 0.01 to 0.007 ft/d (Burow et al., 2004).

The groundwater levels are generally deeper than water levels in the Upper Aquifer (Hotchkiss and Balding 1971). Groundwater levels in the confined aquifer are about -25 to -75 feet msl. The groundwater levels are normally 60 to 200 feet above the top of the Corcoran Clay.

Wells in the Lower Aquifer produce about 700 to 2,500 gpm. The transmissivity typically ranges from 12,000 to 37,000 gpd/ft, but can be 120,000 gpd/ft. The storage coefficient or storativity has been measured to be 0.0001 (Padre, 2004).

Water quality in the Lower Aquifer in the western portions are chloride type water but mostly transitional type of sulfate chloride near the valley margins and sulfate bicarbonate and bicarbonate sulfate near the San Joaquin River (Hotchkiss and Balding, 1971). In general, the TDS ranges from 400 to 1,600 mg/L. Nitrate is typically low in the Lower Aquifer. Wells completed below the Corcoran Clay sometimes have elevated levels of sulfate and TDS above the drinking water maximum contaminant levels (MCLs). Only at one deep location, east of Tracy, are chloride levels elevated (GEI, 2021).

2.7.6 Potentiometric Maps

The Tracy Subbasin GSP (GEI, 2021) used groundwater level measurements in over 226 wells, which have been reported to DWR's CASGEM or Water Data Library systems. To evaluate groundwater levels, the GSP only used wells with known total depths and construction details so that the wells were assigned to a principal aquifer. To supplement data from these wells, additional monitoring wells were located that were being used for other regulatory programs.

Upper Aquifer

Groundwater elevations in the Delta area are typically below sea level because the ground surface in the islands have subsided to below sea level; the drains within the island keep groundwater levels bgs to allow for farming. **Figure A-52** shows a schematic profile for groundwater surfaces that are expected at the islands. Although each island has distinct groundwater elevations, there are similar hydraulics on all islands. Groundwater elevations are higher near the island edges (adjacent to waterways) and deepen equivalent with the deepest land surface and drain. Groundwater elevations in the islands are managed by the elevations of the

drains and canals. There is very little, if any, pumping of wells for agriculture. Because drains and canals control the groundwater elevations, groundwater contours are not developed/monitored for the Delta islands (GEI, 2021).

In the non-Delta areas west of the San Joaquin River, groundwater contours for the Upper Aquifer indicate groundwater elevations are highest near the Coast Ranges and decrease toward the Delta. Flow directions indicate that recharge areas are present along the foothills and that groundwater discharges into the Old River and/or Tom Paine Slough (**Figure A-53**). Groundwater gradients in the non-Delta portions of the Subbasin are the steepest, at approximately 0.008 ft/ft. East of the San Joaquin River, near Lathrop, the river recharges the Upper Aquifer and flows toward a pumping depression near Stockton. Groundwater contours at the southeastern edge of the Subbasin are perpendicular to the Stanislaus-San Joaquin County line, suggesting that there is no flow in the Upper Aquifer between the subbasins, other than the areas of the Delta Mendota Subbasin north of the County line, where water apparently flows into and out of both subbasins.

Lower Aquifer

The Corcoran Clay extends throughout the non-Delta areas and only slightly into the Delta area, at Union Island. Groundwater contours for the Lower Aquifer were developed using data from the CASGEM monitoring wells that are constructed below the Corcoran Clay and supplemented by data from municipal wells (**Figure A-54**). Groundwater monitoring well data were used from the adjacent Delta Mendota Subbasin (GEI, 2021).

Groundwater elevation contours in the Lower Aquifer imply groundwater is entering the subbasin from the south (Delta Mendota Subbasin) and from the east (Eastern San Joaquin Subbasin). Pumping in the vicinity of the City of Tracy has apparently modified this overall regional flow, resulting in a pumping depression towards the City of Tracy. The groundwater levels are expected to be at sea level near the northern edge of the Corcoran Clay extent (GEI, 2021).

The groundwater gradient in fall 2019 from the Delta Mendota and the Eastern San Joaquin subbasins is estimated to be 0.0009 ft/ft into the Tracy Subbasin. Due to the pumping depression, the gradient increases around the City of Tracy. The gradient near the western edge of the subbasin cannot be determined to the lack of monitoring wells constructed below the Corcoran Clay (GEI, 2021).

2.7.7 Water Supply Wells

The California State Water Resources Control Board Groundwater Ambient Monitoring Assessment Program (GAMA), and the Department of Water Resources (DWR) public databases were searched to identify any water supply wells within a one-mile radius of the AOR. A total of 155 water supply wells were identified within 1 mile of the AoR. A map of well locations and table of information are found in **Figure A-55** and the attached **Table A-14**, respectively.

Groundwater in the Subbasin is used for municipal, industrial, irrigation, domestic, stock watering, frost protection, and other purposes. The number of water wells is based on well logs

filed and contained within public records may not reflect the actual number of active wells because many of the wells contained in files may have been destroyed and others may not have been recorded.

There are many more wells in the non-Delta areas, south of the Old River, than in the Delta area of the Subbasin. The depths of wells are generally deeper in the non-Delta portion of the Subbasin as compared to the Delta portion of the Subbasin. Typically, the domestic wells are constructed to shallower depths than the production wells. The municipal wells are generally constructed deeper than either the domestic or production wells (GEI, 2021). The known water well depths and other information are included in the attached **Table A-14**. Some well depths are unknown, but all water supply wells completion intervals are expected to be much shallower than the injection zone.

2.8 Geochemistry [40 CFR 146.82(a)(6)]

2.8.1 Formation Geochemistry

Mokelumne River Formation

As noted in the mineralogy section (Section 2.4.1).

Capay Shale

As noted in the mineralogy section (Section 2.4.1).

H&T Shale

As noted in the mineralogy section (Section 2.4.1).

2.8.2 Fluid Geochemistry

The Mokelumne River Formation contains only saline water within the AoR. No water samples from the Mokelumne River Formation exist within the AoR, so samples from the Rio Vista Gas Field and King Island/PGE Gas Field have been used (see **Figure A-37** for well locations).

The well Midland_Fee_Water_Injection_1 was sampled in 1980 in the Rio Vista Gas Field. The measurement of TDS for the sample is 13,889.4 mg/L. The complete water chemistry is shown in **Figure A-56**.

The well Piacentine_2-27 was sampled in 2013 in the King Island/PGE Gas Field. The measurement of TDS for the sample is 14,000 mg/L. The complete water chemistry is shown in **Figure A-57**.

Salinity calculations were also performed on logs from wells within the AoR, and these showed TDS in the Mokelumne River Formation of approximately 14,000 to 16,000 ppm. A 10% uncertainty was applied to the measured water sample TDS, which resulted in a TDS of 15,500 ppm being used for the computational model. Formation fluid properties at reservoir conditions are shown in **Table A-15**.

No gas is present in the Mokelumne River Formation within the boundaries of the AoR, so no hydrocarbon analysis is available.

2.8.3 Fluid-Rock Reactions

Mokelumne River Formation

Mineralogy and formation fluid interactions have been assessed for the Mokelumne River Formation. The following applies to potential reactions associated with the CO_2 injectate:

- The Mokelumne River Formation has a negligible quantity of carbonate minerals and is instead dominated by quartz and feldspar. These minerals are stable in the presence of CO_2 and carbonic acid and any dissolution or changes that occur will be on grain surfaces.
- The water within the Mokelumne River Formation contains minimal calcium and magnesium cations, which would be expected to react with the CO_2 to form calcium-bearing minerals in the pore space.

Capay Shale

There is no fluid geochemistry analysis for the Capay Shale. Given the low permeability of the rock and the low carbonate content, the Capay Shale is not expected to be impacted by the CO_2 injectate.

H&T Shale

There is no fluid geochemistry analysis for the H&T Shale. Given the low permeability of the rock and the low carbonate content, the H&T Shale is not expected to be impacted by the CO_2 injectate.

Geochemical Modeling

Geochemical modeling for the injectate streams, detailed in Section 7.2 of this document, was conducted using the USGS geochemical modeling software PHREEQC (ph-REdox-Equilibrium) to understand the potential interactions of the injectates with the injection zone and upper confining zone formation mineralogy and fluids. The model was set up using the formation fluid data referenced in Section 2.8.2, and the injection zone and upper confining zone mineralogy data referenced in Section 2.4.1.

Geochemical modeling indicates that for either composition, minimal amounts of minerals will dissolve and precipitate, with expected net change in molar mass of 1.5 to 2%, and as such the formation and formation fluids are compatible with the proposed injectates.

Details of the modeling methodology and results can be found in the attached appendix – “CTV III Geochemical Modeling”.

CTV will review and confirm the geochemical modeling results at pre-operational testing based on injectate sampling to ensure that they are consistent with the model inputs.

2.9 Other Information (Including Surface Air and/or Soil Gas Data, if Applicable)

No additional information to add.

2.10 Site Suitability [40 CFR 146.83]

Sufficient data from both wells and seismic demonstrate the integrity through lateral continuity of the reservoir as well as the confining zone. Regional mapping completed by West Coast Regional Carbon Sequestration Partnership (WESTCARB), CGS, and the National Energy and Technology Lab (NETL) support our local stratigraphy, both indicating lateral continuity and regional thickness across the AoR (Downey, 2010). This study covers formations with sequestration and seal potential from southern Sutter County down to the Stockton Arch Fault San Joaquin County, encompassing an area far beyond the AoR presented in Attachment B.

The vertical confinement and laterally continuous reservoir, described in Attachment A, will compensate for the CO_2 due to it being located within an open system. The Capay Shale is a continuous shale, as described in Section 2.2.2, and will guide the lateral dispersion of CO_2 across the AoR (**Figure A-58**). Surrounding oil and gas fields in the area demonstrate adequate seal capacity in the upper confining zone and surrounding faults. Corrosion resistant alloy (CRA) will be used for completion of the injection and monitoring wells, inhibiting any reaction between CO_2 and wellbores.

Thickness maps and petrophysics demonstrate confinement based on the upper confining zones laterally continuity, low permeability and thickness. A minor fault does extend within the CO_2 plume; however, thickness maps support an adequate seal across this offset. Pressures along bounding faults will be estimated using computational modeling and in-zone monitoring wells to mitigate the possibility of fault reactivation.

Due to the regional continuity and low permeability of the upper confining zone (Capay Shale), no secondary confinement is necessary; however, another shale barrier does exist above the Domengine Formation monitoring sand. This creates another impermeable zone of confinement separating the injection zone from the USDW.

CTV's estimates storage for the project area is up to 70.7 million metric tons (MMT) of CO_2. This value was arrived at through computational modeling as described below.

As discussed in **Attachment B: Area of Review and Corrective Action Plan**, a dynamic model was generated for each target injection zone with data from the static model (structure, porosity, absolute permeability, net to gross ratio, facies), special core analysis (relative permeability and capillary pressure), pressure, volume, temperature (PVT) analysis (fluid PVT), geochemical analysis (water salinity). Injector locations are based on geologic interpretation, petrophysical properties, and economic optimization. Injection rates were analyzed with flexibility to handle offset well failure during the project period. Injectors were also designed with a maximum allowable injection pressure limit. To assure storage site safety during the injection period, reservoir pressure was also controlled by critical pressure. Dynamic model results predicted a storage volume of 70.6 MMT at 28 years, using six CO_2 injection wells.

3. AoR and Corrective Action

CTV's AoR and Corrective Action plan pursuant to 40 CFR 146.82(a)(4), 40 CFR 146.82(a)(13) and 146.84(b), and 40 CFR 146.84(c) describes the process, software, and results to establish the AoR, and the wells that require corrective action.

AoR and Corrective Action GSDT Submissions
GSDT Module: AoR and Corrective Action ***Tab(s):*** All applicable tabs Please use the checkbox(es) to verify the following information was submitted to the GSDT: ☒ Tabulation of all wells within AoR that penetrate confining zone ***[40 CFR 146.82(a)(4)]*** ☒ AoR and Corrective Action Plan *[40 CFR 146.82(a)(13) and 146.84(b)]* ☒ Computational modeling details ***[40 CFR 146.84(c)]***

4. Financial Responsibility

CTV's Financial Responsibility demonstration pursuant to 140 CFR 146.82(a)(14) and 40 CFR 146.85 is met with a line of credit for Injection Well Plugging and Post-Injection Site Care and Site Closure and insurance to cover Emergency and Remedial Responses.

Financial Responsibility GSDT Submissions
GSDT Module: Financial Responsibility Demonstration ***Tab(s):*** Cost Estimate tab and all applicable financial instrument tabs Please use the checkbox(es) to verify the following information was submitted to the GSDT: ☐ Demonstration of financial responsibility ***[40 CFR 146.82(a)(14) and 146.85]***

5. Injection and Monitoring Well Construction

CTV plans to drill six new injectors for the CTV III storage project. New injection wells C1, C2, E1, E2, W1, and W2 are planned and designed specifically for CO_2 sequestration purposes. These wells will target selective intervals within the injection zone to optimize plume development and injection conformance. Additionally, three new monitoring wells are required to support the storage project. M1 and M2 will be injection zone monitoring wells, and D1 will be an above-zone monitoring well. Two USDW monitoring wells, US1 and US2, will also be constructed prior to injection. **Figure A-59** shows the locations of the new wells.

All planned new wells will be constructed with components that are compatible with the injectate and formation fluids encountered such that corrosion rates and cumulative corrosion over the duration of the project are acceptable. The proposed well materials will be confirmed based on actual CO_2 composition such that material strength is sufficient to withstand all loads encountered throughout the life of the well with an acceptable safety factor incorporated into the design. Casing points will be verified by trained geologists using real-time drilling data such as logging while drilling (LWD) and mud logs to ensure non-endangerment of USDWs. Due to the depth of the base of USDW, an intermediate casing string will be used to isolate the USDW. Cementing design, additives, and placement procedures will be sufficient to ensure isolation of the injection zone and protection of USDW using cementing materials that are compatible with injectate, formation fluids, and subsurface pressure and temperature conditions.

Appendix C-1: Injection and Monitoring Well Schematics provides casing diagram figures for all injection and monitoring wells with construction specifications and anticipated completion details in graphical and/or tabular format.

Injection wells will have wellhead equipment sufficient to shut off injection at surface. The project does not anticipate risk factors that warrant downhole shut-off devices, such as high temperature, high pressure, presence of hydrogen sulfide, proximity to populated areas, or high likelihood of damage to the wellhead.

5.1 Proposed Stimulation Program [40 CFR 146.82(a)(9)]

There are no proposed stimulation programs currently.

5.2 Construction Procedures [40 CFR 146.82(a)(12)]

Injection and monitoring wells will be drilled during pre-operational testing, and no abnormal drilling and completion challenges are anticipated. The drilling histories of nearby wells provide key information to drilling professionals and identify the expected conditions to be encountered. The wells will be constructed with objectives to achieve target CO_2 injection rates, to prevent migration of fluids out of the injection zone, to protect the shallow formations, and to allow for monitoring, as described by the following:

- Well designs will be sufficient to withstand all anticipated load cases including safety factors.

- Multiple cemented casing strings will protect shallow USDW-bearing zones from contacting injection fluid.
- All casing strings will be cemented in place with volume sufficient to place cement to surface using industry-proven recommended practices for slurry design and placement
- Cement bond logging (CBL) will be used to verify presence of cement in the production casing annulus through and above the confining layer.
- Mechanical integrity testing (MIT) will be performed on the tubing and the tubing/casing annulus.
- Upper completion design enables monitoring devices to be installed downhole, cased hole logs to be acquired and MIT to be conducted.
- All wellhead equipment and downhole tubulars will be designed to accommodate the dimensions necessary for deployment of monitoring equipment such as wireline-conveyed logging tools and sampling devices.
- Realtime surface monitoring equipment with remote connectivity to a centralized facility and alarms provides continual awareness to potential anomalous injection conditions.
- Annular fluid (packer fluid) density and additives to mitigate corrosion provide additional protection against mechanical or chemical failure of production casing and upper completion equipment.

Well materials used will be compatible with the CO_2 injectate and will limit corrosion.

- Wellhead: stainless steel or other corrosion resistant alloy.
- Casing: 13Cr L-80 or other corrosion resistant alloy in specified sections of production string (i.e., flow-wetted casing).
- Cement: Portland cement has been used extensively in enhanced oil recovery (EOR) injectors. Data acquired from existing wells supports that the materials are compatible with CO_2 where good cement bond between formation and casing exists.
- Tubing: 13Cr L-80 or other corrosion resistant alloy.
- Packer: corrosion resistant alloy and hardened elastomer.

Well materials follow the following standards:

- API Spec 5CT / ISO 11960 – Specification for Casing and Tubing
- API Spec 5CRA / ISO 13680 – Specification for Corrosion-Resistant Alloy Seamless Tubes for use as Casing, Tubing, and Coupling Stock
- API Spec 10A / ISO 10426-1 – Cements and Materials for Cementing
- API Spec 11D1 / ISO 14310 – Downhole Equipment – Packers and Bridge Plugs
- API Spec 6A / ISO 10423 – Specification for Wellhead and Tree Equipment

As required by §146.86(b)(1), casing and tubing material sizes, thicknesses, and grades were selected by evaluating the proposed well design internal pressures, external pressures, and axial loads that the well will be expected to withstand throughout construction and operations. Temperature effects under static or dynamic conditions, based on load scenario, have been incorporated into the modelling results. The design results indicate the materials selected have strengths sufficient to withstand all worst-case load scenarios and include industry-standard safety factors.

CTV will confirm that the properties of the CO_2 stream are consistent with design assumptions based on pre-op injectate sampling.

5.2.1 Casing and Cementing

Well-specific casing diagrams including casing specifications are presented in **Appendix C-1: Injection and Monitoring Well Schematics** to meet the requirements of 40 CFR 146.86(b)(1)(iv). These specifications allow for the safe operation at bottomhole injection conditions not to exceed the maximum injection pressures specified in the Operational Procedures Appendix.

The injection zone pressure is neither significantly depleted nor over-pressured, and the temperature is approximately 151°F. These conditions are not extreme, and standard cementing and casing best practices are sufficient to ensure successful placement and isolation. Industry standard practices and procedures for designing and placing primary cement in the casing annuli will be used to ensure mechanical integrity of cement and casing. Staged cementing is not an anticipated requirement.

Surface casing will be designed to protect the base of fresh water at a depth of around 400 feet TVD. Casing is planned to be set at 600 feet. Class G portland cement—an API grade cement—meets API standard specifications for this application. Accelerator additives will be used to speed up the thickening time of the cement, lost circulation additive may be used as macro plugging material, and extender additives may be used to protect shallow formations by reducing the weight of cement.

The intermediate casing will be set at a depth sufficient to cover the USDW. The depth to the base of USDW is expected to be encountered at approximately 2,541 feet TVD. Casing will be set or below 2,550 feet TVD to ensure protection of the USDW. Class G portland cement will be circulated to surface with retarding additives (depending on pump time) to decrease the speed of cement hydration as well as friction reducer additives to improve upon the flow properties of the cement slurry. Anti-foam additives, fluid loss additives, lost circulation material, dispersants, and extenders may also be considered based on industry best practices for slurry design to ensure effective placement of cement.

The long casing string will be set 120 feet into the H&T Shale. A combination of Class G portland lead slurry and Class G portland tail slurry with CO_2 resistant additives will be used to cement the long string. The tail slurry will be circulated from TD into the confining layer. The lead slurry will provide isolation of the long string casing in and above the confining layer to surface. Anti-foam additives, fluid loss additives, lost circulation material, dispersants, and extenders may also be considered based on industry best practices for slurry design to ensure

effective placement of cement, along with considering the addition of silica flour for strength retrogression.

Operational parameters acquired throughout the pressure pumping operation will be used to compare modeled versus actual pressure and rate. The presence of circulated cement at surface will also be a primary indicator of effective cement placement. Cement evaluation logging will be conducted to confirm cement placement and isolation.

5.2.2 Tubing and Packer

The information in the tables provided in **Appendix C-1: Injection and Monitoring Well Schematics** is representative of completion equipment that will be used and meets the requirements at 40 CFR 146.86(c). Tubing and packer selection and specifications will be determined during pre-operational testing and will be sufficient to withstand all load scenarios considering internal pressure, external pressure, axial loading, and temperature effects.

5.2.3 Annular Fluid

4% KCl completion fluid treated with corrosion inhibitor and biocide will be circulated in the tubing/casing annulus at the time of tubing installation. The corrosion inhibitor and biocide additives will be compatible with the wellbore environment and bottomhole temperatures to prevent internal corrosion of the 7-inch casing and external corrosion of the tubing.

5.2.4 Injectate and Formation Fluid Properties

CTV is planning to construct a carbon capture and sequestration "hub" project (i.e., a project that collects CO_2 from multiple sources over time and injects the CO_2 stream(s) via a Class VI UIC permitted injection well(s)). Therefore, CTV is currently considering multiple sources of anthropogenic CO_2 for the project. CO_2 will be sourced from a blue hydrogen and ammonia plant (up to 377,000 tonnes per annum) that will be located in proximity to the storage site, direct air capture and other CO_2 sources in the project area. Minor constituents associated with the CO_2 stream may include, for example, water content (<25 lb/mmscf), oxygen, hydrogen sulfide (H_2S), and SO_x compounds. The CO_2 stream will be sampled at the transfer point from the source and analyzed according to the analytical methods described in Table 4 of the QASP and Table 1 of **Attachment C: Testing and Monitoring Plan**.

The anticipated injection temperature at the wellhead is 90 to 130°F.

The Injectate 1 and Injectate 2 compositions and properties are detailed in Section 7.2.

No corrosion is expected in the absence of free phase water provided that the entrained water is kept in solution with the CO_2. This is ensured by the <25 lb/mmscf injectate specification limit, and this specification will be a condition of custody transfer at the capture facility. For transport through pipelines, which typically use standard alloy pipeline materials, this specification is critical to the mechanical integrity of the pipeline network, and out of specification product will be immediately rejected. Therefore, all product transported through pipeline to the injection wellhead is expected to be dry-phase CO_2 with no free-phase water present.

Injectate water solubility will vary with depth and time as temperature and pressures change. The water specification is conservative to ensure water solubility across super-critical operating ranges. CRA tubing will be used in the injection wells to mitigate any potential corrosion impact should free-phase water from the reservoir become present in the wellbore, such as during shut-in events when formation liquids, if present, could backflow into the wellbore. CTV may further optimize the maximum water content specification prior to injection based on technical analysis.

Geochemical analysis and properties of the connate formation water has been provided in Section 2.8. Water geochemistry representative of the project area does not indicate corrosiveness to standard cement and casing materials. A formation water analysis will be obtained during pre-operational testing and reviewed to ensure compatibility with well construction materials.

5.2.5 Alarms and Shut-Off Devices

As described in the Testing and Monitoring Plan, injection wells will be configured with real-time injection rate, injection pressure, and annular pressure monitoring and alarms. The Operating Procedures plan details the maximum injection rate and pressure thresholds for alarms and shut-off devices.

A surface shut-off valve will be installed on the wellhead and configured with automation and communication to the Central Control Facility (CCF). The valve will be used by the CCF operator remotely to respond to an emergency by shutting in the well. The valve will be configured to automatically shut-in the well if tubing or annular alarm thresholds are exceeded.

The project does not anticipate risk factors that warrant downhole shut-off devices, such as high temperature, high pressure, presence of hydrogen sulfide, proximity to populated areas, or high likelihood of damage to the wellhead.

6. Pre-Operational Logging and Testing

CTV has attached a pre-operational logging and testing plan pursuant to 40 CFR 146.82(a)(8) and 40 CFR 146.87.

Pre-Operational Logging and Testing GSDT Submissions
GSDT Module: Pre-Operational Testing ***Tab(s):*** Welcome tab Please use the checkbox(es) to verify the following information was submitted to the GSDT: ☒ Proposed pre-operational testing program ***[40 CFR 146.82(a)(8) and 146.87]***

7. Well Operation

7.1 Operational Procedures [40 CFR 146.82(a)(10)]

CTV has provided detailed operational procedures for each injection well. These procedures and parameters are provided for all injectors in the Operational Procedures document attached with this application.

7.2 Proposed Carbon Dioxide Stream [40 CFR 146.82(a)(7)(iii) and (iv)]

CTV is planning to construct a carbon capture and sequestration "hub" project (i.e., a project that collects CO_2 from multiple sources over time and injects the CO_2 stream(s) via a Class VI UIC permitted injection well(s)). Therefore, CTV is currently considering multiple sources of anthropogenic CO_2 for the project. CO_2 will be sourced from a blue hydrogen and ammonia plant (up to 377,000 tonnes per annum) that will be located in proximity to the storage site, direct air capture and other CO_2 sources in the project area. CTV would expect the CO_2 stream will be sampled at the transfer point from the source and analyzed according to the analytical methods described in Table 4 of the QASP and Table 1 of **Attachment C: Testing and Monitoring Plan**. Should the injectate not meet the minimum requirements, it will be rejected.

The anticipated injection temperature at the wellhead is 90 to 130°F.

For the purposes of geochemical modeling, CO_2 plume modeling, AoR determination, and well design, two major types of Injectate compositions were considered based on the source:

- Injectate 1: A potential injectate stream composition from a direct air capture (DAC) or a pre-combustion source (such as a blue hydrogen facility) or a post-combustion source (such as a natural gas fired power plant or steam generator). The primary impurity in the injectate is nitrogen.
- Injectate 2: A potential injectate stream composition from a biofuel capture source (such as a biodiesel plant that produces biodiesel from a biologic source feedstock) or from an oil and gas refinery. The primary impurity in the injectate is light end hydrocarbons (methane and ethane).

The compositions for these two injectates are shown in **Table A-16**, and are based on engineering design studies and literature.

For geochemical and plume modeling scenarios, these injectate compositions were simplified to a 4-component system, shown in **Table A-17**, and then normalized for use in the modeling. The 4-component simplified compositions cover 99.9% by mass of Injectates 1 and 2 and cover particular impurities of concern (H_2S and SO_2). The estimated properties of the injectates at downhole conditions are specified in **Table A-18**.

No corrosion is expected in the absence of free-phase water provided that the entrained water is kept in solution with the CO_2. This is ensured by the <25 lb/mmscf injectate specification limit, and this specification will be a condition of custody transfer at the capture facility. For transport through pipelines, which typically use standard alloy pipeline materials, this specification is

critical to the mechanical integrity of the pipeline network, and out of specification product will be immediately rejected. Therefore, all product transported through pipeline to the injection wellhead is expected to be dry-phase CO_2 with no free-phase water present.

Injectate water solubility will vary with depth and time as temperature and pressures change. The water specification is conservative to ensure water solubility across super-critical operating ranges. CRA tubing will be used in the injection wells to mitigate any potential corrosion impact should free-phase water from the reservoir become present in the wellbore, such as during shut-in events when formation liquids, if present, could backflow into the wellbore. CTV may further optimize the maximum water content specification prior to injection based on technical analysis.

8. Testing and Monitoring

CTV's Testing and Monitoring plan pursuant to 40 CFR 146.82 (a) (15) and 40 CFR 146.90 describes the strategies for testing and monitoring to ensure protection of the USDW, injection well mechanical integrity, and plume monitoring.

Testing and Monitoring GSDT Submissions
GSDT Module: Project Plan Submissions ***Tab(s):*** Testing and Monitoring tab Please use the checkbox(es) to verify the following information was submitted to the GSDT: ☒ Testing and Monitoring Plan [40 CFR 146.82(a)(15) and 146.90]

9. Injection Well Plugging

CTV's Injection Well Plugging Plan pursuant to 40 CFR 146.92 describes the process, materials and methodology for injection well plugging.

Injection Well Plugging GSDT Submissions
GSDT Module: Project Plan Submissions ***Tab(s):*** Injection Well Plugging tab Please use the checkbox(es) to verify the following information was submitted to the GSDT: ☒ Injection Well Plugging Plan [40 CFR 146.82(a)(16) and 146.92(b)]

10. Post-Injection Site Care (PISC) and Site Closure

CTV has developed a Post-Injection Site Care and Site Closure plan pursuant to 40 CFR 146.93 (a) to define post-injection testing and monitoring.

At this time CTV is not proposing an alternative PISC time frame.

PISC and Site Closure GSDT Submissions
GSDT Module: Project Plan Submissions ***Tab(s):*** PISC and Site Closure tab Please use the checkbox(es) to verify the following information was submitted to the GSDT: ☒ PISC and Site Closure Plan [40 CFR 146.82(a)(17) and 146.93(a)]
GSDT Module: Alternative PISC Timeframe Demonstration ***Tab(s):*** All tabs (only if an alternative PISC timeframe is requested) Please use the checkbox(es) to verify the following information was submitted to the GSDT: ☐ Alternative PISC timeframe demonstration ***[40 CFR 146.82(a)(18) and 146.93(c)]***

11. Emergency and Remedial Response

CTV's Emergency and Remedial Response plan pursuant to 40 CFR 164.94 describes the process and response to emergencies to ensure USDW protection.

Emergency and Remedial Response GSDT Submissions
GSDT Module: Project Plan Submissions ***Tab(s):*** Emergency and Remedial Response tab Please use the checkbox(es) to verify the following information was submitted to the GSDT: ☐ Emergency and Remedial Response Plan *[40 CFR 146.82(a)(19) and 146.94(a)]*

12. Injection Depth Waiver and Aquifer Exemption Expansion

No depth waiver or Aquifer Exemption expansion is being requested as part of this application

Injection Depth Waiver and Aquifer Exemption Expansion GSDT Submissions
GSDT Module: Injection Depth Waivers and Aquifer Exemption Expansions ***Tab(s):*** All applicable tabs Please use the checkbox(es) to verify the following information was submitted to the GSDT: ☐ Injection Depth Waiver supplemental report ***[40 CFR 146.82(d) and 146.95(a)]*** ☐ Aquifer exemption expansion request and data ***[40 CFR 146.4(d) and 144.7(d)]***

13. References

Bartow. 1985. Maps showing Tertiary stratigraphy and structure of the Northern San Joaquin Valley, California. United States Geological Survey (USGS).

Berkstresser, C.F. Jr. 1973. Base of Fresh Ground-Water -- Approximately 3,000 micromhos -- in the Sacramento Valley and Sacramento-San Joaquin Delta, California. U.S. Geological Survey Water-Resource Inv. 40-73. 1973

Bertoldi, G., R. Johnston, and K. Evenson. 1991. Groundwater in the Central Valley, California - A Summary Report. USGS Professional Paper 1401-A. https://doi.org/10.3133/pp1401A.

Beyer, L.A. Summary of Geology and Petroleum Plays Used to Assess Undiscovered Recoverable Petroleum Resources of Sacramento Basin Province, California. United States Department of the Interior Geological Survey, 1988.

Burow, K.R., J.L. Shelton, J.A. Hevesi, and G.S. Weissmann. 2004. Hydrologic Characterization of the Modesto Area, San Joaquin Valley, California. Preliminary Draft. U.S. Geological Survey. Water-Resources Investigation Report. Prepared in cooperation with Modesto Irrigation District. Sacramento, California.

B. Wetenhall et al. / International Journal of Greenhouse Gas Control 30 (2014) 197–211

California Department of Water Resources (DWR). 1995. Sacramento Delta San Joaquin Atlas.

California DWR. 2006. California's Groundwater, Bulletin 118. San Joaquin Valley Groundwater Basin Tracy Subbasin. Last updated November 2021.

Chiquet, Pierre & Daridon, J.L. & Broseta, Daniel & Thibeau, S.. (2009). CO2/Water Interfacial Tensions under Pressure and Temperature and Conditions of CO2 Geological Storage. Energy Convers. Manage.. 50. 431-431.

Davis G.H., J.H. Green, S.H. Olmstead, and D.W. Brown 1959. Ground water conditions and storage capacity in the San Joaquin Valley, California. U.S. Geological Survey Water Supply Paper No. 1469, 287 p.

Davis, K.E., 1988. *Survey of Methods to Determine Total Dissolved Solids Concentrations*. U.S. Environmental Protection Agency Underground Injection Control Program. Prepared by Ken E. Davis Associates under subcontract to Engineering Enterprises, INC. EPA LOE Contract No. 68-03-3416, Work Assignment No. 1-0-13, Keda Project No. 30-956.

Downey, C. and J. Clinkenbeard. 2006. An overview of geologic carbon sequestration potential in California, California Energy Commission, PIER Energy-Related Environmental Research Program.

Downey, C. and J. Clinkenbeard. 2010. Preliminary Geologic Assessment of the Carbon Sequestration Potential of the Upper Cretaceous Mokelumne River, Starkey, and Winters Formations – Southern Sacramento Basin, California. California Geological Survey.

Fjaer, E., R.M. Holt, A.M. Raaen, and P. Horsrud. (2008). *Petroleum Related Rock Mechanics* (2nd ed.). Elsevier Science.

GEI Consultants, Inc. (GEI) 2007. Tracy Regional Groundwater Management Plan.

GEI. 2021. Tracy Subbasin Groundwater Sustainability Plan. November 1, 2021.

Graham, S.A., C. McCloy, M. Hitzman, R. Ward, and R. TurnerR. 1984. Basin Evolution During Chance from Convergent to Transform Continental Margin in Central California. The American Association of Petroleum Geologists Bulletin V.68 No. 3.

Haeri, Foad & Tapriyal, Deepak & Sanguinito, Sean & Fuchs, Samantha & Shi, Fan & Dalton, Laura & Baltrus, John & Howard, Bret & Matranga, Christopher & Crandall, Dustin & Goodman, Angela. (2020). CO2-Brine Contact Angle Measurements on Navajo, Nugget, Bentheimer, Bandera Brown, Berea, and Mt. Simon Sandstones. Energy & Fuels. XXXX. 10.1021/acs.energyfuels.0c00436.

Hotchkiss, W.R. and G.O. Balding. 1971. Geology, hydrology, and water quality of the Tracy-Dos Palos area, San Joaquin Valley, California. U.S. Geological Survey. Open-File Report. Hotchkiss and Balding. 1971.

Heidbach, O., M. Rajabi, X. Cui, K. Fuchs, B. Müller, J. Reinecker, K. Reiter, M. Tingay, F. Wenzel, F. Xie, M.O. Ziegler, M.-L. Zoback, and M.D. Zoback (2018): The World Stress Map database release 2016: Crustal stress pattern across scales. Tectonophysics, 744, 484-498, doi:10.1016/j.tecto.2018.07.007

Heidbach, O., M. Rajabi, K. Reiter, M. Ziegler, and WSM Team. 2016. World Stress Map Database Release 2016. GFZ Data Services, doi:10.5880/WSM.2016.001

Hydrofocus. 2015. San Joaquin County and Delta Quality Coalition Groundwater Quality Assessment Report, April 27, 2015.

IEAGHG. 2011. Effects of impurities on geological storage of CO_2. International Energy Agency Greenhouse Gas programme

Ingram G.M., J.L. Urai, and M.A. Naylor. 1997. in Hydrocarbon Seals: Importance for Exploration and Production, Sealing processes and top seal assessment, Norwegian Petroleum Society (NPF) Special Publication, eds Moller-Pedersen P., Koestler A. G. 7, pp 165–175.

Ingram, G. and J. Urai. 1999. Top-seal leakage through faults and fractures: the role of mudrock properties. Geological Society, London, Special Publications. 158. 125-135. 10.1144/GSL.SP.1999.158.01.10.

Johnson, D.S. 1990. Depositional environment of the Upper Cretaceous Mokelumne River Formation, Sacramento Basin. California. American Assoc. of Petroleum Geologists Bulletin 74: 5 1990: 686 p.

Juhasz, I. 1979. The Central Role Of Qv And Formation-water Salinity In The Evaluation Of Shaly Formations*. *The Log Analyst*, 20.

Leong, J.K. and J.R. Tenzer. 1994. Production Optimization of a Mature Gas Field. Paper presented at the SPE Western Regional Meeting, Long Beach, California.

Lohr, Celeste & Hackley, Paul. (2018). [Open Access] Using mercury injection pressure analyses to estimate sealing capacity of the Tuscaloosa marine shale in Mississippi, USA: Implications for carbon dioxide sequestration. International Journal of Greenhouse Gas Control. 78. 375-387. 10.1016/j.ijggc.2018.09.006.

Lund Snee, J.-E. and M. Zoback. 2020. Multiscale variations of the crustal stress field throughout North America", Nature Communications 11, 1951.

Magoon, L.B. and Z.C. Valin. 1995. Sacramento Basin Province (009). United States Department of the Interior Geological Survey, National assessment of United States oil and gas resources-results, methodology, and supporting data.

Medeiros, M., et al., 2018. *Technical Feasibility of Compressed Air Storage (CAES) Utilizing a Porous Rock Reservoir*. Report Number DOE-PGE-00198-1. March 2018.

Mount, V. and J. Suppe. 1992. Present-day stress orientations adjacent to active strike-slip faults - California and Sumatra. Journal of Geophysical Research. 971. 11995-12013. 10.1029/92JB00130.

Nilsen, T.H. and S.H. Clarke Jr. 1975. Sedimentation and Tectonics in the Early Tertiary Continental Borderland of Central California. Geological Survey Professional Paper 925.

O'Geen, A., M. Saal, H. Dahlke, D. Doll, R. Elkins, A. Fulton, G. Fogg, T. Harter, J. Hopmans, C. Ingels, F. Niederholzer, S.S. Sandoval, P. Verdegaal, and M. Walkinshaw. 2015. Soil suitability index identifies potential areas for groundwater banking on agricultural lands.

Padre and Associates, Inc. 2004. personnel communication with Mike Burke regarding aquifer testing at City of Tracy Well 8.

Page, R.W. 1986. Geology of the Fresh Ground-Water Basin of the Central Valley, California, with Texture Maps and Sections. USGS Professional Paper 1401-C.

Shafer, John & Neasham, John & Group, Reservoir. (2000). Mercury porosimetry protocol for rapid determination of petrophysical and reservoir quality properties. Proceeding of the International Symposium of the Society of Core Analysts, SCA.

Sullivan, R. and M. Sullivan. 2012. Sequence Stratigraphy and Incised Valley Architecture of the Domengine Formation, Black Diamond Mines Regional Preserve and the Southern Sacramento Basin, California, U.S.A. Journal of Sedimentary Research.

Towell, T. 1992. Public Health and Safety- Seismic and Geological Hazards. July.

U.S. Environmental Protection Agency Underground Injection Control Program. 1988. Survey of Methods to Determine Total Dissolved Solids Concentrations. Prepared by Ken E. Davis Associates under subcontract to Engineering Enterprises, INC. EPA LOE Contract No. 68-03-3416, Work Assignment No. 1-0-13, Keda Project No. 30-956.

Unruh, J.R. and C.S. Hitchcock. 2009. Characterization of Potential Seismic Sources in the Sacramento-San Joaquin Delta, California. U.S. Geological Survey National Earthquake Hazards Reduction Program.

Williamson, C.R. and D.R. Hill. 1981. Submarine-Fan Deposition of the Upper Cretaceous Winters Sandstone, Union Island Gas Field, Sacramento Valley, California.: The Society of Economic Paleontologists and Mineralogists (SEPM) Deep-Water Clastic Sediments (CW2).

Wagner, D.L., E.J. Bortugno, and R.D. McJunkin. 1991. Geologic Map of the San Francisco – San Jose Quadrangle. California Geological Survey, Regional Geologic Map No. 5A, 1:250,000 scale.

Yielding, G., P. Bretan, and B. Freeman. 2010. Fault Seal Calibration: A Brief Review. Geological Society, London, Special Publications. 347. 243-255. 10.1144/SP347.14

Figures

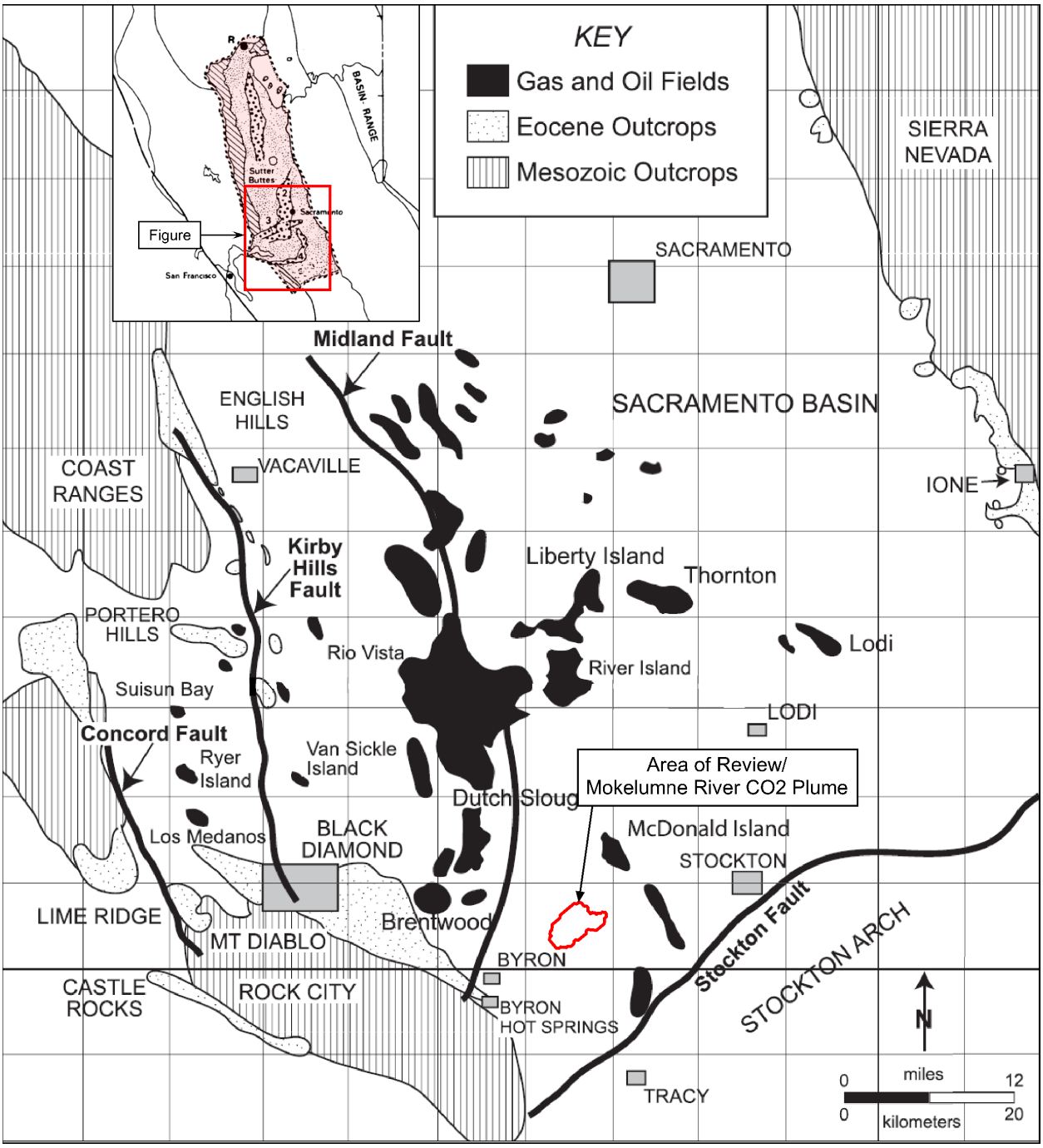

Figure A-1. Location map of the project area with the proposed injection AoR (red) in relation to the Sacramento Basin.

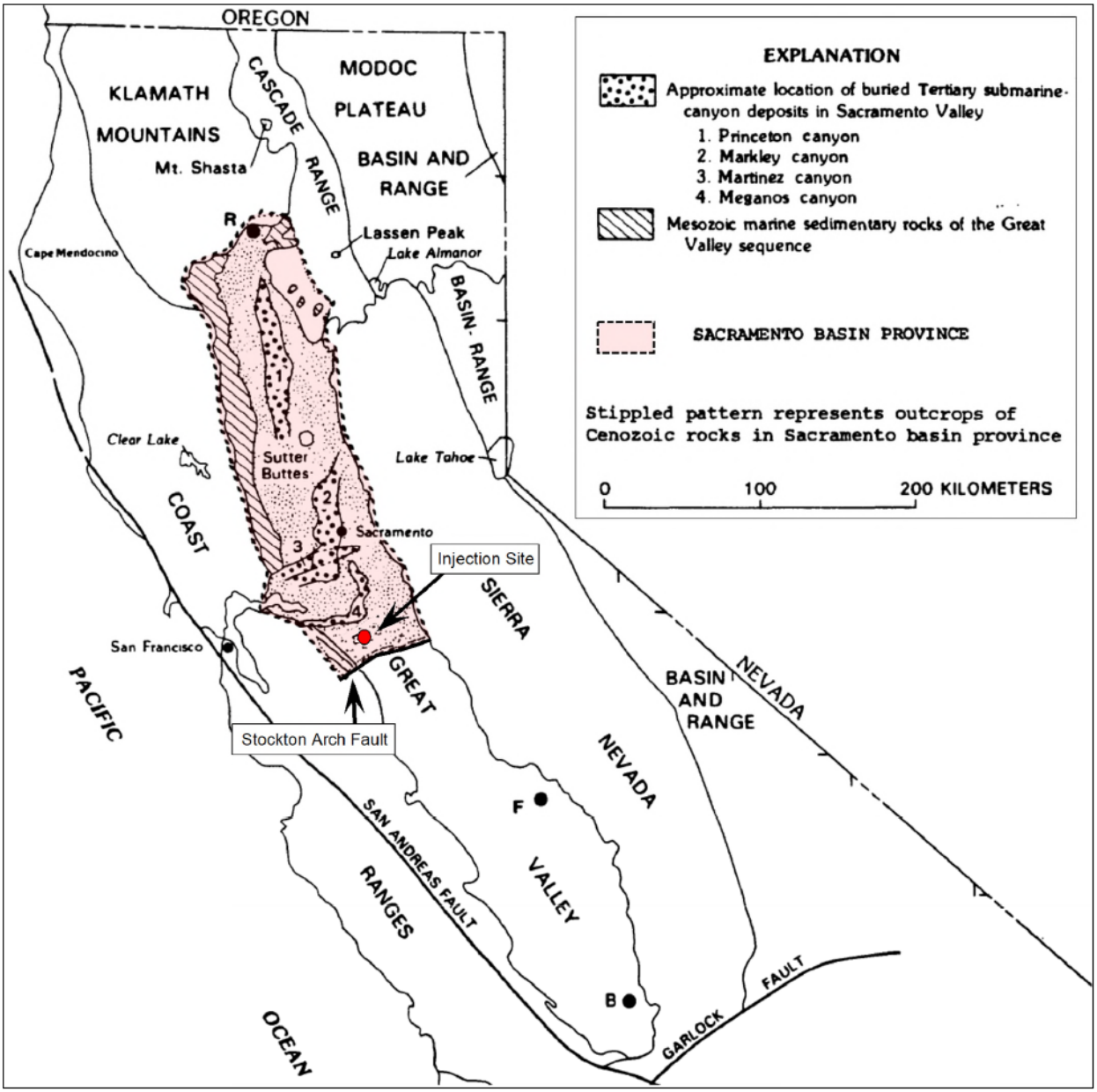

Figure A-2. Location map of California modified from Beyer (1988) and Sullivan (2012). The Sacramento Basin regional study area is outlined by a dashed black line. B – Bakersfield; F – Fresno; R – Redding.

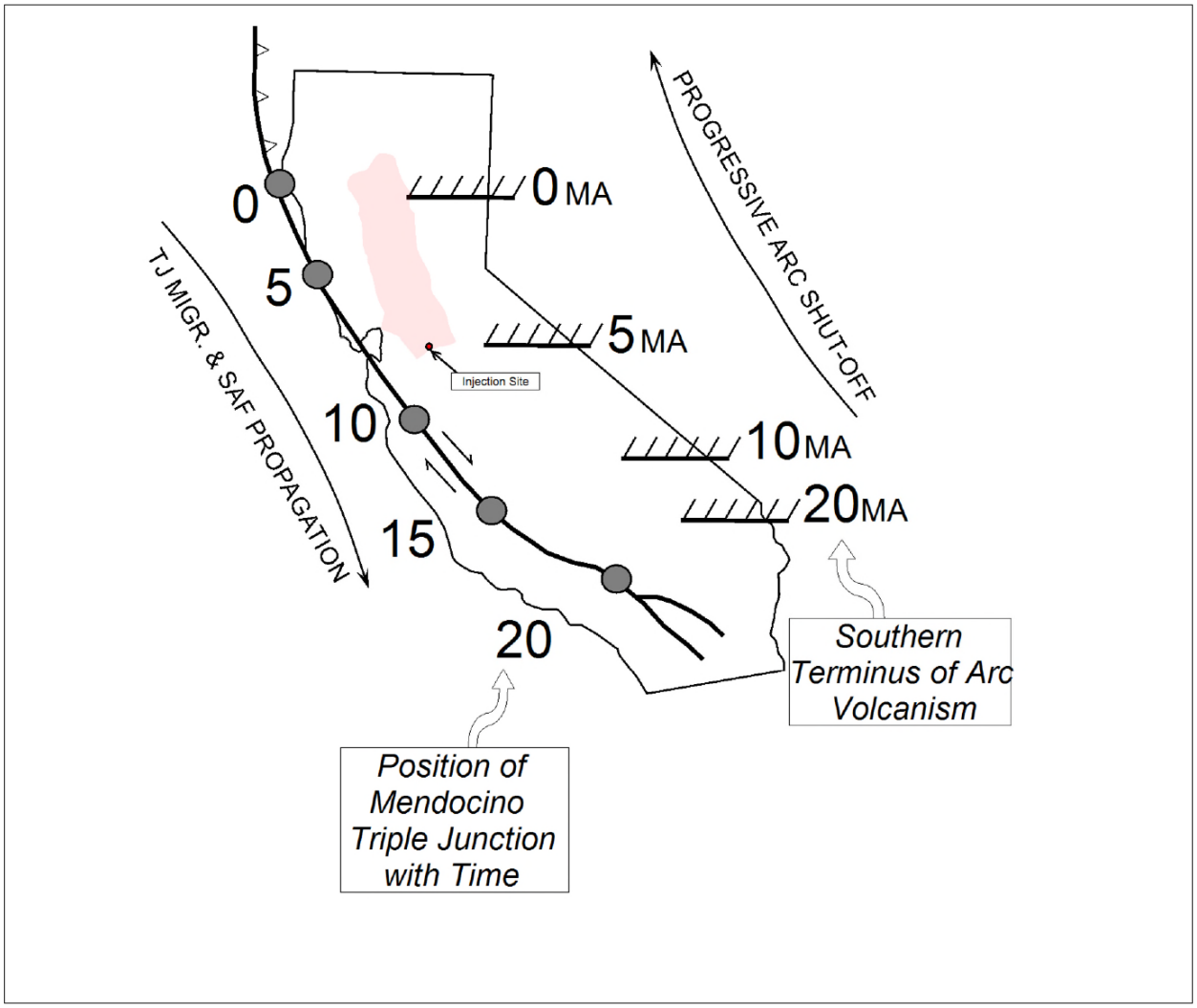

Figure A-3. **Migrational position of the Mendocino triple junction (connection point of the Gorda, North American, and Pacific plates) on the west and migrational position of Sierran arc volcanism in the east (Graham, 1984). The figure indicates space-time relations of major continental-margin tectonic events in California during Miocene.**

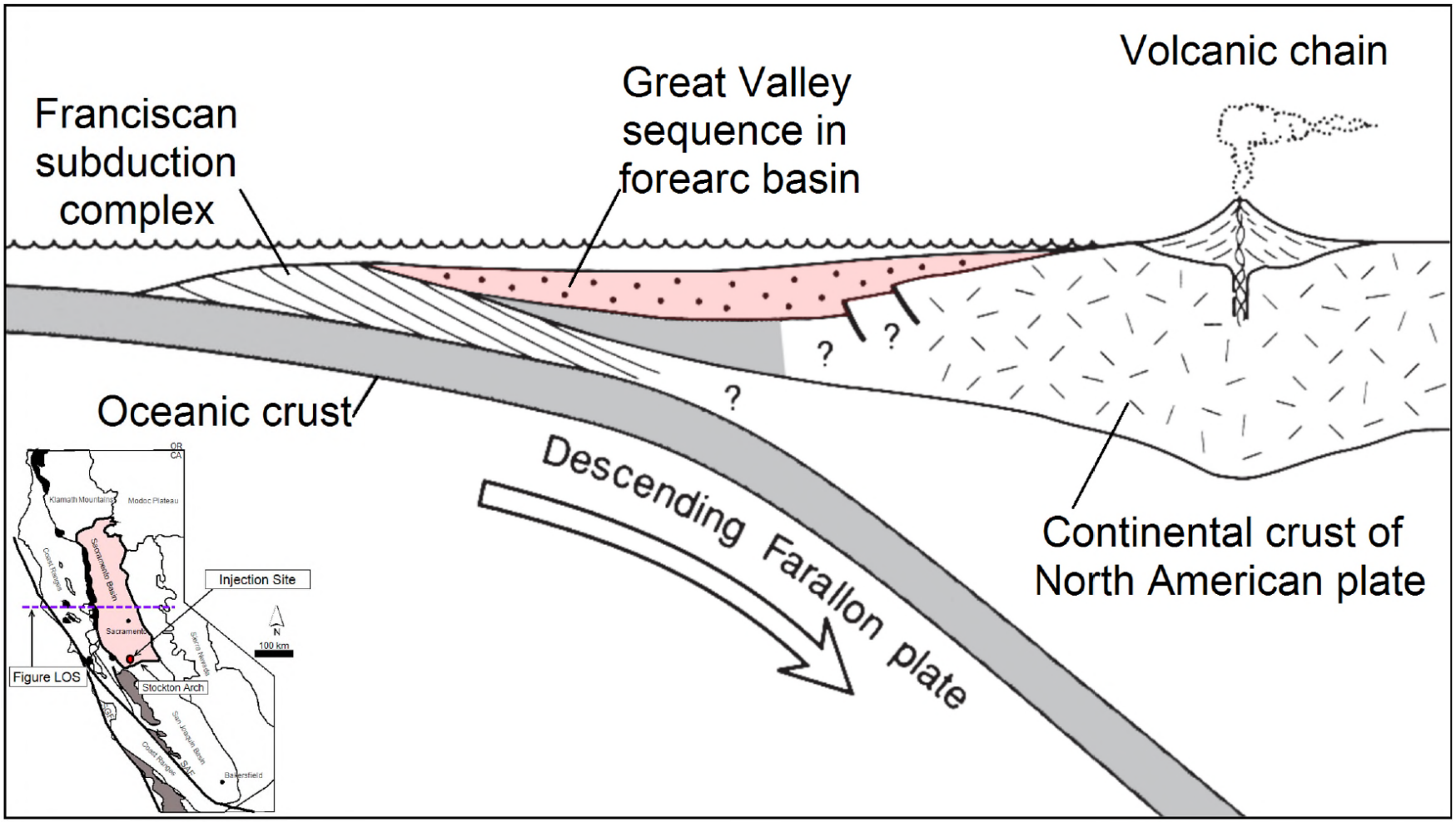

Figure A-4. **Schematic west to east cross section of California, highlighting the Sacramento Basin, as a continental margin during late Mesozoic. The oceanic Farallon plate was forced below the west coast of the North American continental plate.**

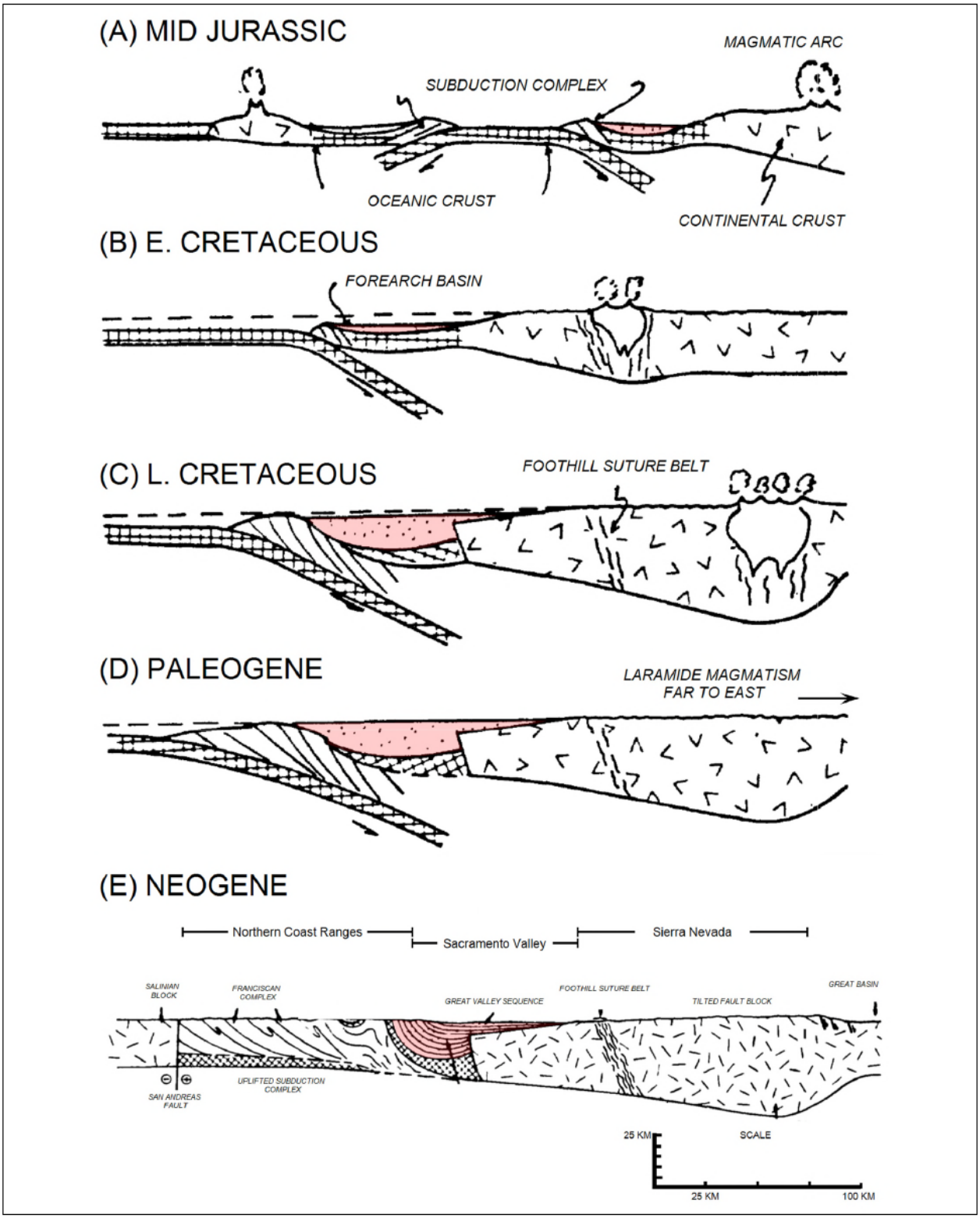

Figure A-5. Evolutionary stages showing the history of the arc-trench system of California from Jurassic (A) to Neogene (E) (modified from Beyer, 1988).

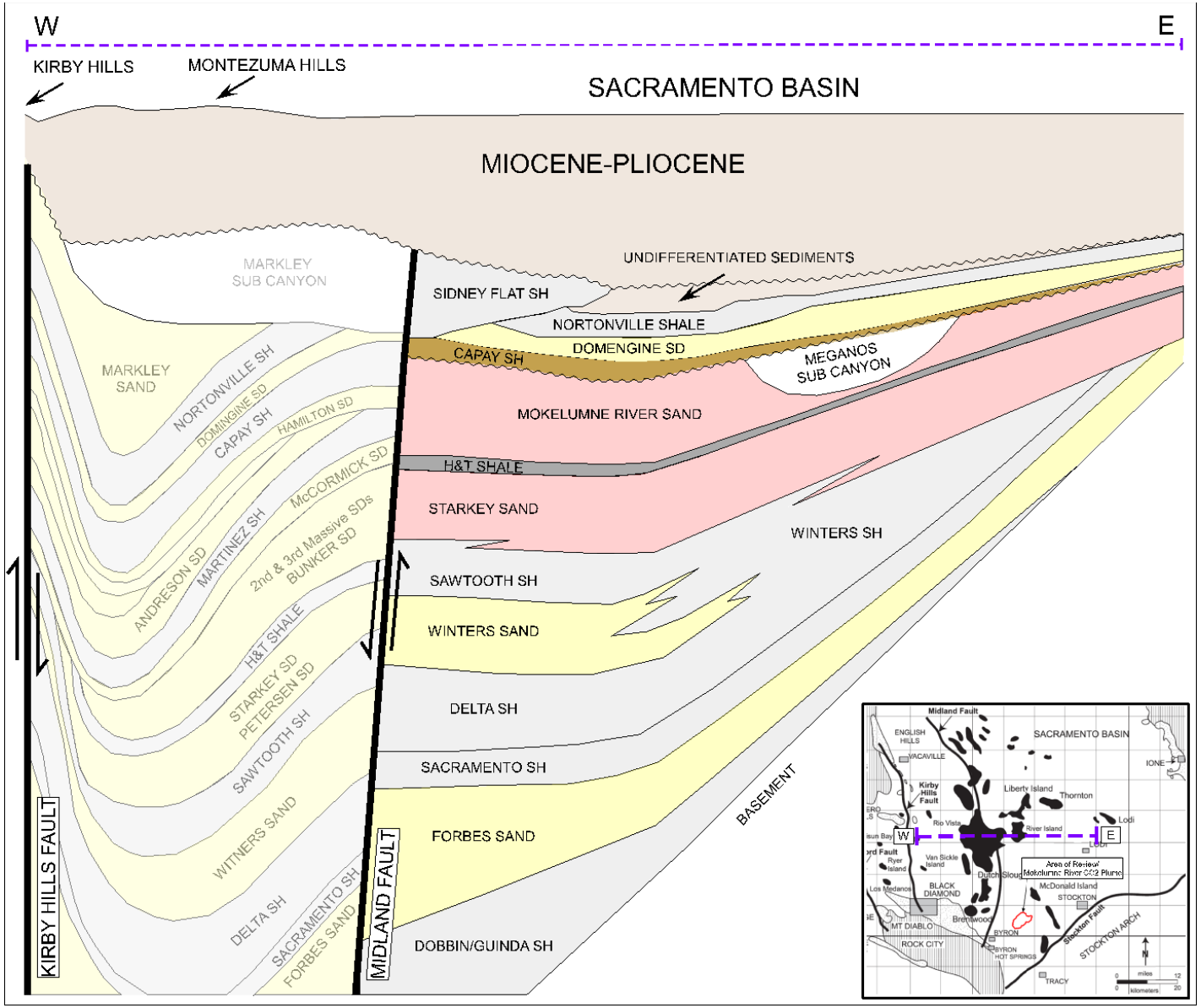

Figure A-6. Schematic west to east cross section in the Sacramento basin.

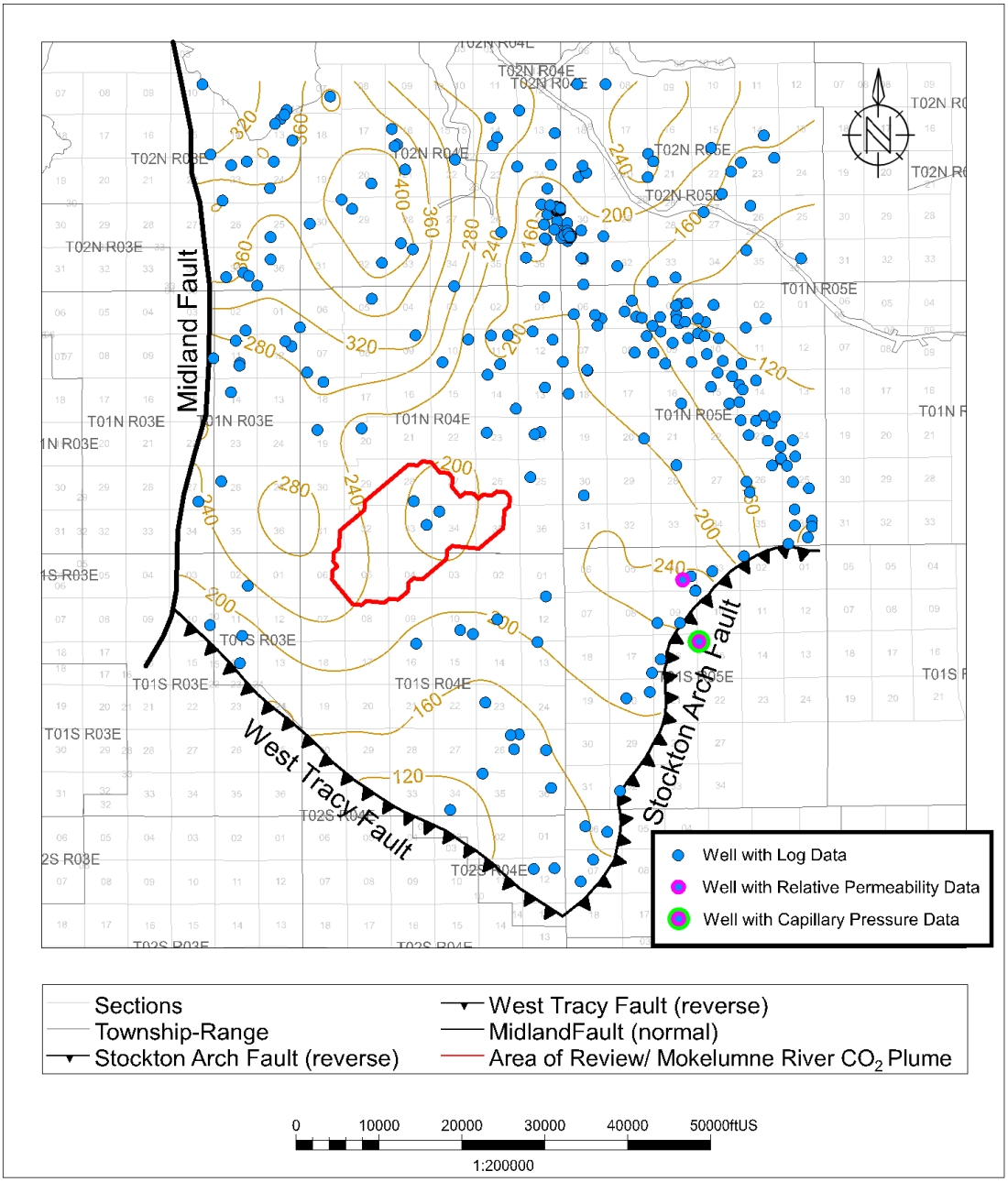

Figure A-7. Capay Shale isopach map for the greater Victoria Island area. Wells shown as blue dots on the map penetrate the Capay Shale and have open-hole logs.

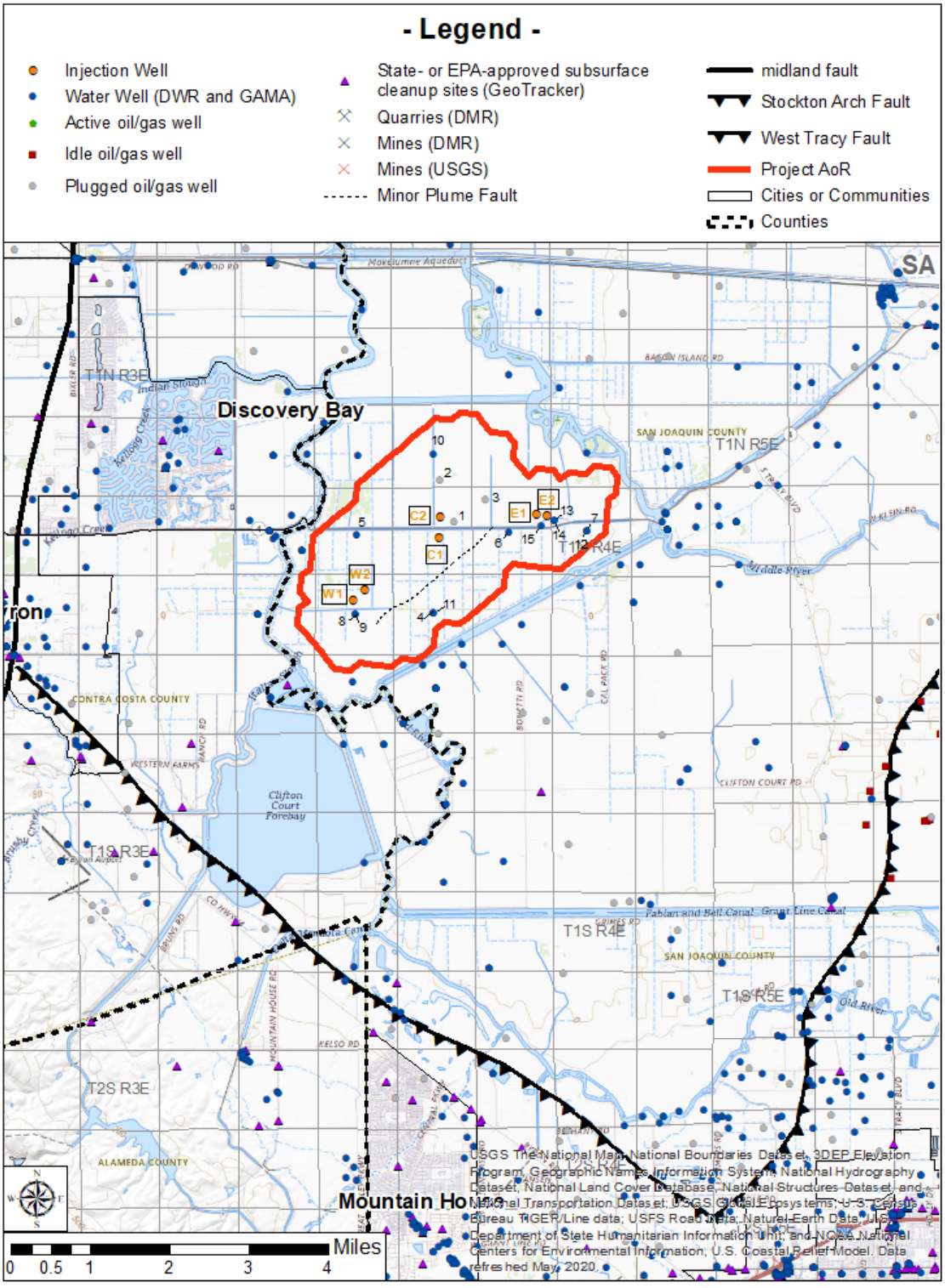

Figure A-8. Summary map of the oil or gas wells, water wells, State- or EPA-approved subsurface cleanup sites, and surface features in the project area. Water wells from California Division of Drinking Water (DWR) and Groundwater Ambient Monitoring and Assessment (GAMA) program. No known mines, quarries, springs or tribal lands are identified near the Area of Review.

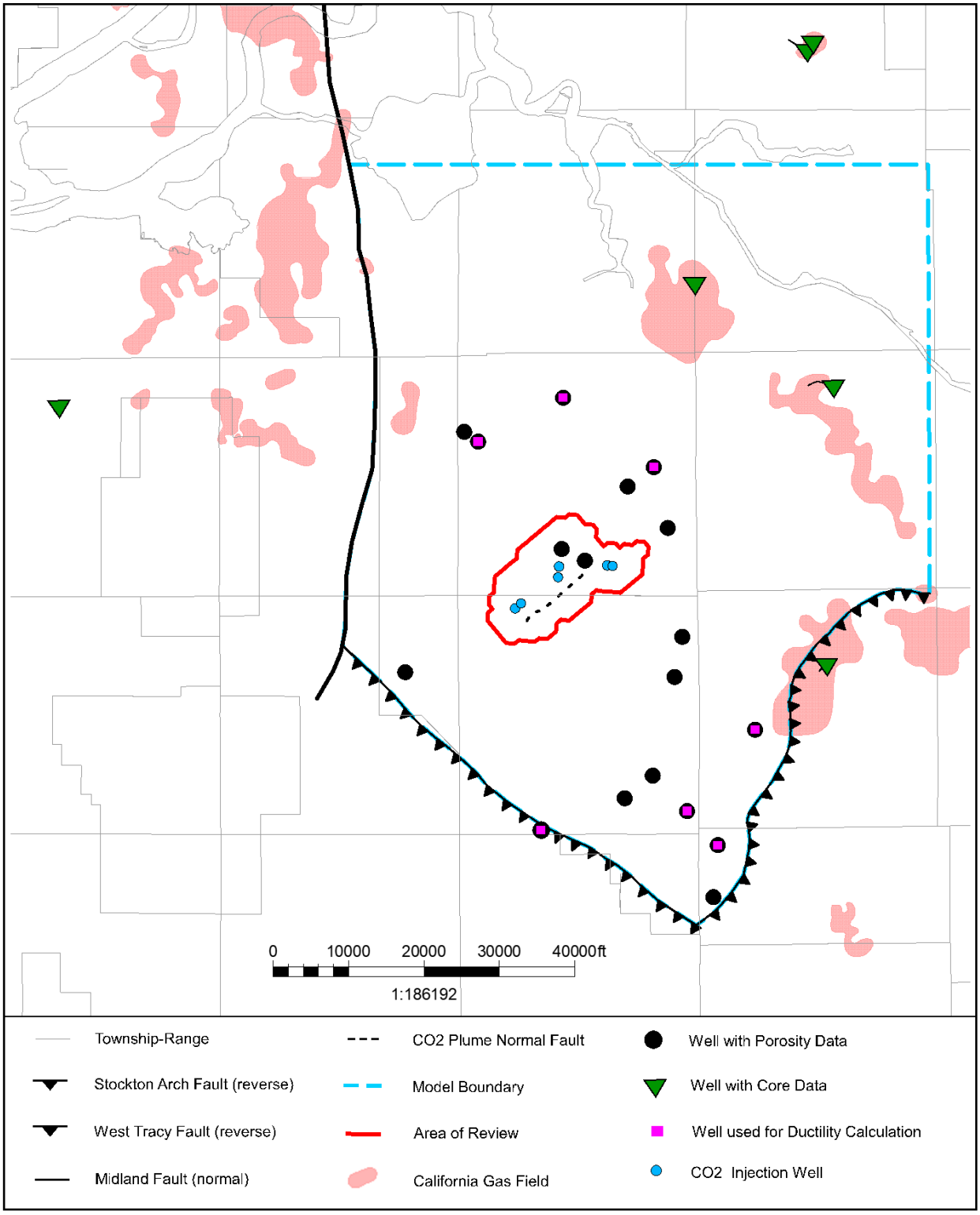

Figure A-9. Wells drilled in the project area with porosity data are shown in black. Wells with core are shown in green, and wells used for ductility calculation are shown in pink.

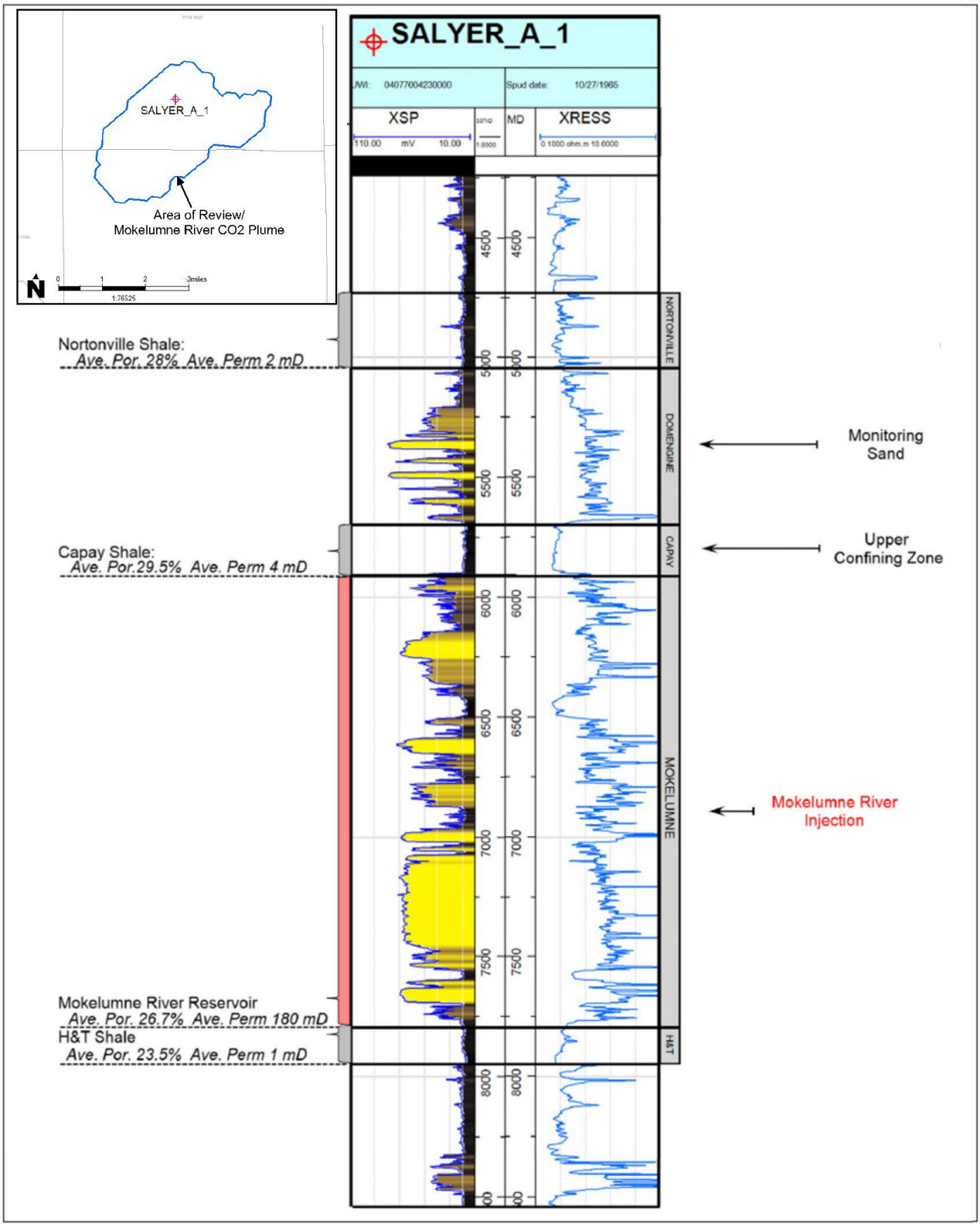

Figure A-10. Type well taken from within the AoR boundary showing confining and injection zone average rock properties.

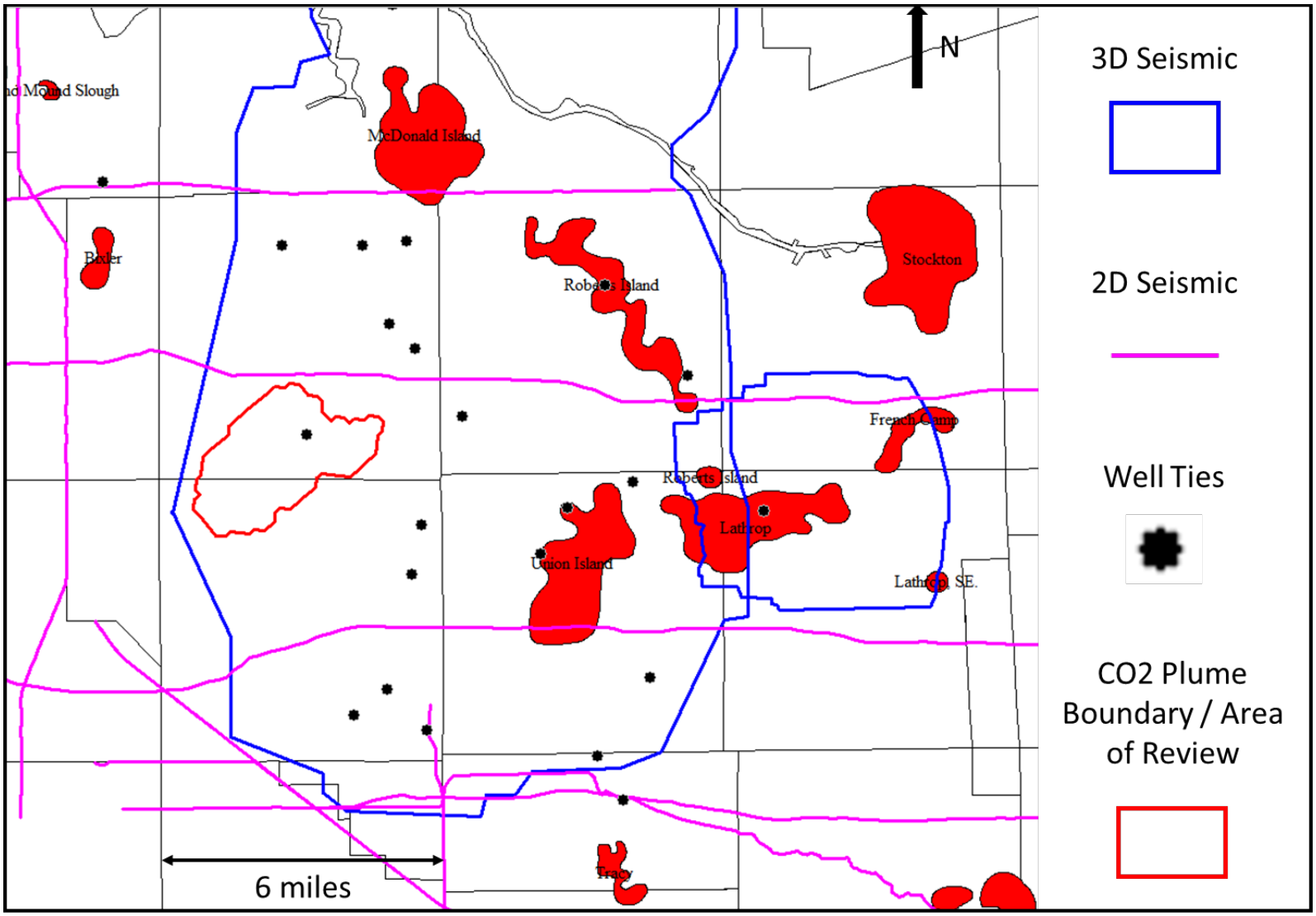

Figure A-11. Summary map and area of seismic data used to build structural model. The 3D surveys were acquired in 1998 and reprocessed in 2013. The 2D seismic were acquired between 1980 and 1985. California gas fields are shown for reference.

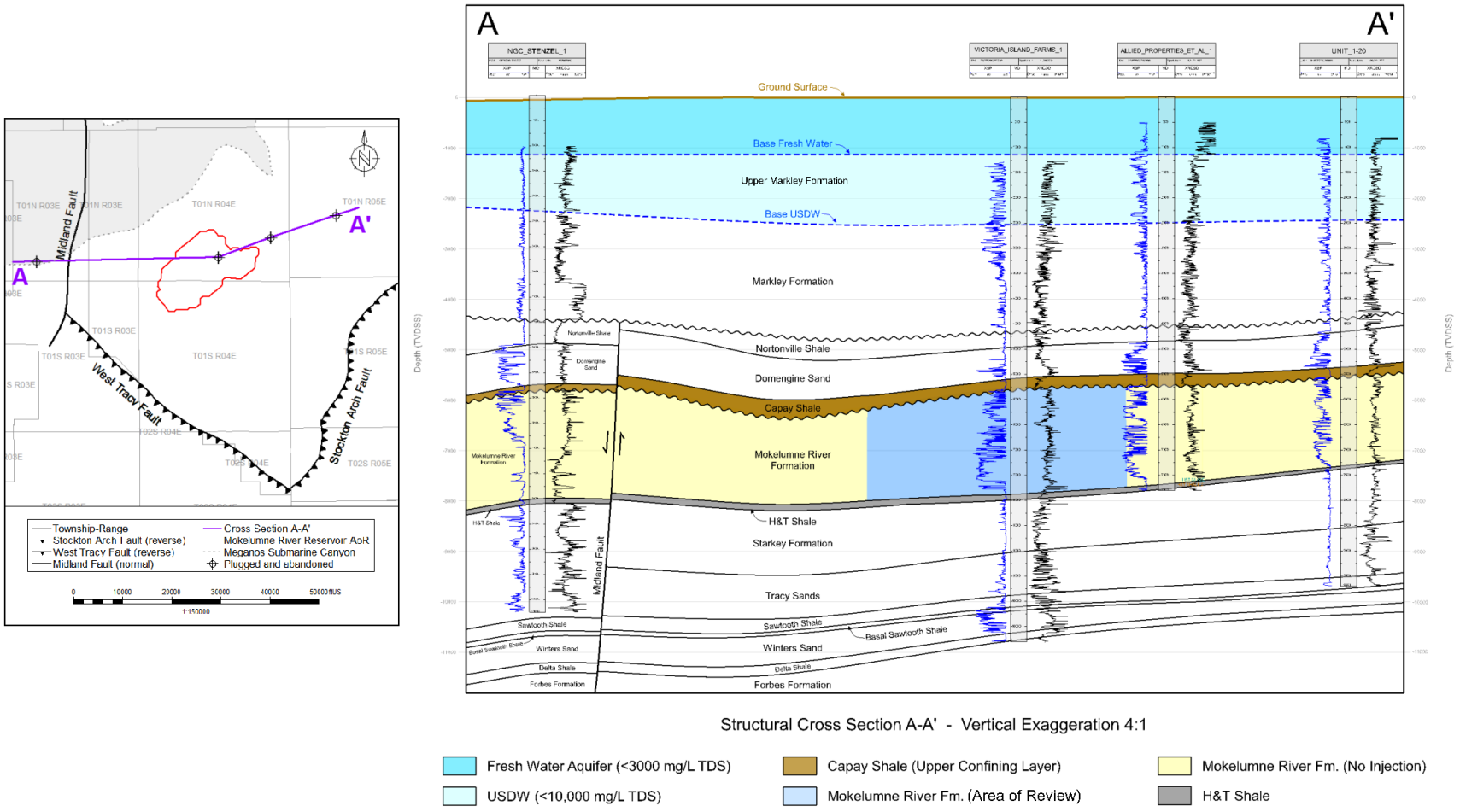

Figure A-12. Cross section showing stratigraphy and lateral continuity of major formations across the project area.

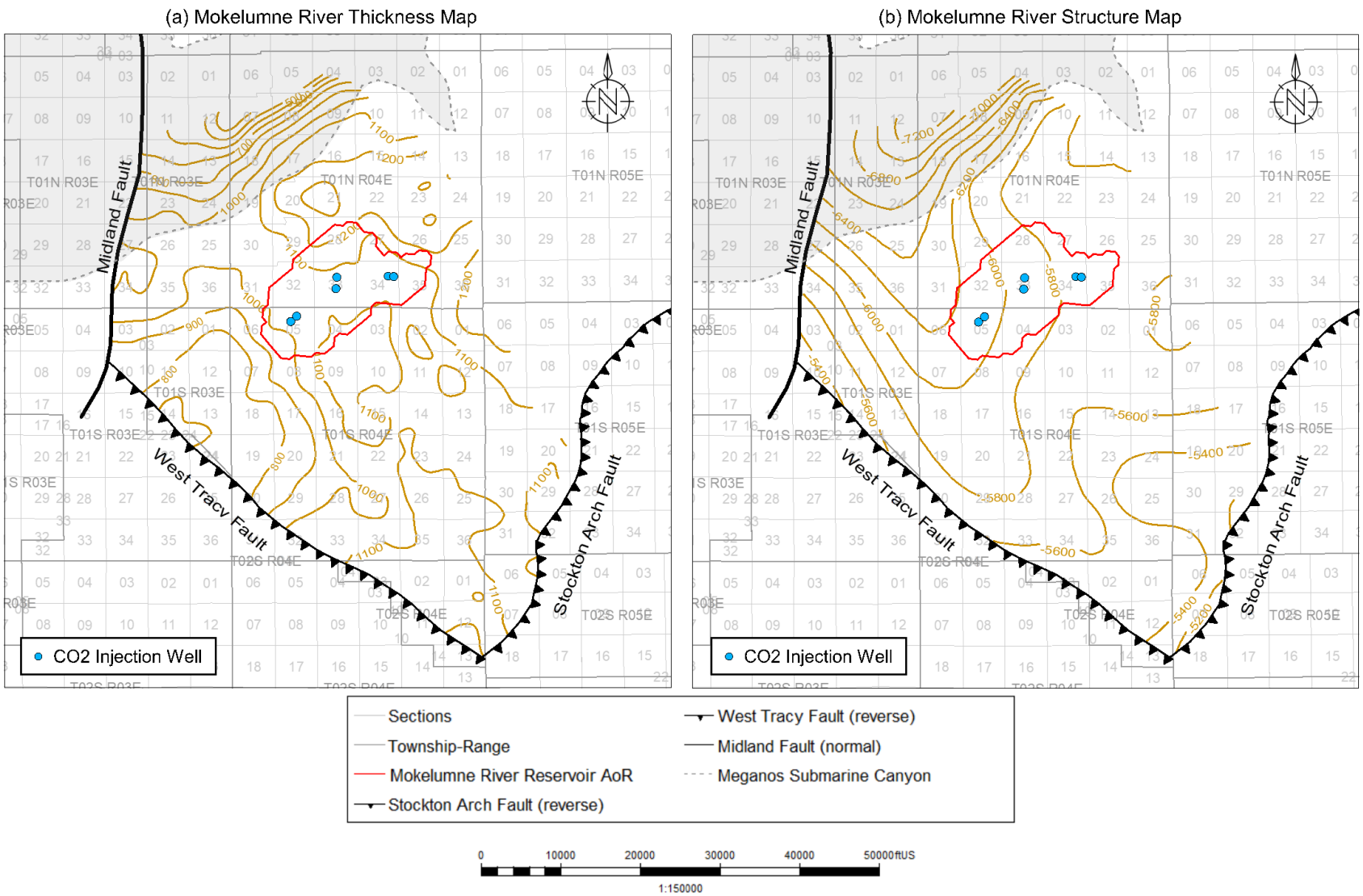

Figure A-13. (a) Mokelumne River Formation thickness map. (b) Mokelumne River Formation structure map

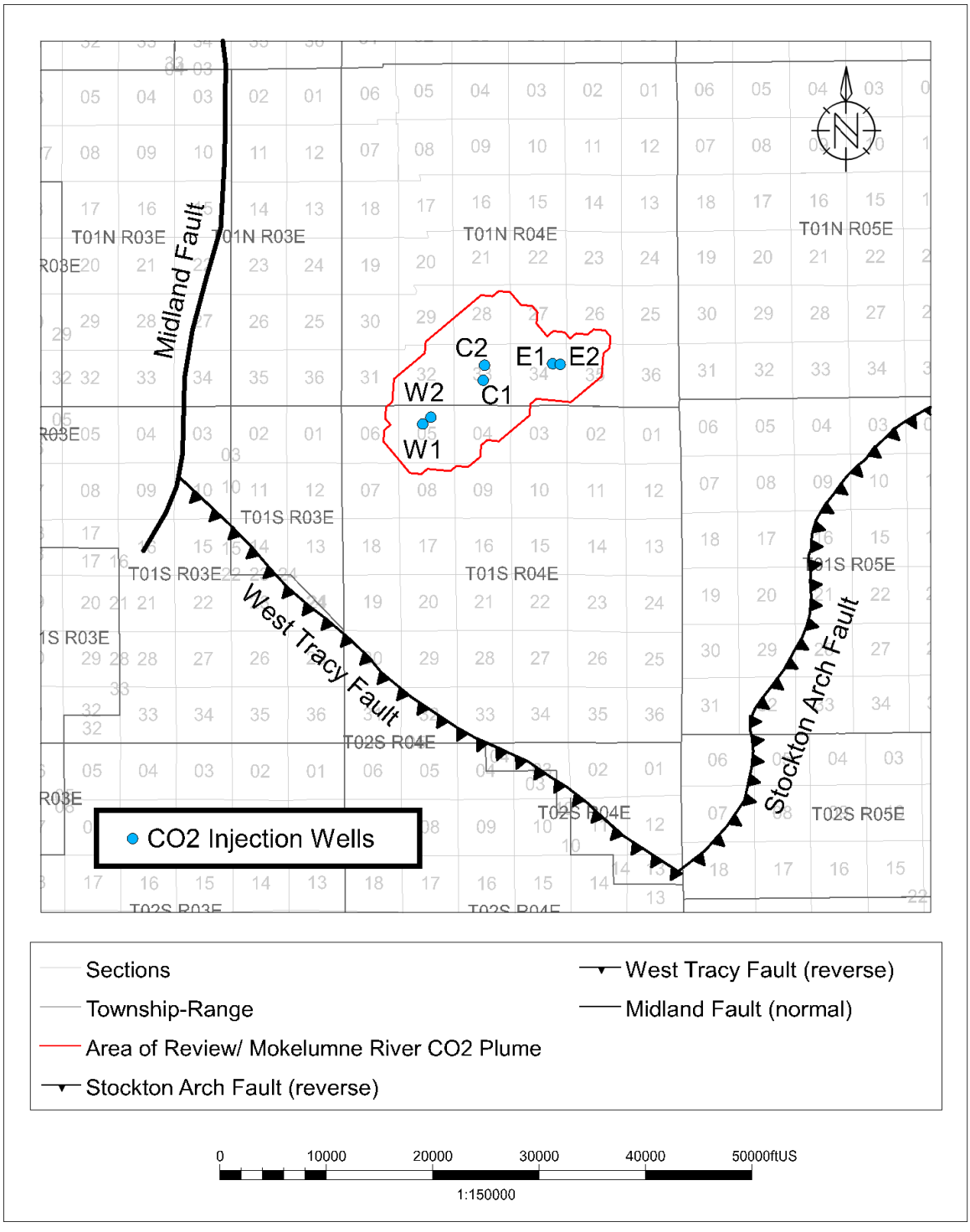

Figure A-14. Injection well location map for the project area. The three groups of injection wells (W1 & W2, C1 & C2, E1 & E2) are approximately 7,000 feet apart.

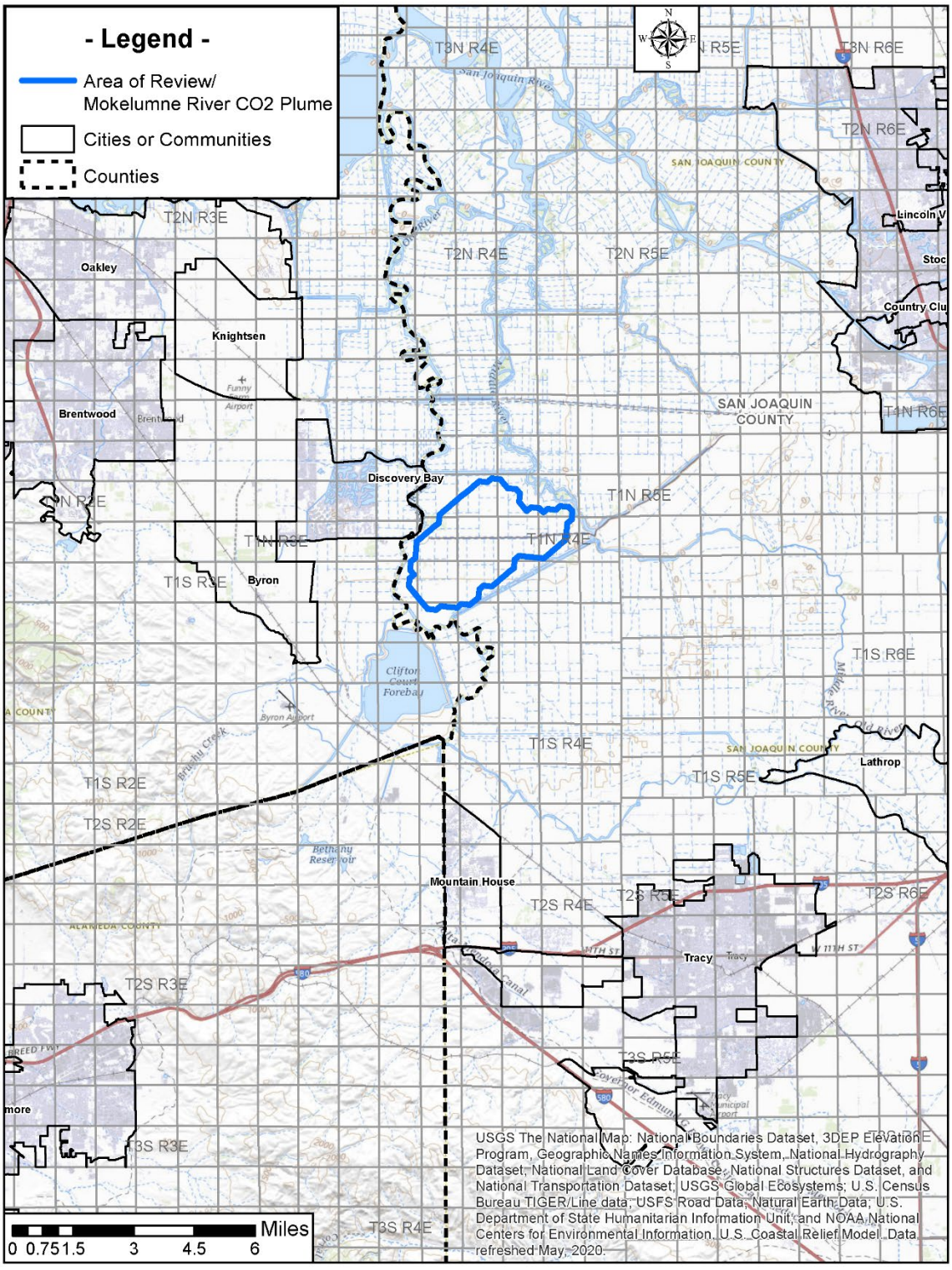

Figure A-15. Surface features and the AoR.

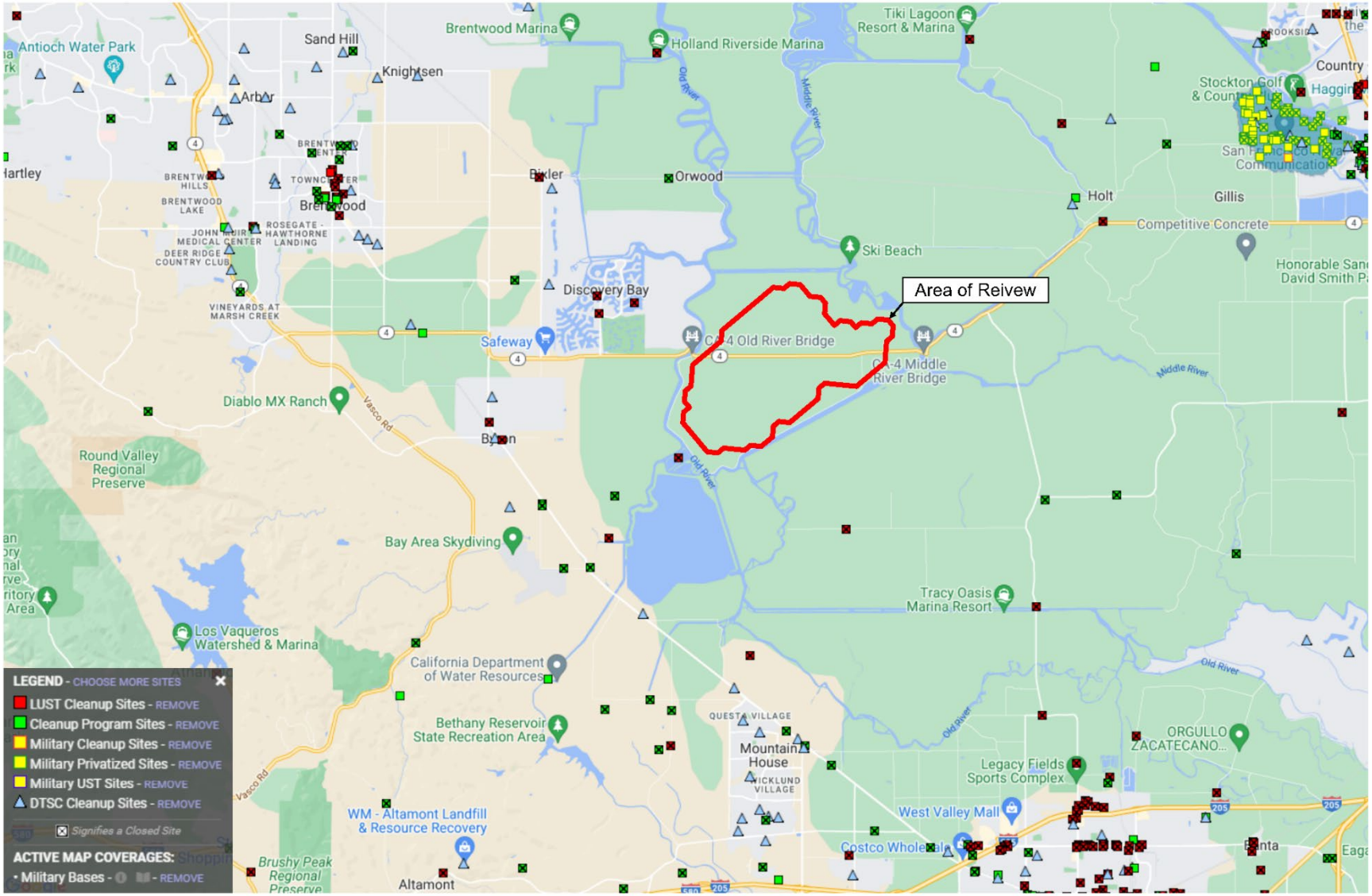

Figure A-16. State or EPA subsurface cleanup sites.

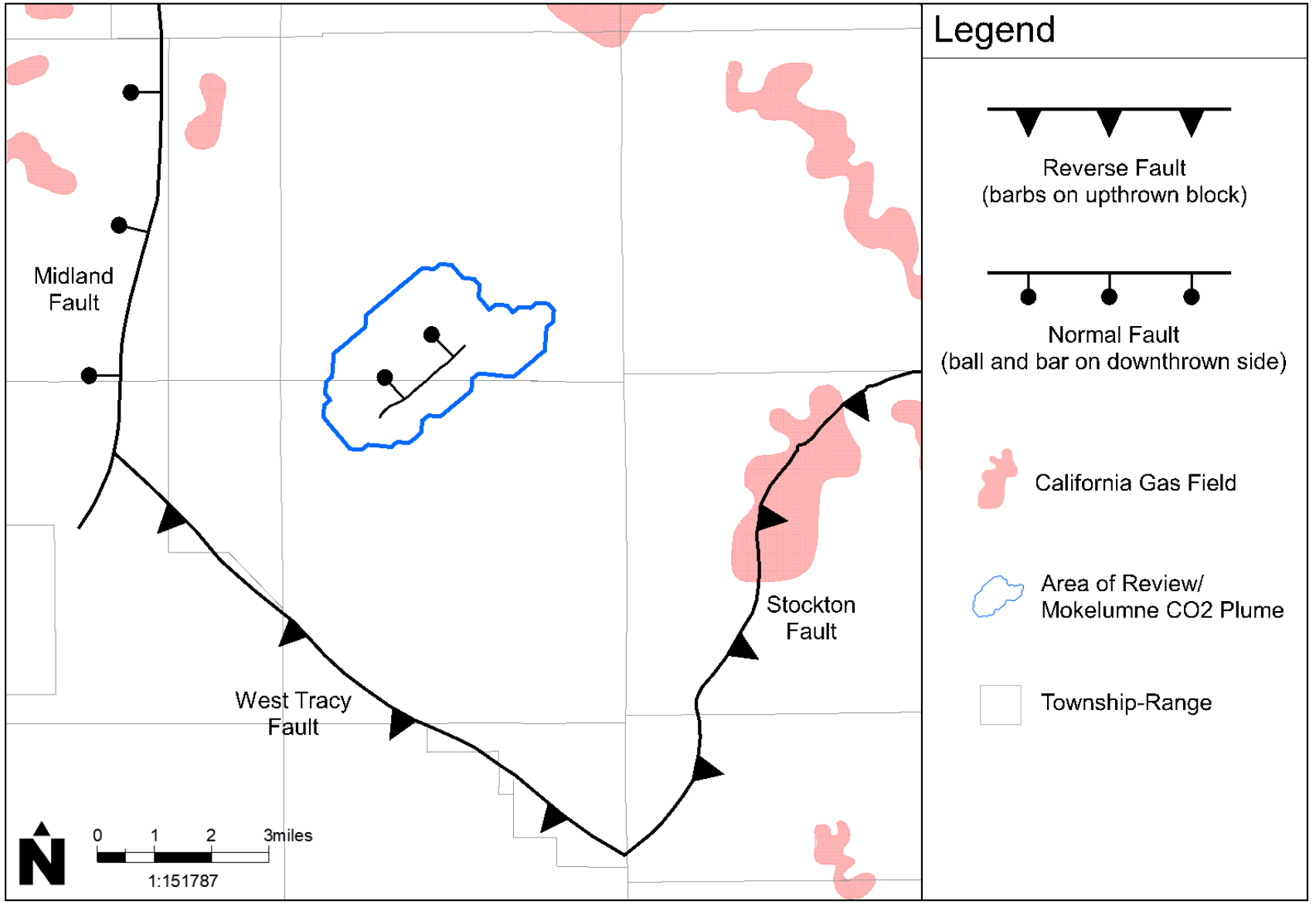

Figure A-17. Faults interpreted from seismic, well, and published data that intersect the project area.

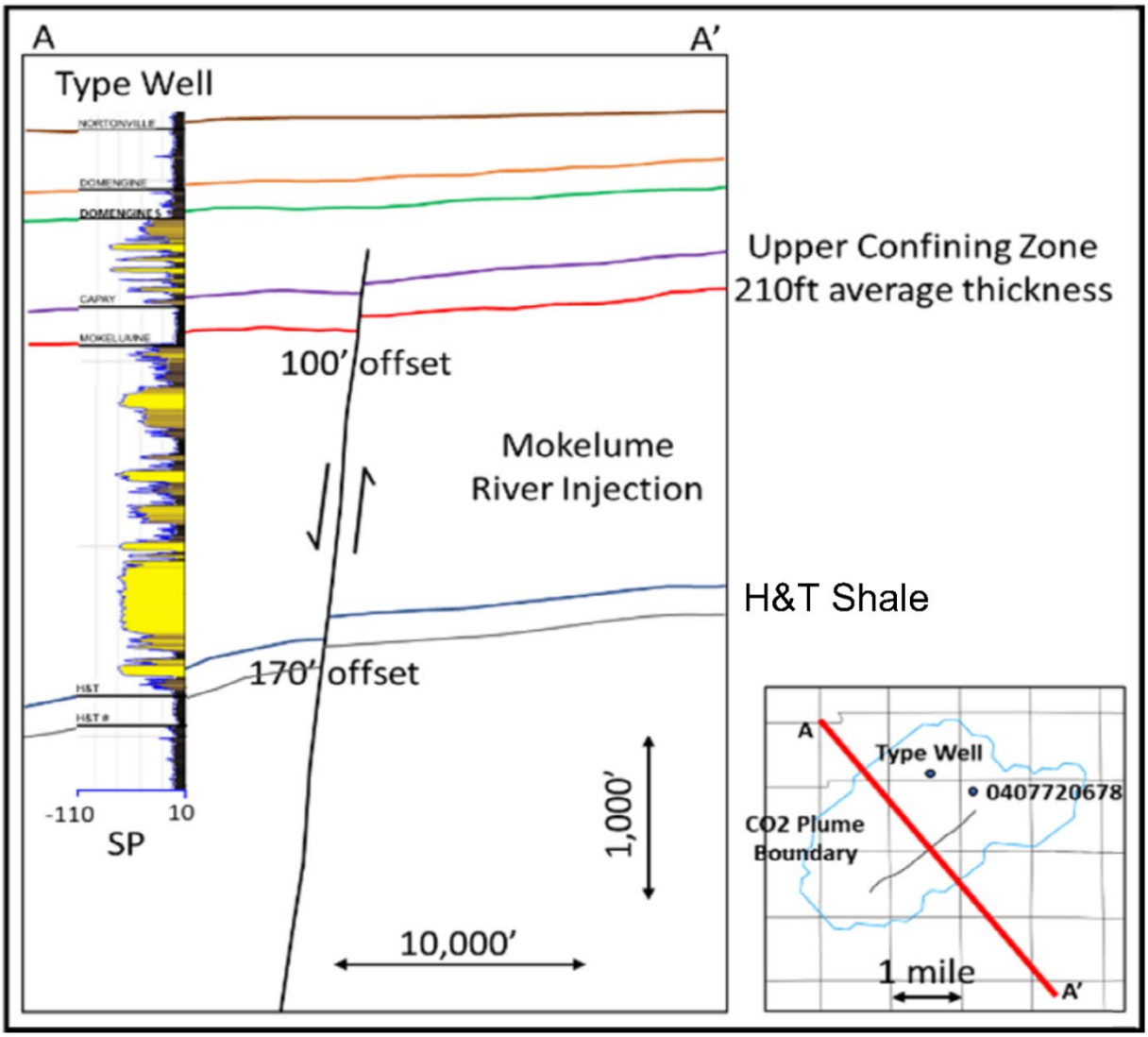

Figure A-18. Schematic cross-section across the normal fault within the CO_2 plume boundary. Properties of the Capay Shale will be confirmed in pre-operational testing and this fault will be monitored during injection in the Domengine sands above.

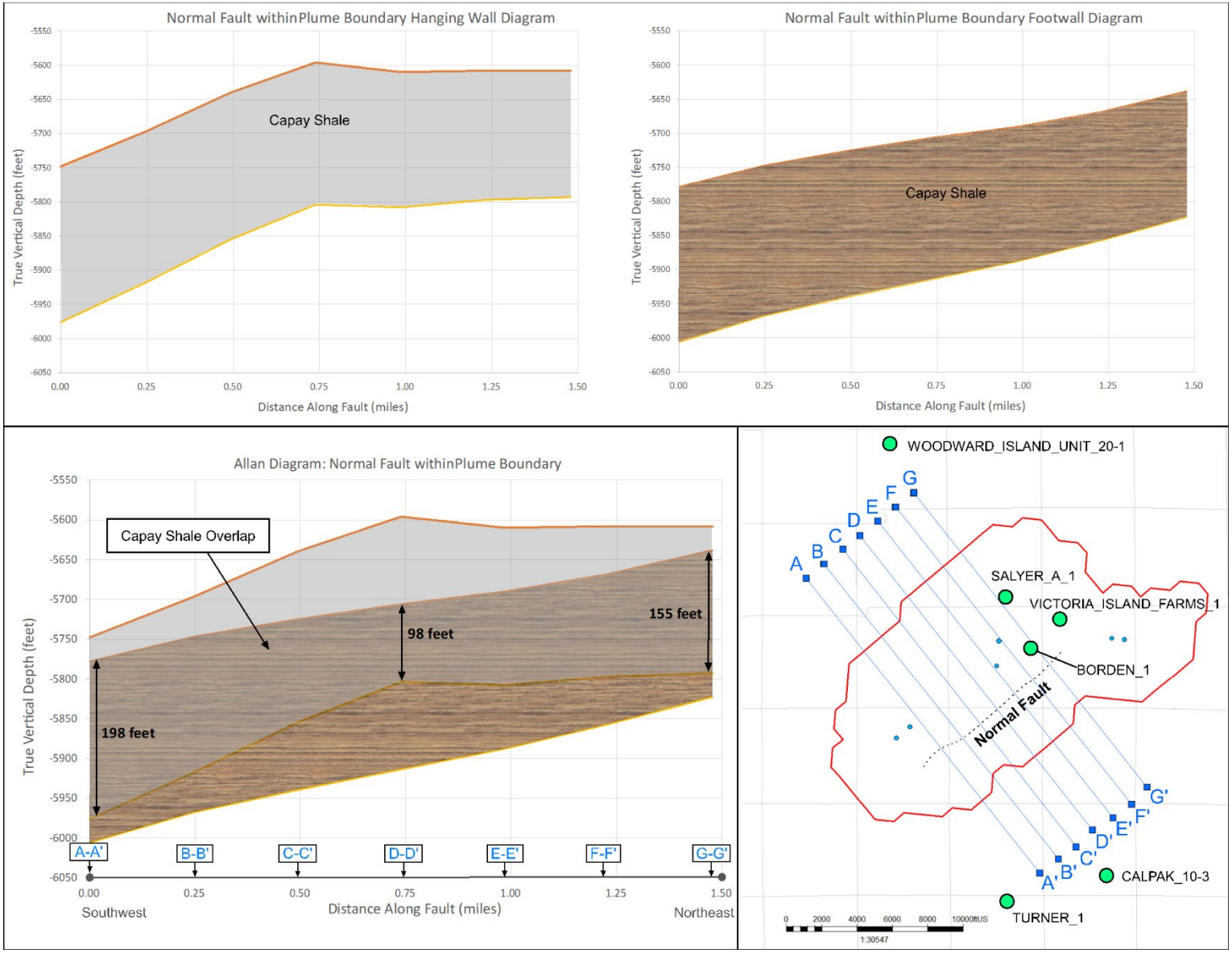

Figure A-19a. Allan diagram for the normal fault within the CO_2 plume boundary.

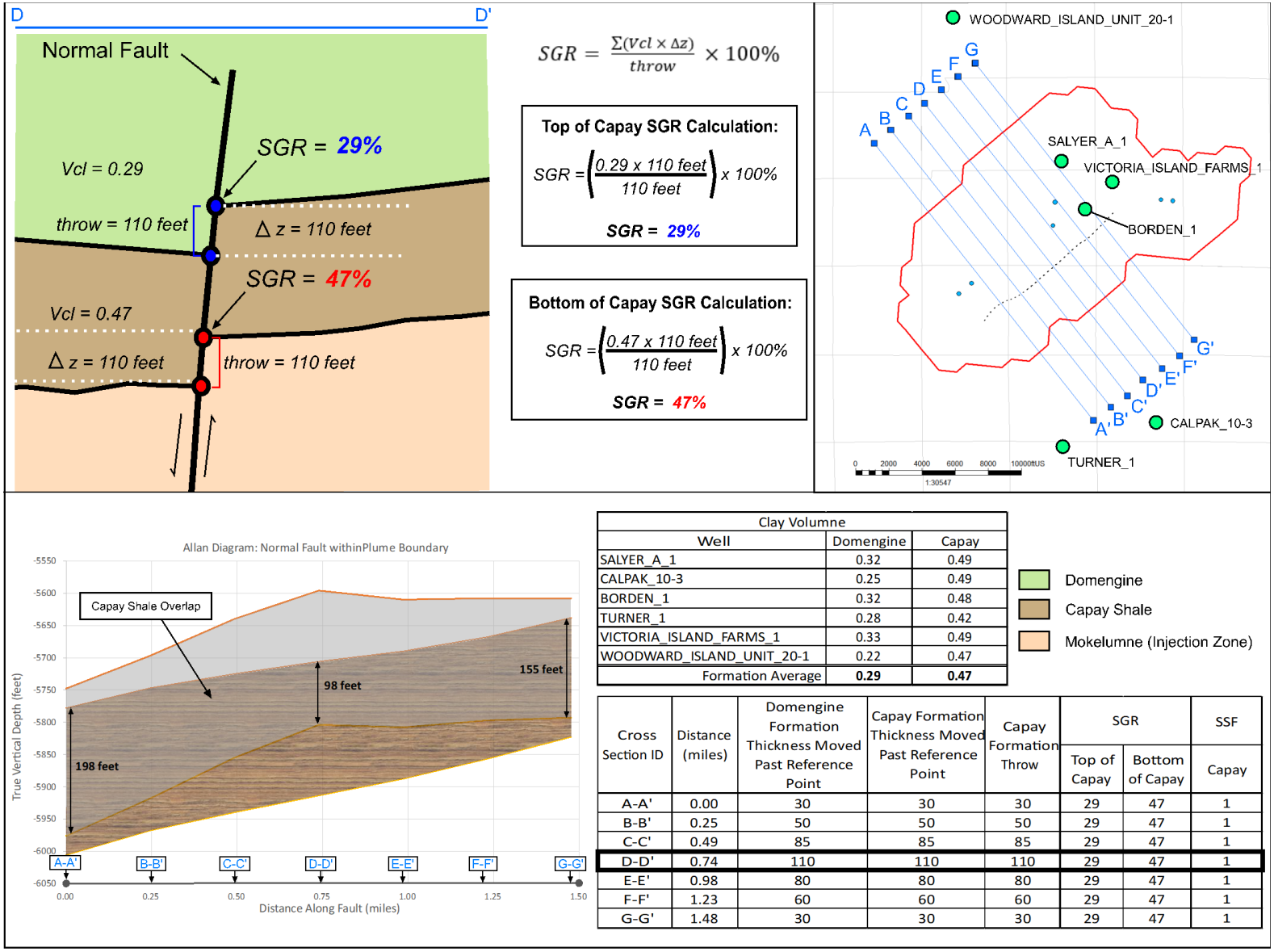

Clay Volumne		
Well	Domengine	Capay
SALYER_A_1	0.32	0.49
CALPAK_10-3	0.25	0.49
BORDEN_1	0.32	0.48
TURNER_1	0.28	0.42
VICTORIA_ISLAND_FARMS_1	0.33	0.49
WOODWARD_ISLAND_UNIT_20-1	0.22	0.47
Formation Average	**0.29**	**0.47**

Cross Section ID	Distance (miles)	Domengine Formation Thickness Moved Past Reference Point	Capay Formation Thickness Moved Past Reference Point	Capay Formation Throw	SGR		SSF
					Top of Capay	Bottom of Capay	Capay
A-A'	0.00	30	30	30	29	47	1
B-B'	0.25	50	50	50	29	47	1
C-C'	0.49	85	85	85	29	47	1
D-D'	0.74	110	110	110	29	47	1
E-E'	0.98	80	80	80	29	47	1
F-F'	1.23	60	60	60	29	47	1
G-G'	1.48	30	30	30	29	47	1

Figure A-19b. Shale Gouge Ratio Calculation Example for the normal fault within the CO_2 plume boundary.

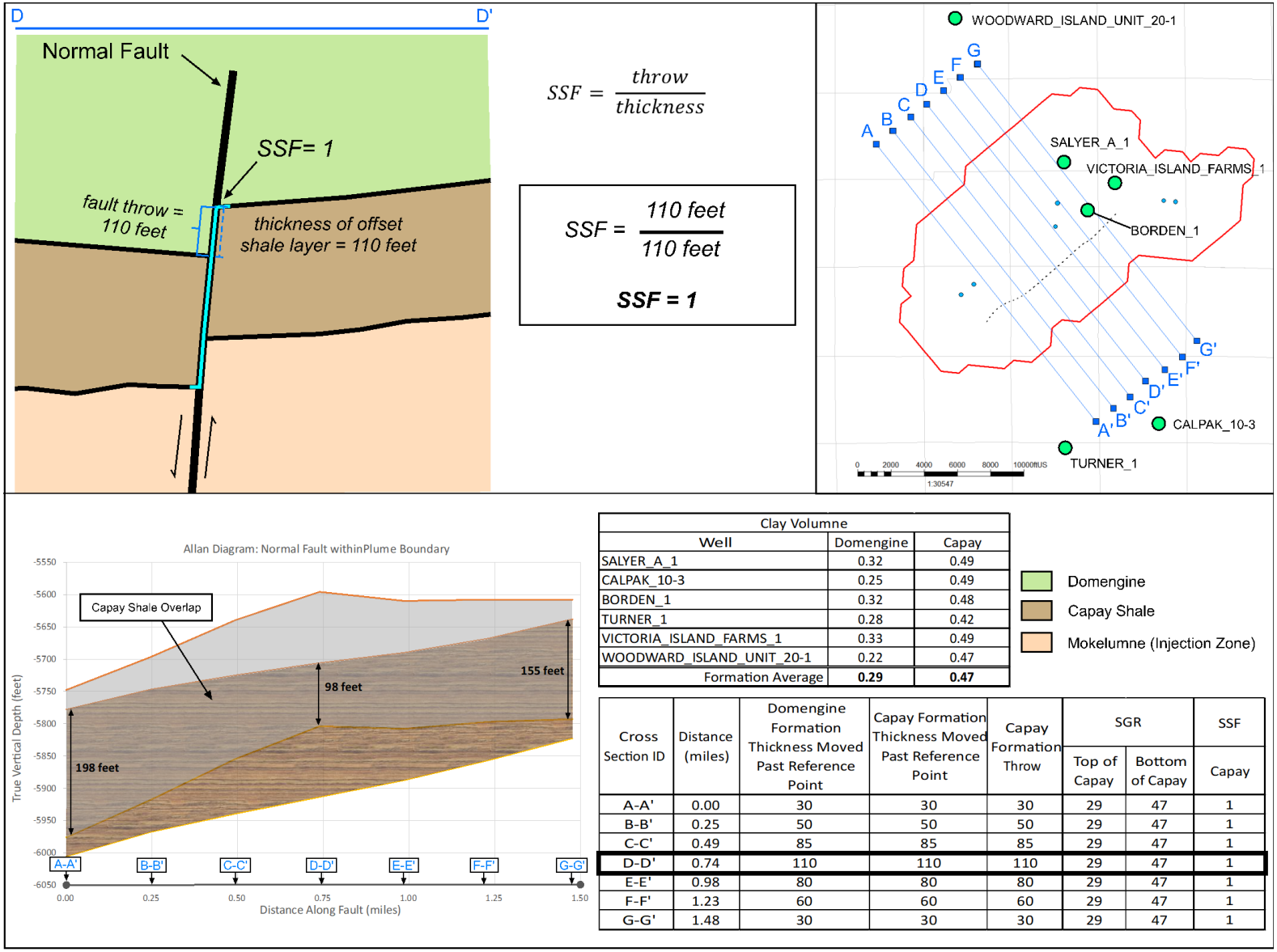

Clay Volumne		
Well	Domengine	Capay
SALYER_A_1	0.32	0.49
CALPAK_10-3	0.25	0.49
BORDEN_1	0.32	0.48
TURNER_1	0.28	0.42
VICTORIA_ISLAND_FARMS_1	0.33	0.49
WOODWARD_ISLAND_UNIT_20-1	0.22	0.47
Formation Average	**0.29**	**0.47**

Cross Section ID	Distance (miles)	Domengine Formation Thickness Moved Past Reference Point	Capay Formation Thickness Moved Past Reference Point	Capay Formation Throw	SGR		SSF
					Top of Capay	Bottom of Capay	Capay
A-A'	0.00	30	30	30	29	47	1
B-B'	0.25	50	50	50	29	47	1
C-C'	0.49	85	85	85	29	47	1
D-D'	0.74	110	110	110	29	47	1
E-E'	0.98	80	80	80	29	47	1
F-F'	1.23	60	60	60	29	47	1
G-G'	1.48	30	30	30	29	47	1

Figure A-19c. Shale Smear Factor Calculation Example for the normal fault within the CO_2 plume boundary.

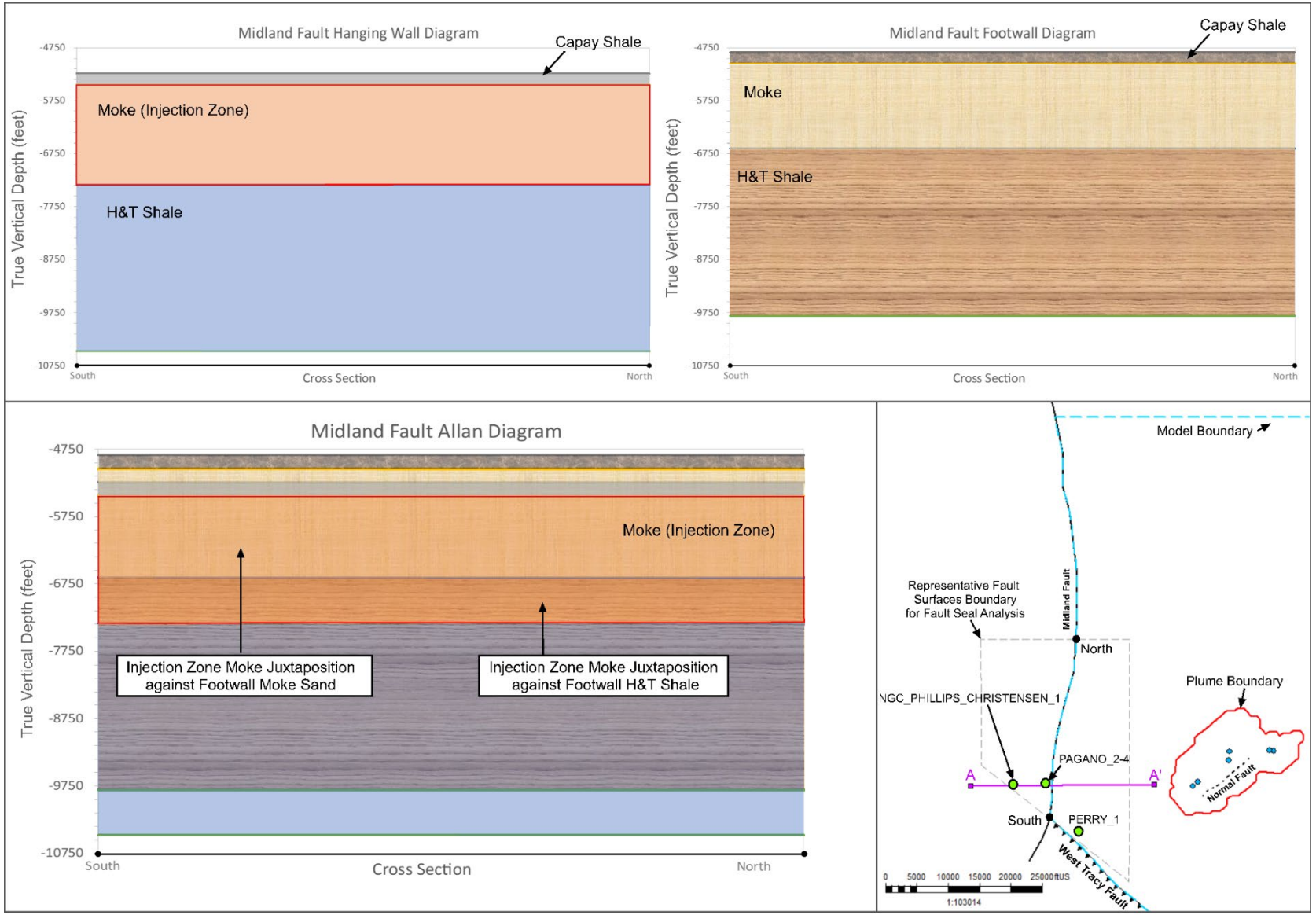

Figure A-20a. Allan diagram for the Midland Fault.

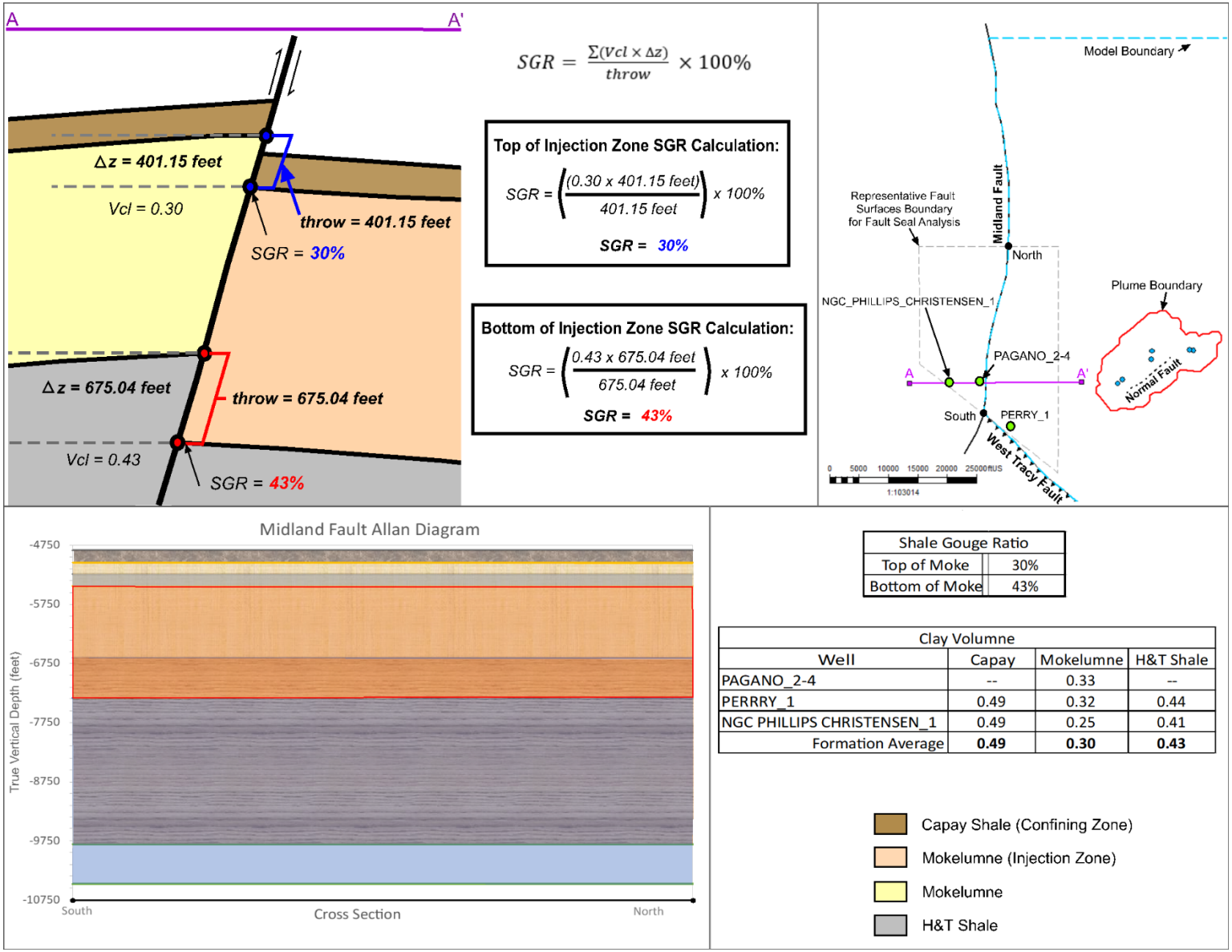

Figure A-20b. Shale Gouge Ratio Calculation for the Midland Fault.

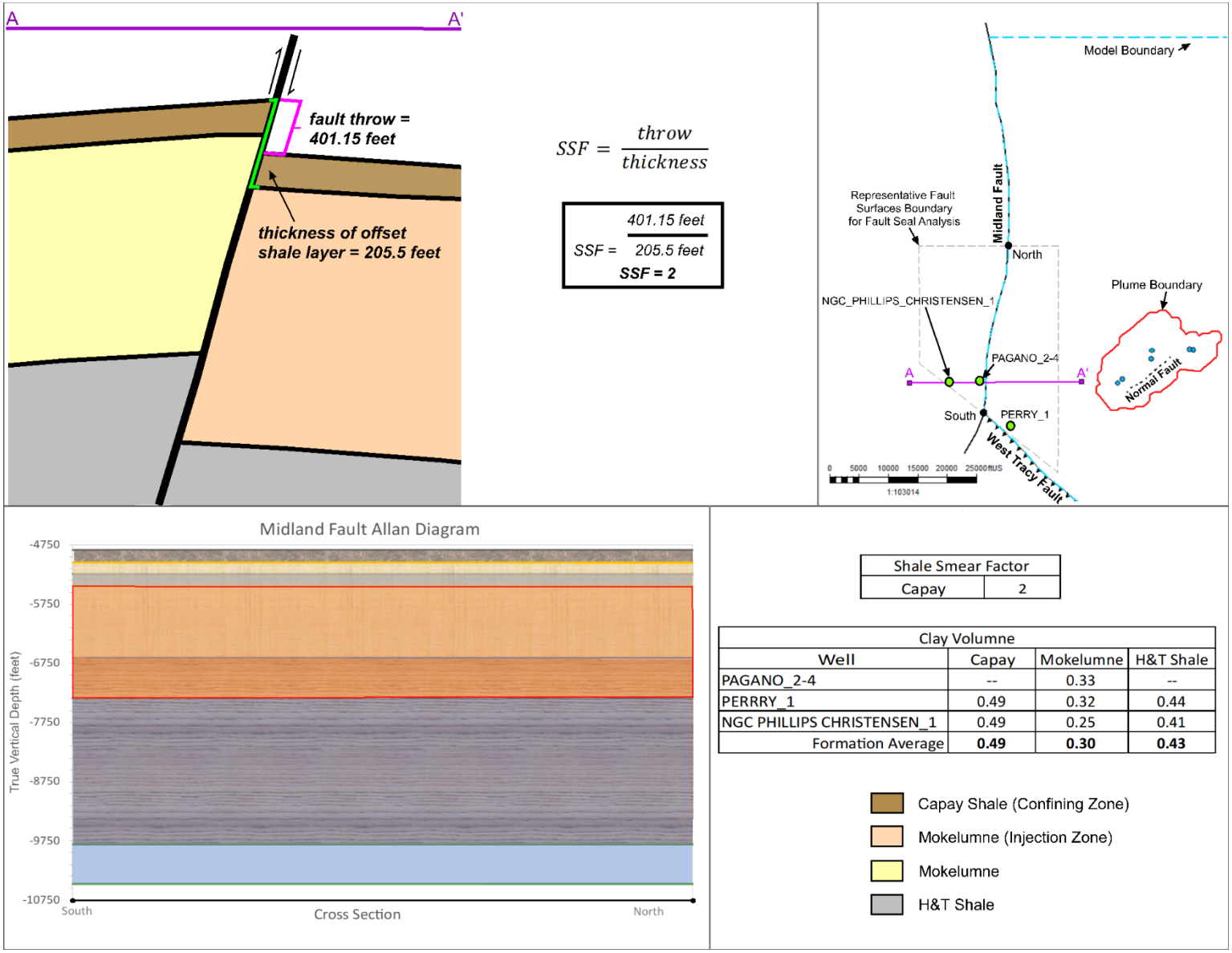

Figure A-20c. Shale Smear Factor Calculation for the Midland Fault.

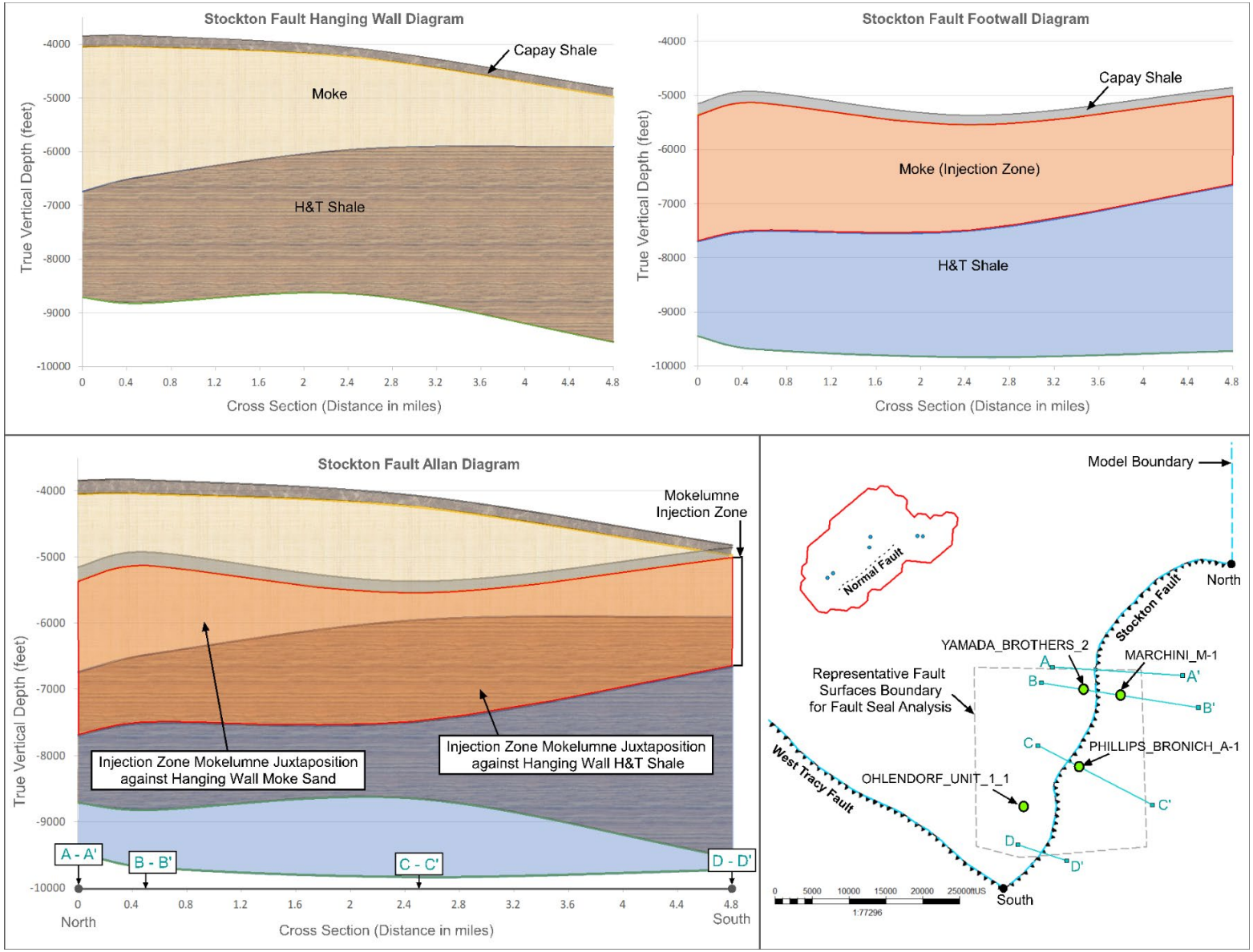

Figure A-21a. Allan diagram for the Stockton Fault.

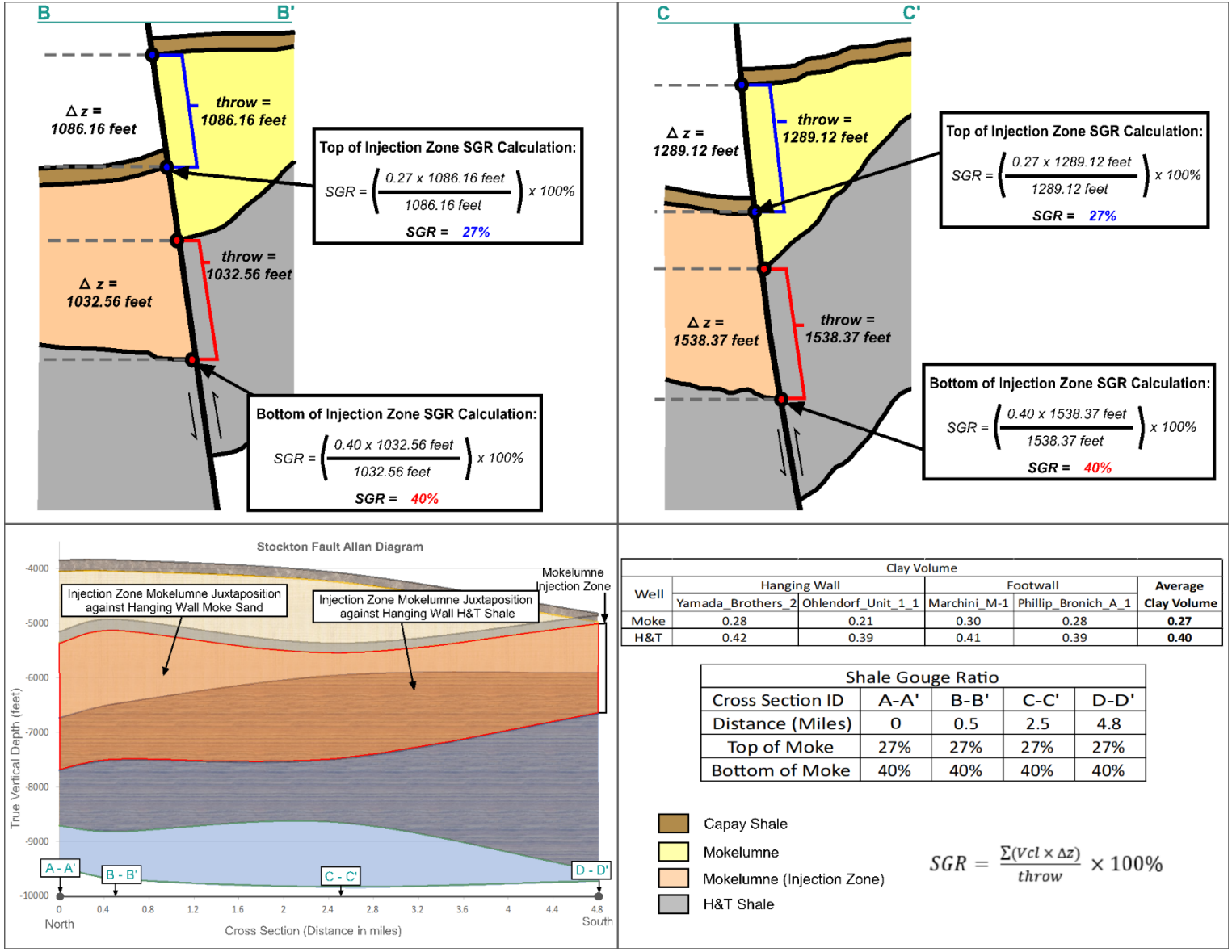

Clay Volume					
Well	Hanging Wall		Footwall		Average
	Yamada_Brothers_2	Ohlendorf_Unit_1_1	Marchini_M-1	Phillip_Bronich_A_1	Clay Volume
Moke	0.28	0.21	0.30	0.28	**0.27**
H&T	0.42	0.39	0.41	0.39	**0.40**

Shale Gouge Ratio				
Cross Section ID	A-A'	B-B'	C-C'	D-D'
Distance (Miles)	0	0.5	2.5	4.8
Top of Moke	27%	27%	27%	27%
Bottom of Moke	40%	40%	40%	40%

Capay Shale
Mokelumne
Mokelumne (Injection Zone)
H&T Shale

$$SGR = \frac{\sum(Vcl \times \Delta z)}{throw} \times 100\%$$

Figure A-21b. Example Shale Gouge Ratio Calculations for the Stockton Fault.

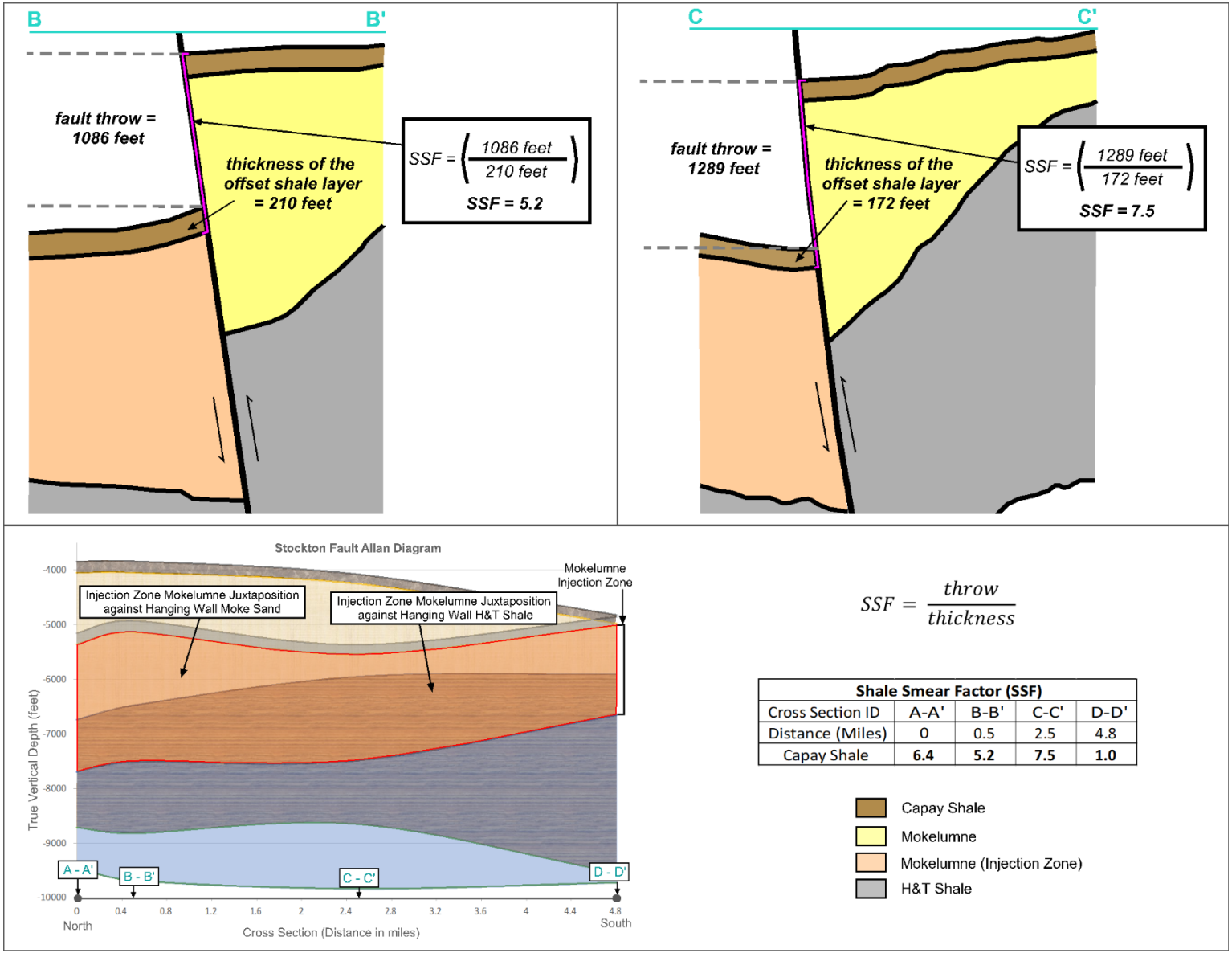

Figure A-21c. Example Shale Smear Factor Calculations for the Stockton Fault.

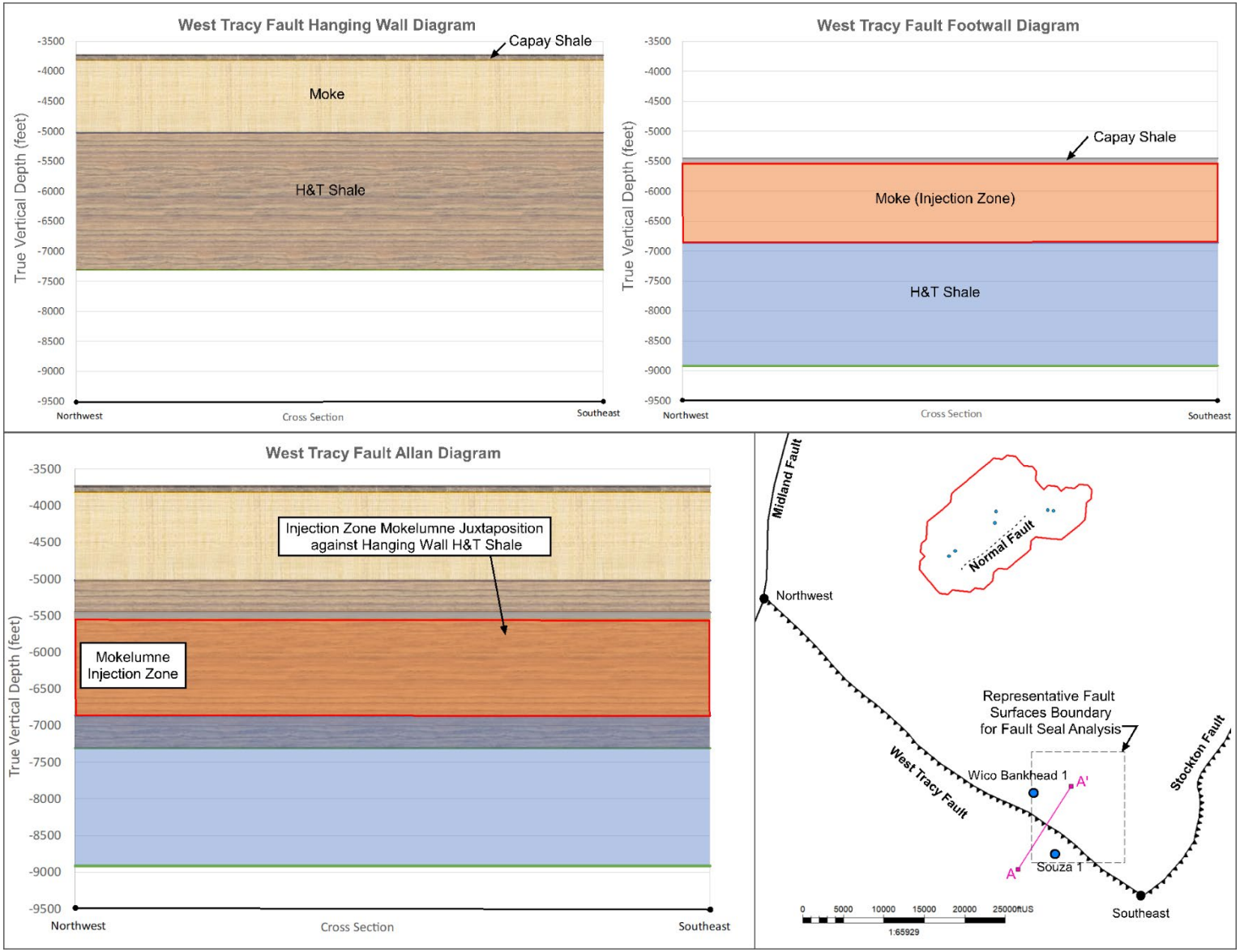

Figure A-22a. Allan diagram for the West Tracy Fault.

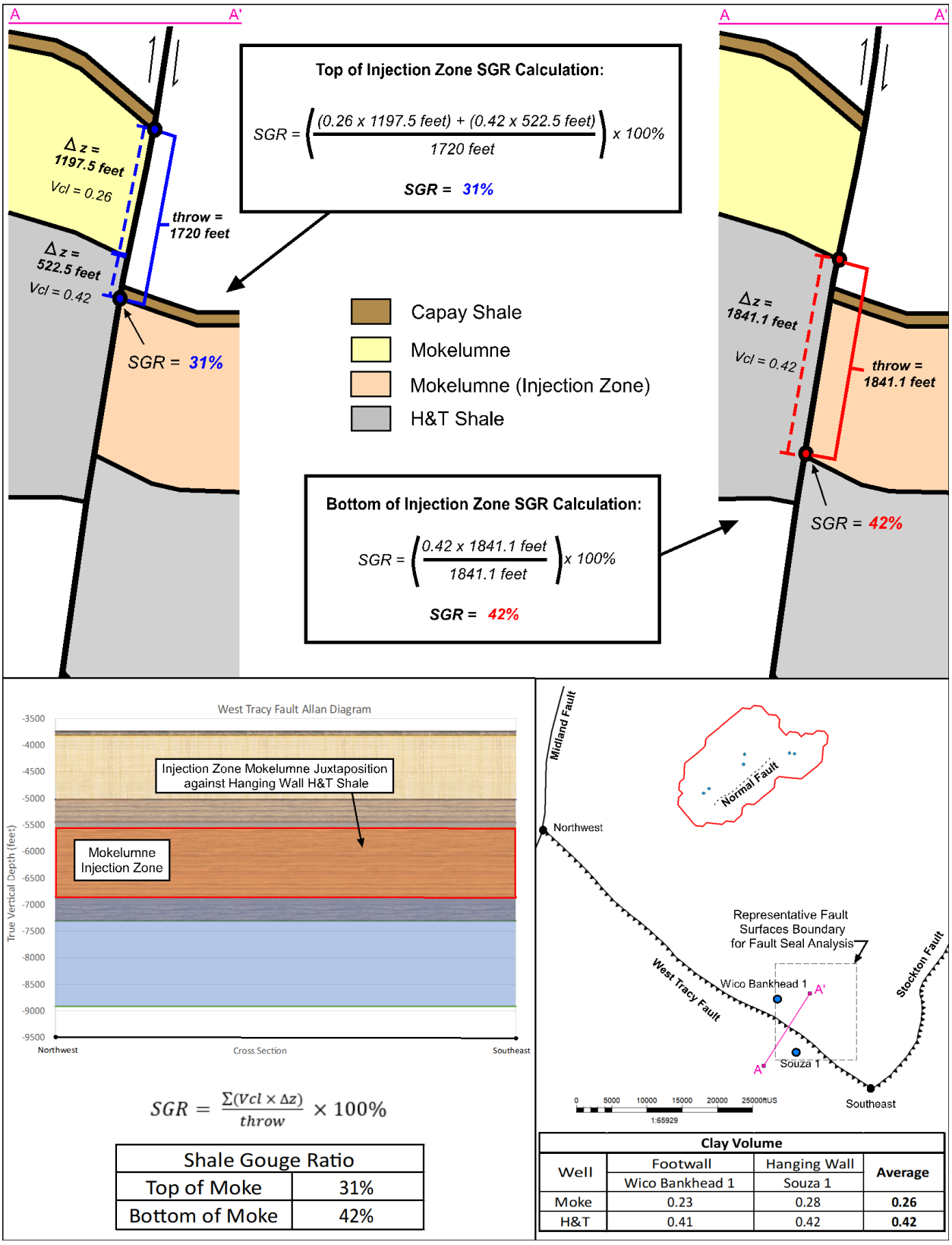

$$SGR = \frac{\Sigma(Vcl \times \Delta z)}{throw} \times 100\%$$

Shale Gouge Ratio	
Top of Moke	31%
Bottom of Moke	42%

Clay Volume			
Well	Footwall	Hanging Wall	Average
	Wico Bankhead 1	Souza 1	
Moke	0.23	0.28	**0.26**
H&T	0.41	0.42	**0.42**

Figure A-22b. Shale Gouge Ratio Calculations for the West Tracy Fault.

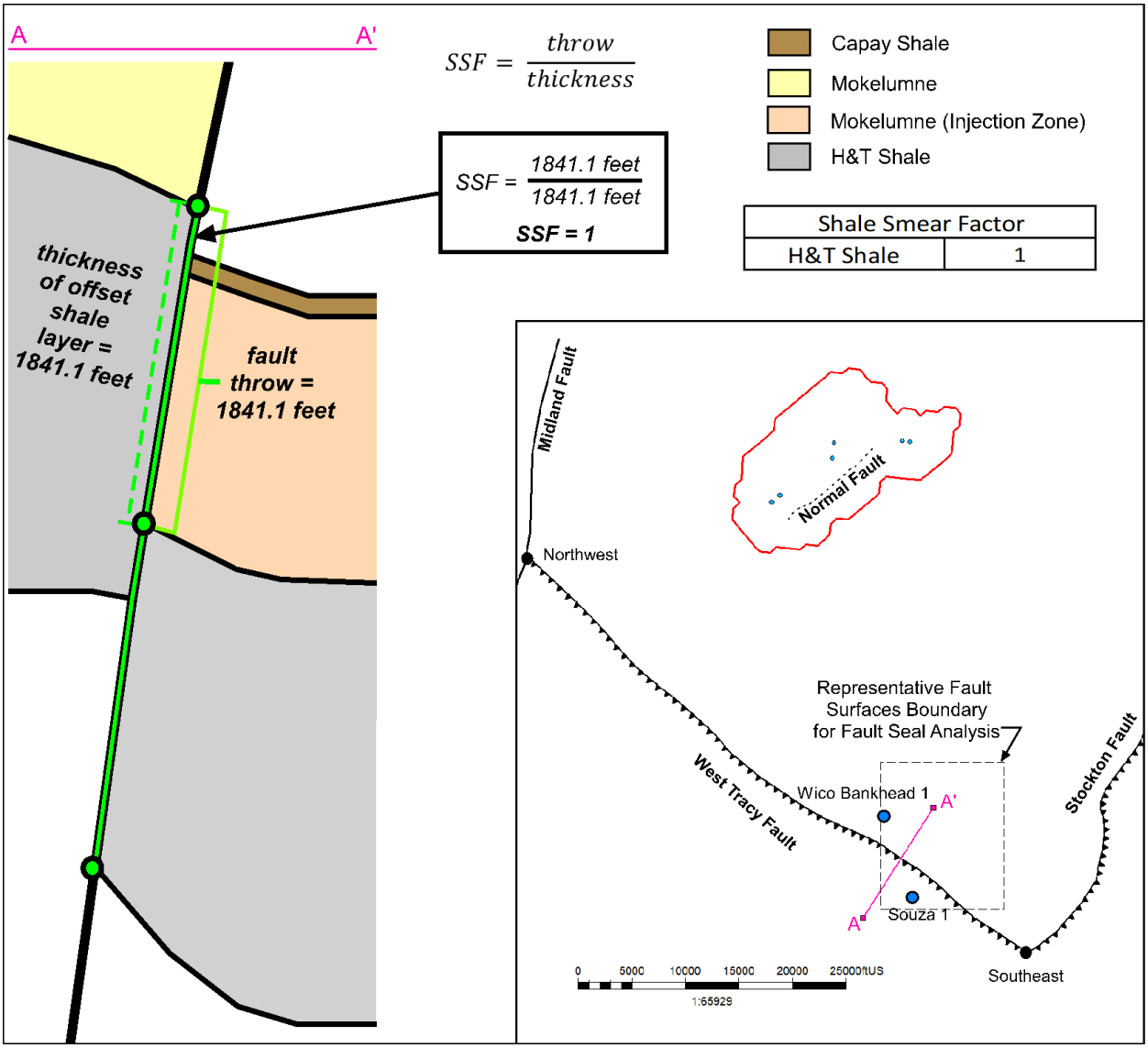

Figure A-22c. Shale Smear Factor Calculation for the West Tracy Fault.

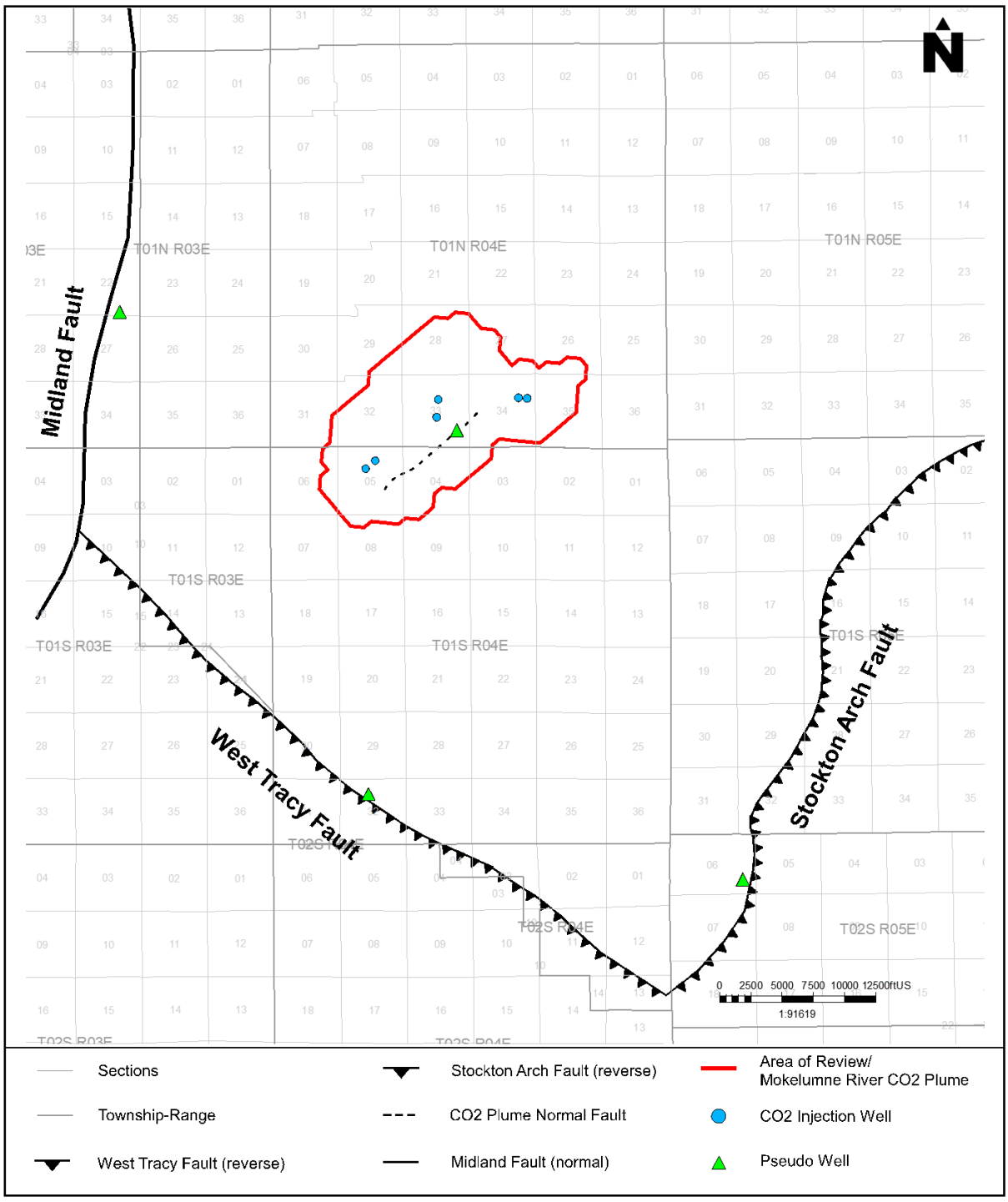

Figure A-23. Green triangles show pseudo well locations at central areas along the normal fault located in the CO_2 plume and the three bounding faults relative to the project area. Pressure data were extracted from the plume model to capture the expected pressure values at each location. Average of these results are presented in Table A-4.

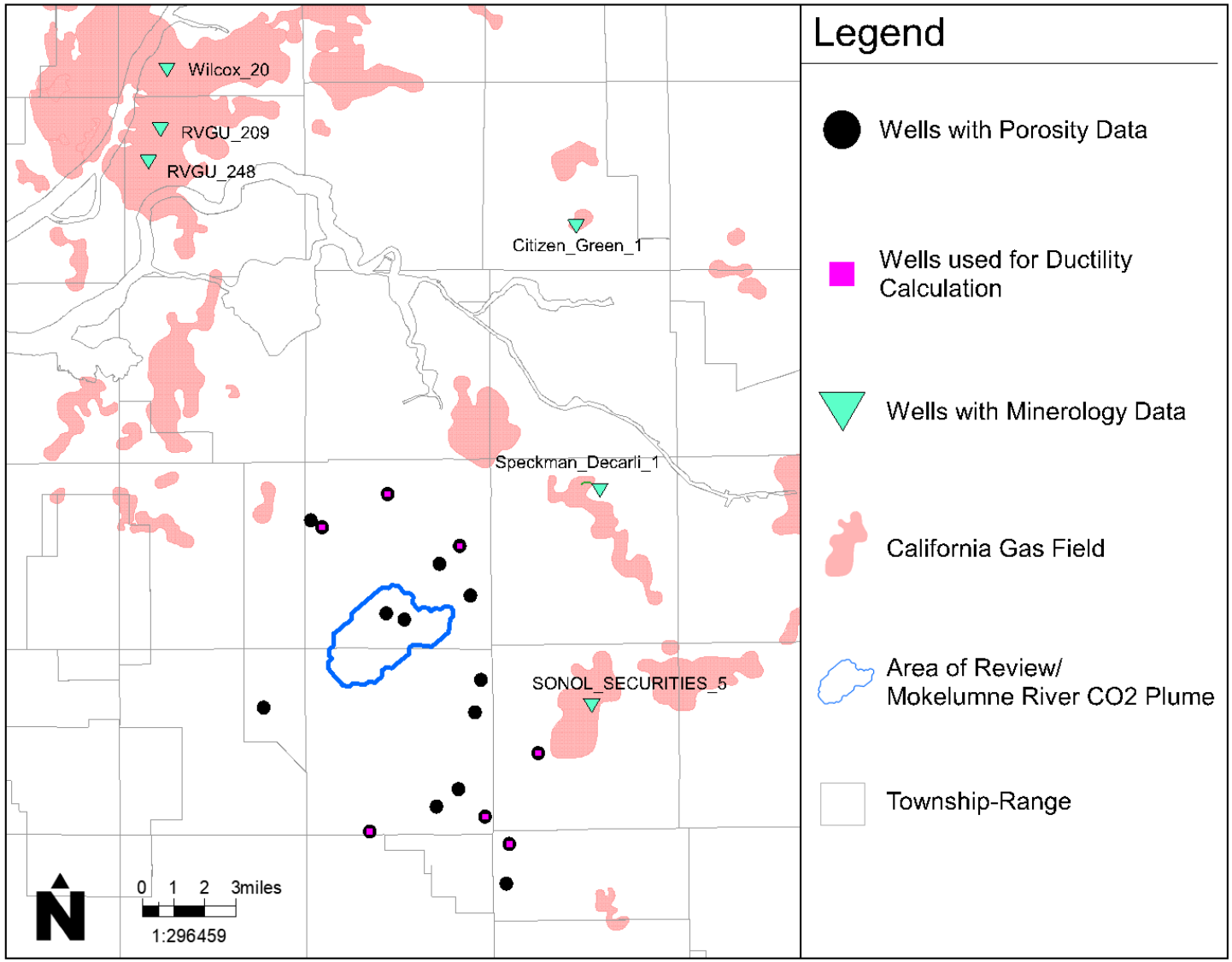

Figure A-24. Map showing location of wells with mineralogy data relative to the AoR.

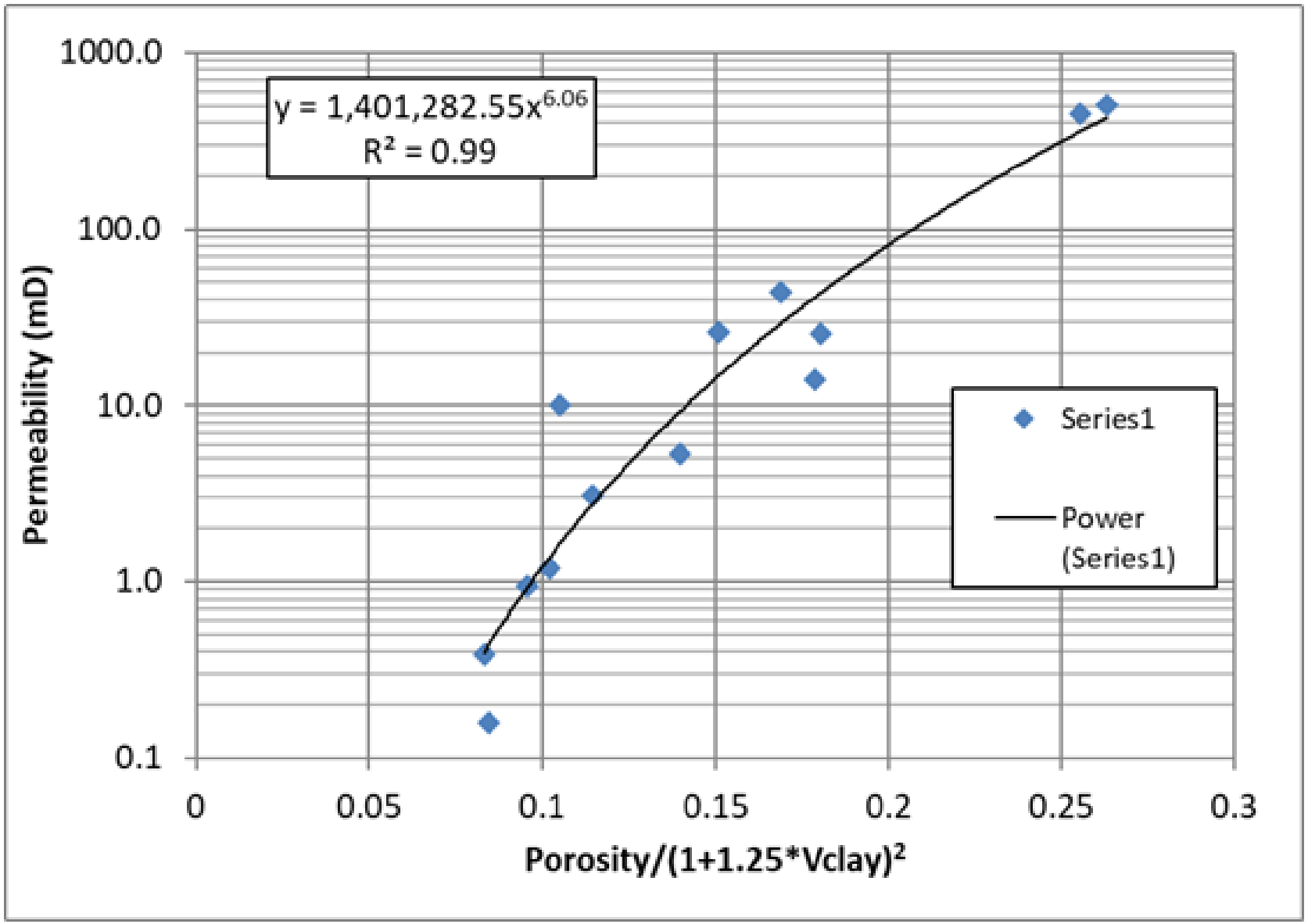

Figure A-25. Permeability transform for Sacramento basin zones.

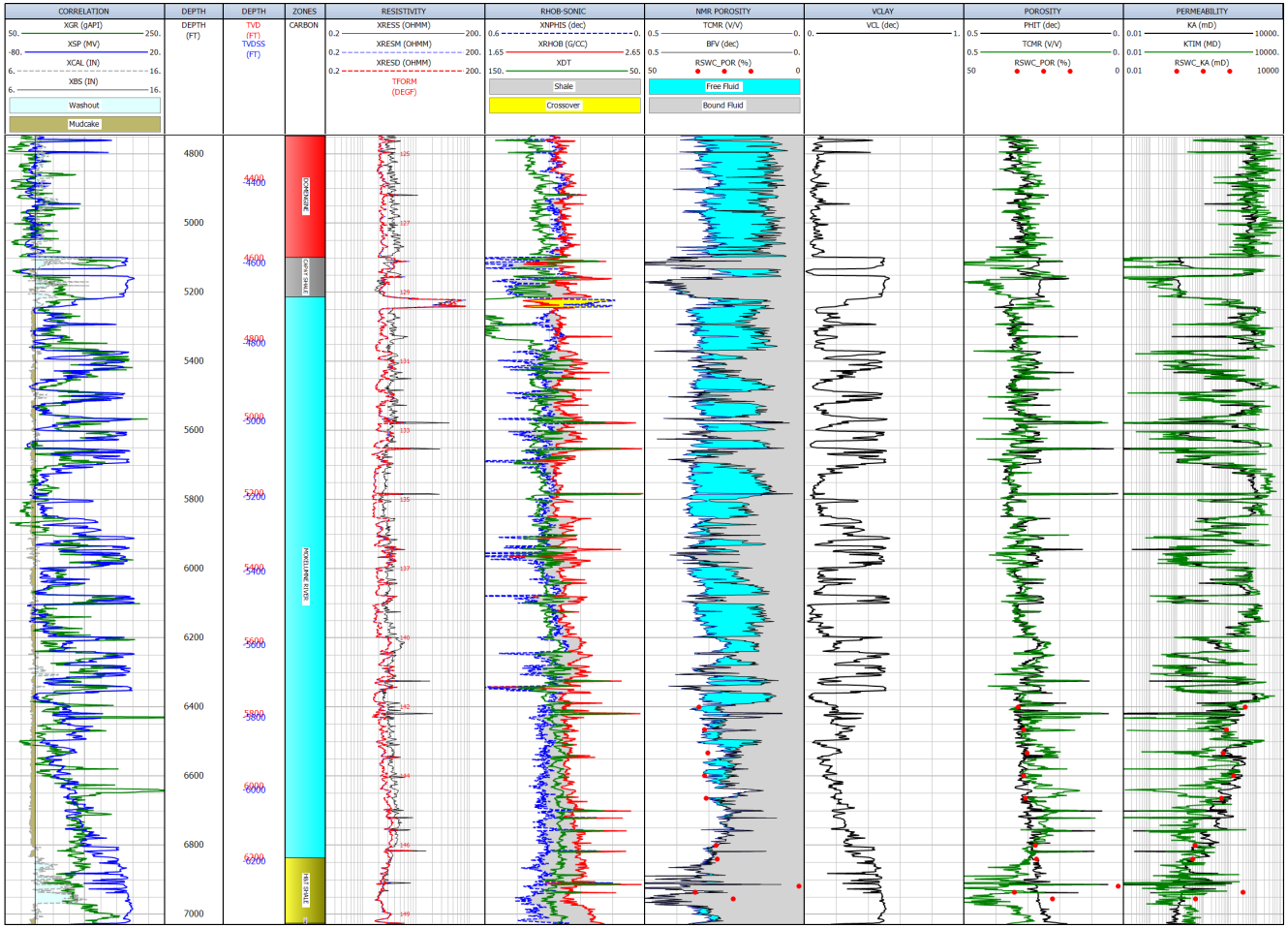

Figure A-26. Example log from the Citizen_Green_1 well in King Island Gas Field. The last track shows a comparison of the permeability calculated from the transform (black) shown in Figure A-20 to permeability calculated from an NMR log (green) and rotary sidewall core permeability (red dots). Track 1: Correlation and caliper logs. Track 2: Measured depth. Track 3: Vertical depth and vertical subsea depth. Track 4: Zones. Track 5: Resistivity. Track 6: Compressional sonic, density, and neutron logs. Track 7: NMR total porosity and bound fluid. Track 8: Volume of clay. Track 9: Porosity calculated from sonic and NMR total porosity (green). Track 10: Permeability calculated using transform and NMR Timur-Coates permeability.

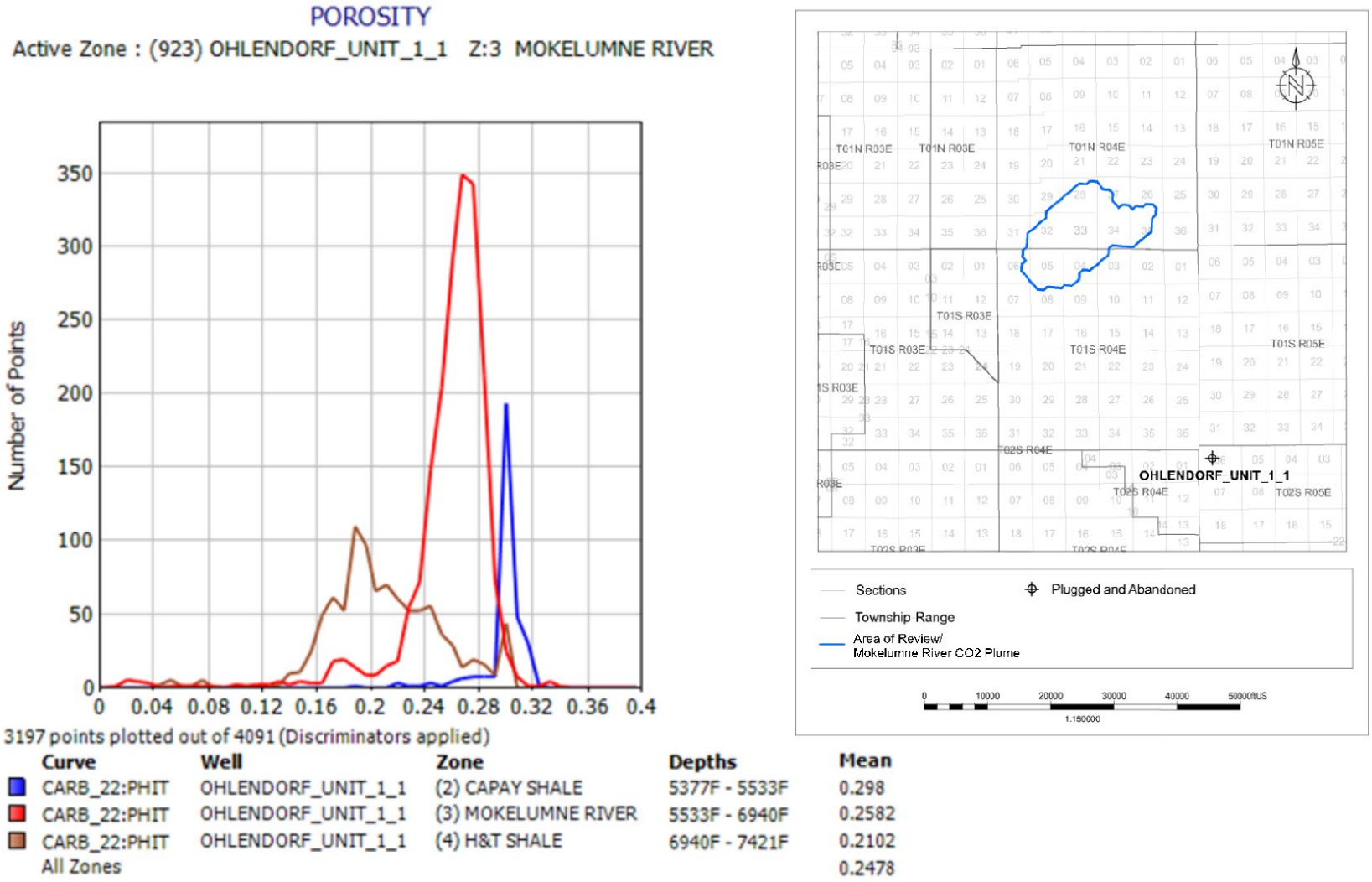

Figure A-27. Porosity histogram for well Ohlendorf_Unit_1_1. In the histogram, blue represents the Capay Shale, red the Mokelumne River Formation, and brown the H&T Shale. For the two shale intervals, only data with VCL>0.25 is shown, and for the Mokelumne River Formation only data with VCL≤0.25 is shown.

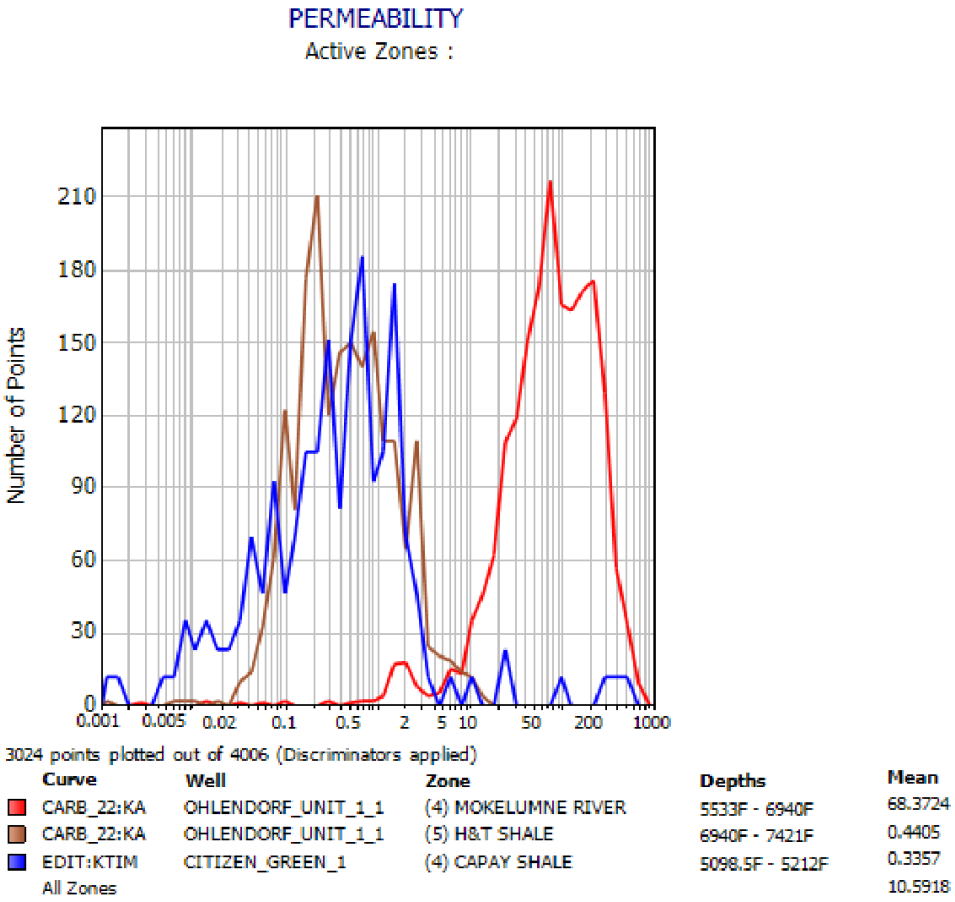

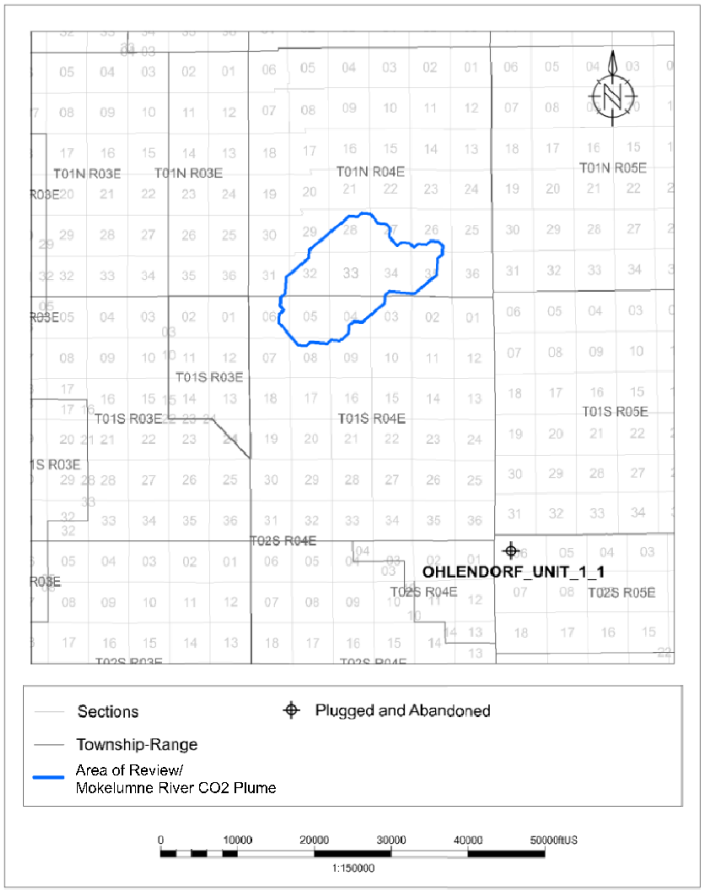

Figure A-28. Permeability histogram for wells Ohlendorf_Unit_1_1 and Citizen_Green_1. In the histogram, blue represents the Capay Shale, red the Mokelumne River Formation, and brown the H&T Shale. For the two shale intervals, only data with VCL>0.25 is shown, and for the Mokelumne River Formation only data with VCL≤0.25 is shown.

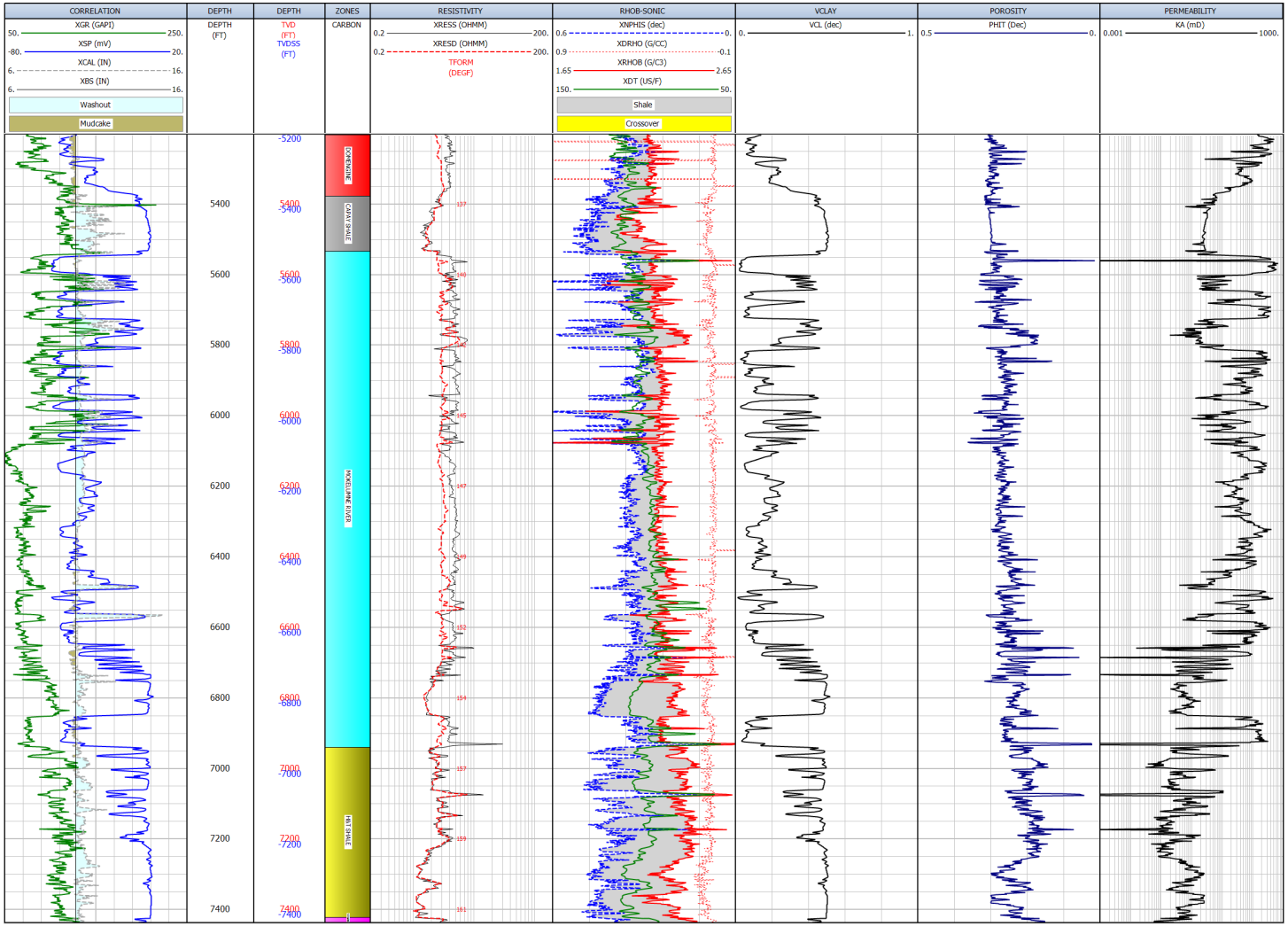

Figure A-29. Log plot for well Ohlendorf_Unit_1_1, showing the log curves used as inputs into calculations of clay volume, porosity and permeability, and their outputs. Track 1: Correlation and caliper logs. Track 2: Measured depth. Track 3: Vertical depth and vertical subsea depth. Track 4: Zones. Track 5: Resistivity. Track 6: Compressional sonic, neutron, and density logs. Track 7: Volume of clay. Track 8: Porosity calculated from log curves. Track 9: Permeability calculated using transform. See Figure A-30 for well location.

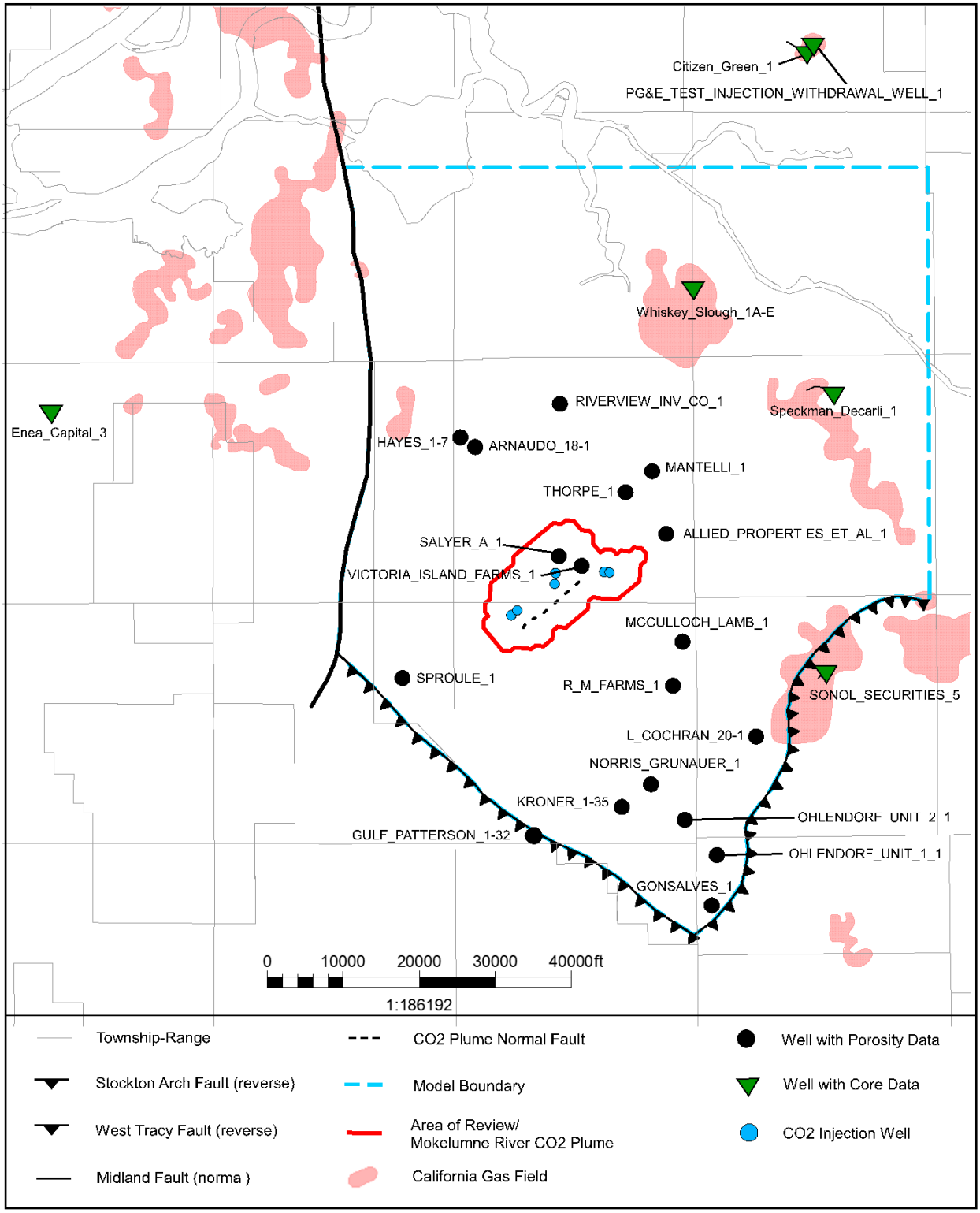

Figure A-30. Map of wells with porosity and permeability data.

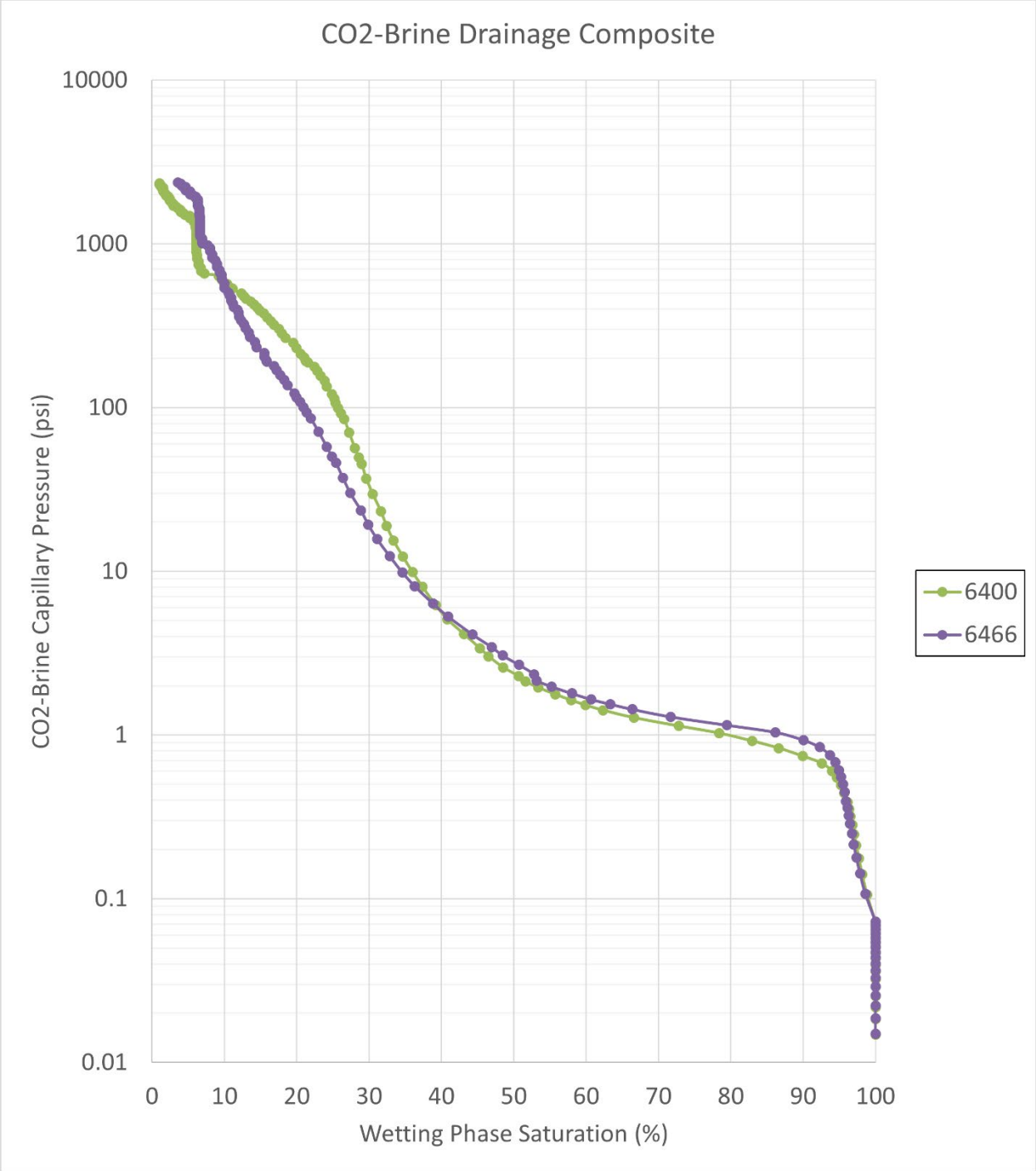

Figure A-31. Capillary pressure versus wetting phase saturation for core data from the Citizen_Green_1 well. Samples are labeled by their depth.

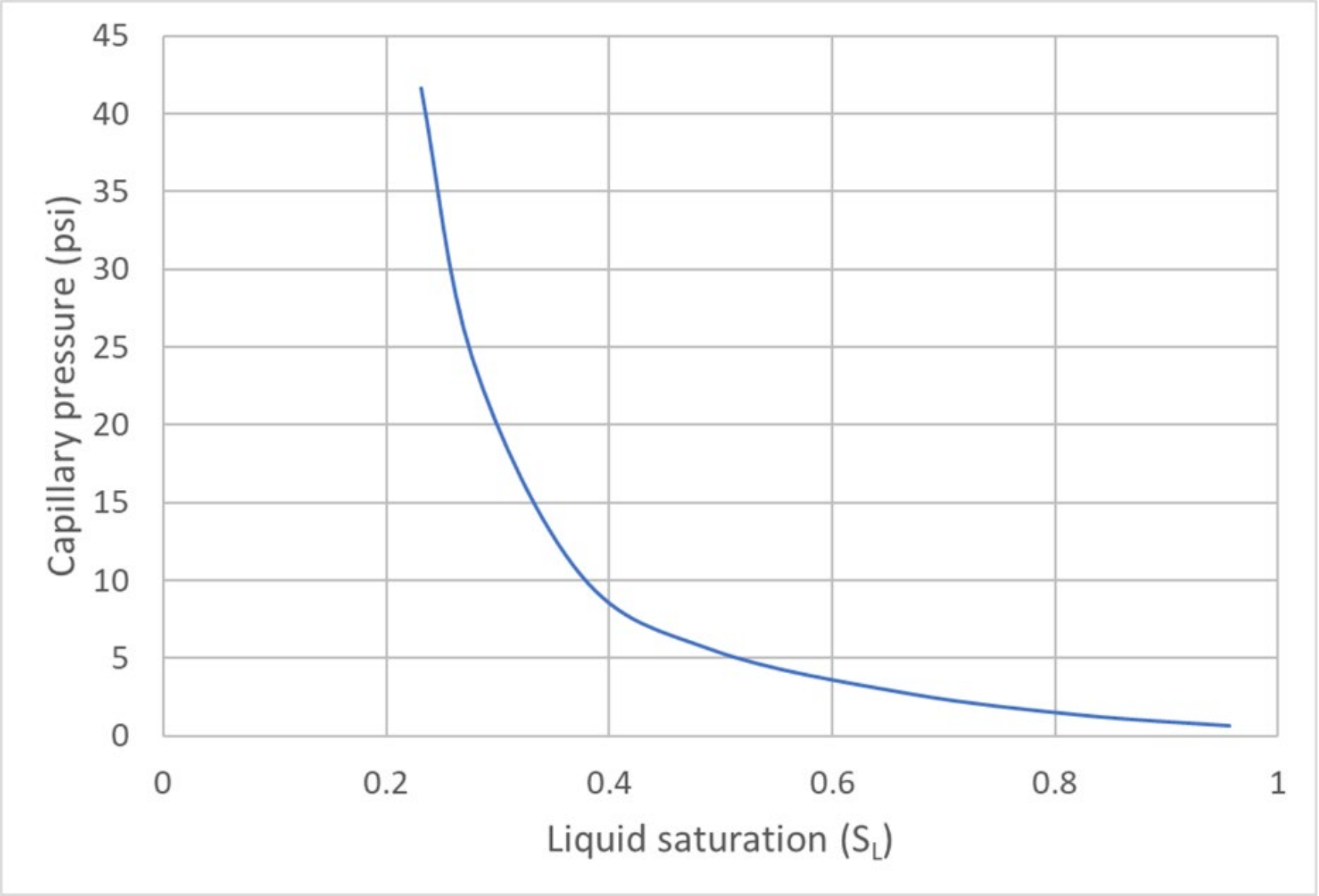

Figure A-32. Injection zone capillary pressure used for computational modeling.

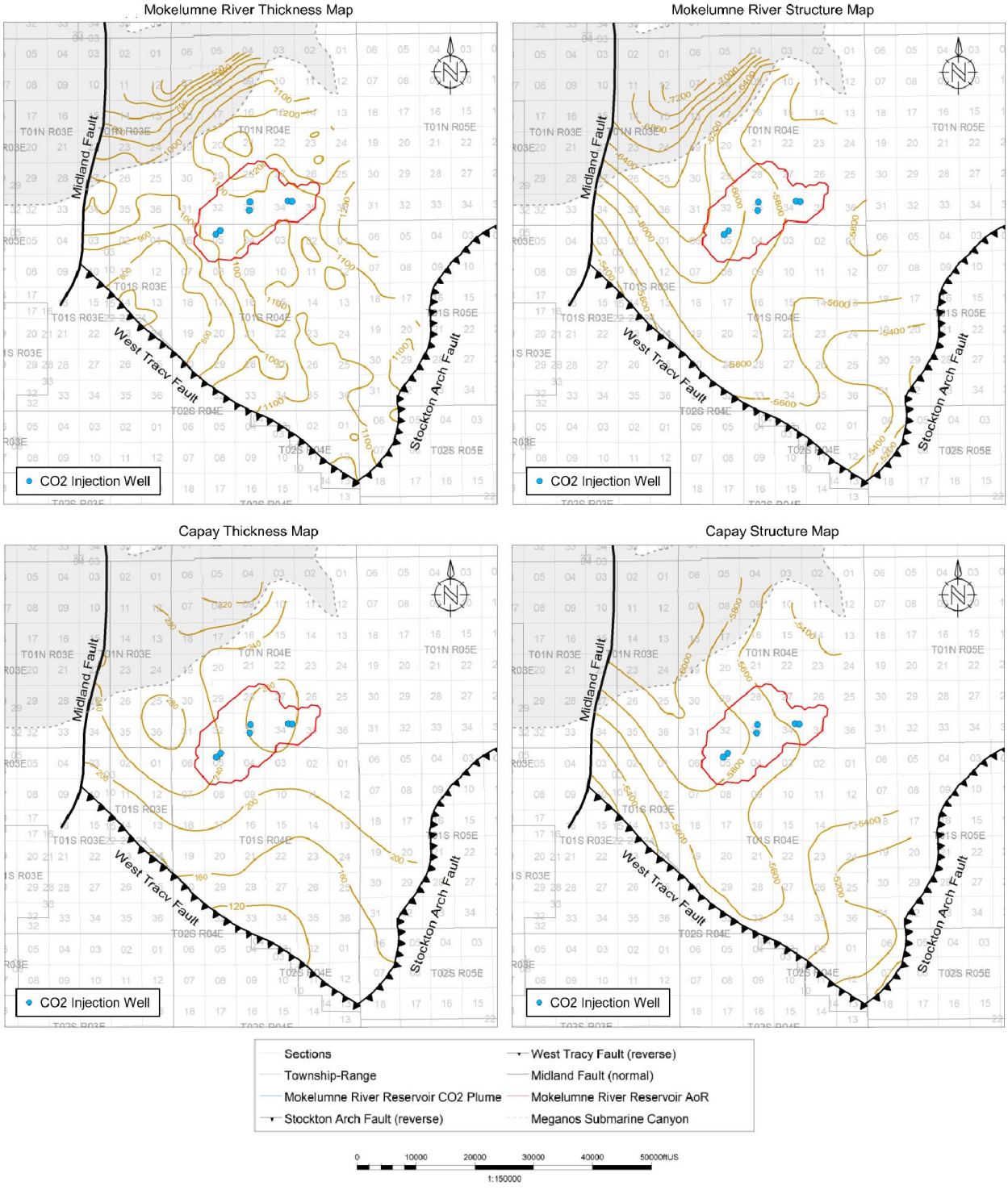

Figure A-33. Thickness and structure maps for the Mokelumne River and Capay Shale Formations within the vicinity of the AoR.

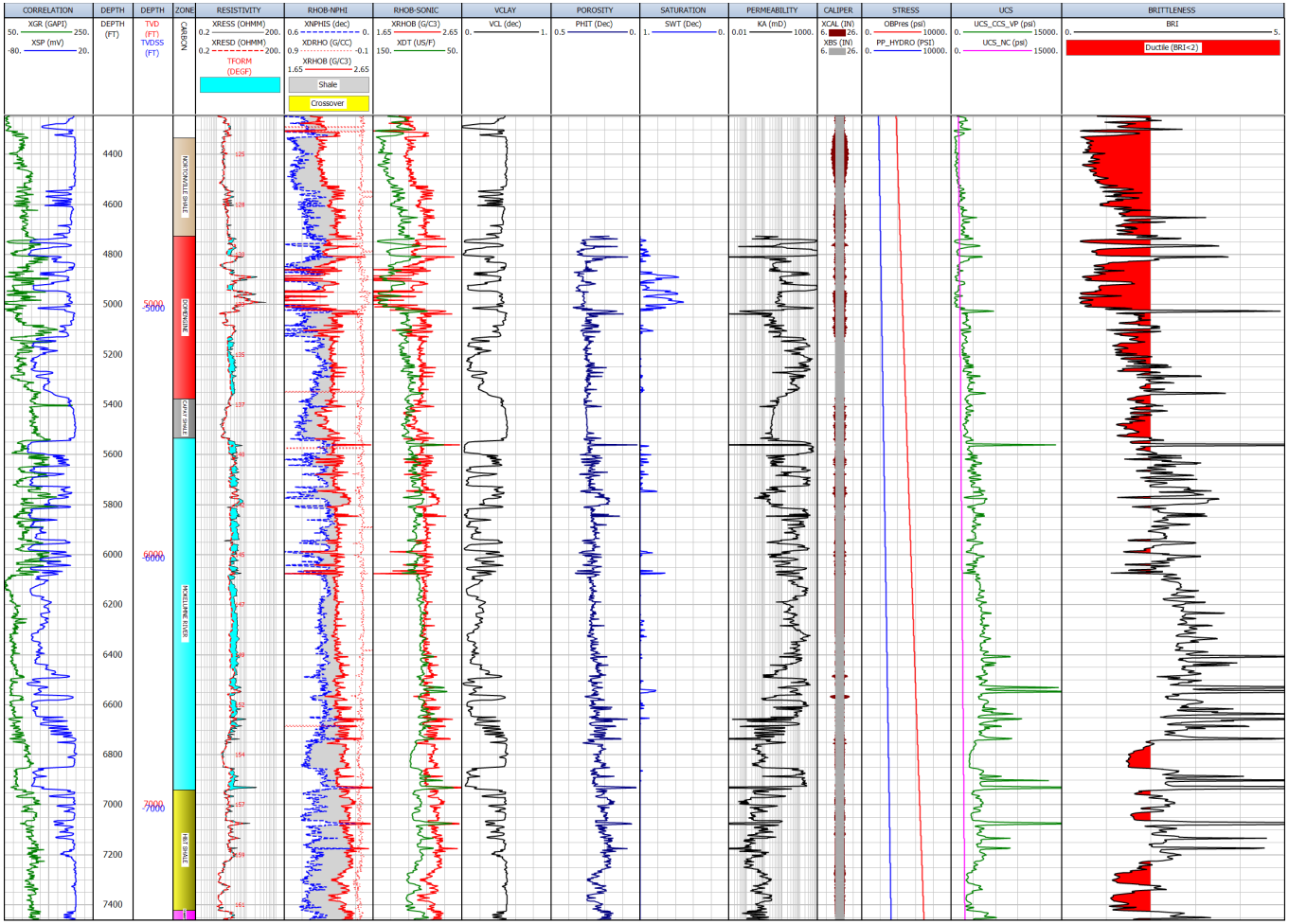

Figure A-34. Unconfined compressive strength and ductility calculations for well Ohlendorf_Unit_1_1. The Capay Shale ductility is less than two, as is the shallower Nortonville Shale. Track 1: Correlation logs. Track 2: Measured depth. Track 3: Vertical depth and vertical subsea depth. Track 4: Zones. Track 5: Resistivity. Track 6: Density and neutron logs. Track 7: Density and compressional sonic logs. Track 8: Volume of clay. Track 9: Porosity calculated from sonic and density. Track 10: Water saturation. Track 11: Permeability. Track 12: Caliper. Track 13: Overburden pressure and hydrostatic pore pressure. Track 14: UCS and UCS_NC. Track 15: Brittleness. See Figure A-30 for well location.

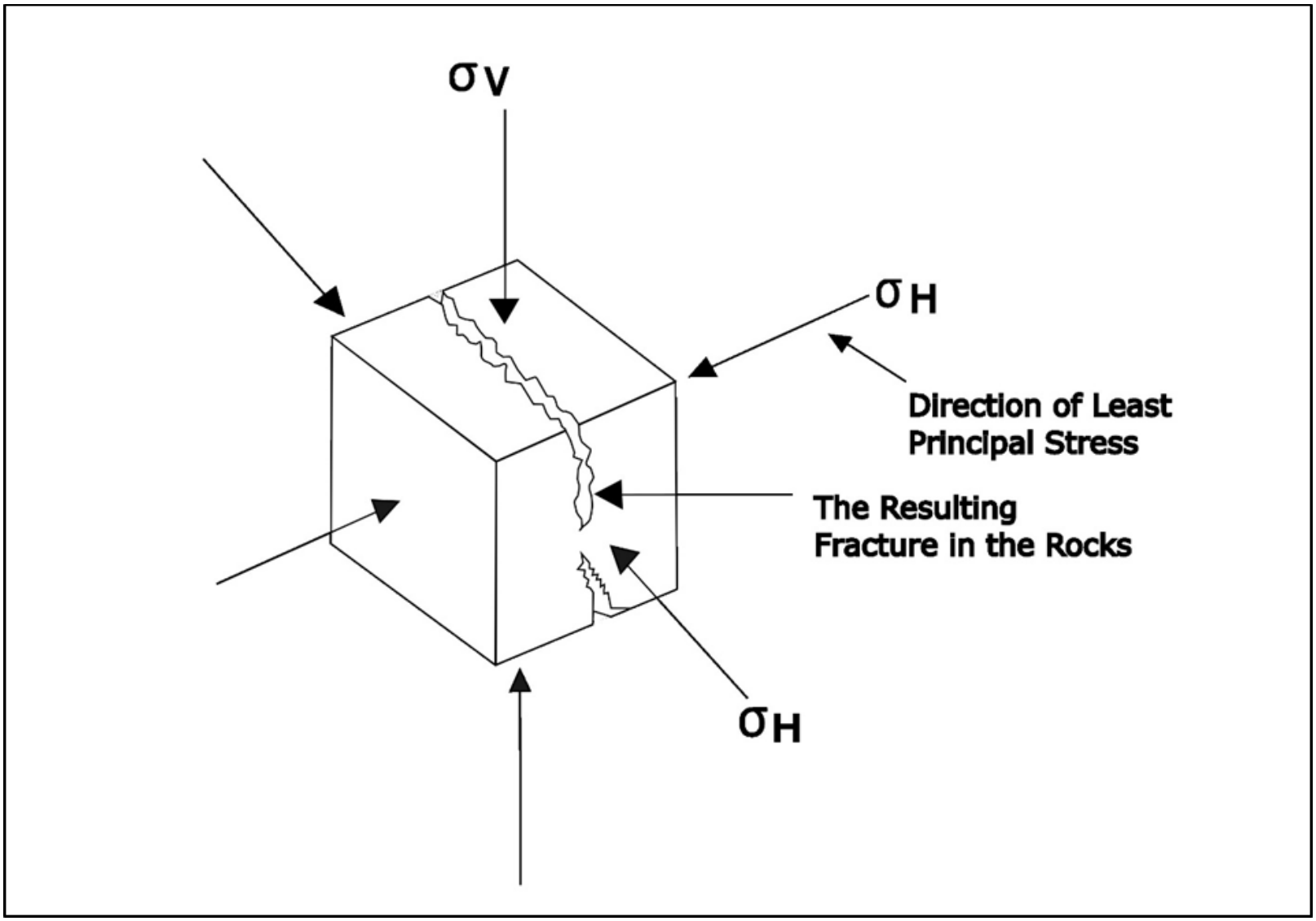

Figure A-35. Stress diagram showing the three principal stresses and the fracturing that will occur perpendicular to the minimum principal stress.

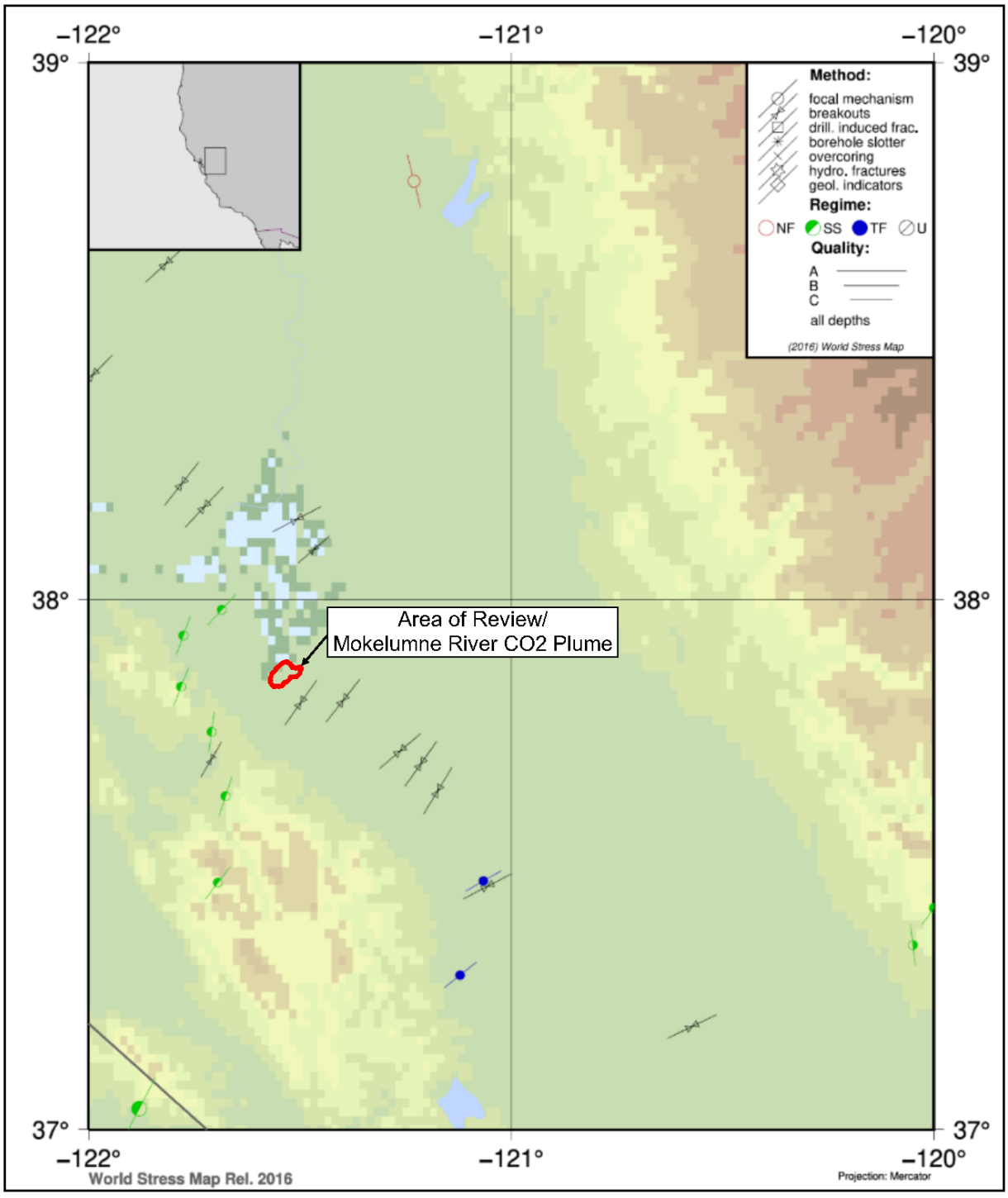

Figure A-36. World Stress Map output showing S_{Hmax} azimuth indicators and earthquake faulting styles in the Sacramento Basin (Heidbach et al., 2016). In red is the outline of the Mokelumne River Formation AoR. The background coloring represents topography.

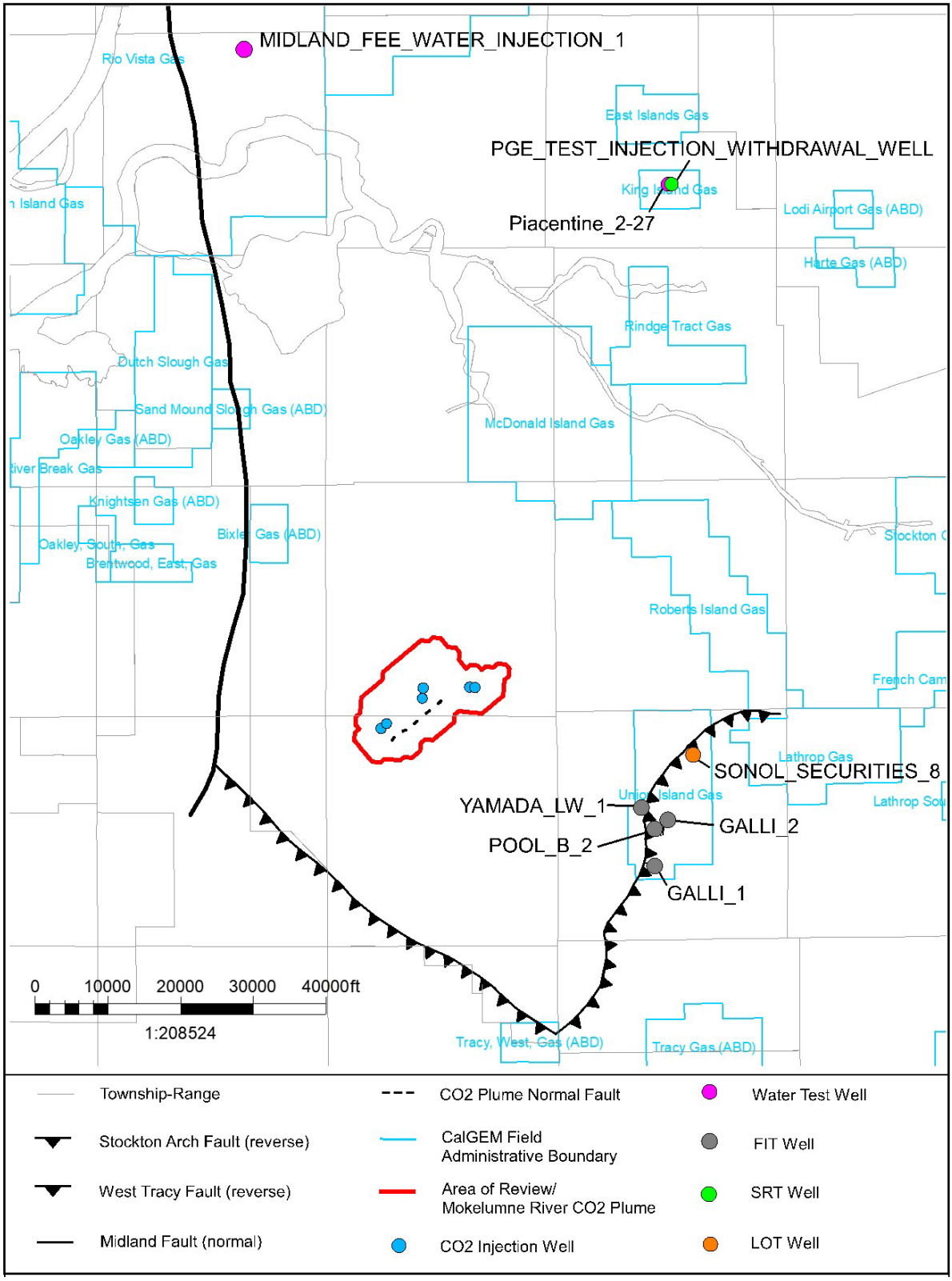

Figure A-37. Map showing the locations of wells with water tests, formation integrity tests (FITs), step rate tests (SRTs), and leak off tests (LOTs).

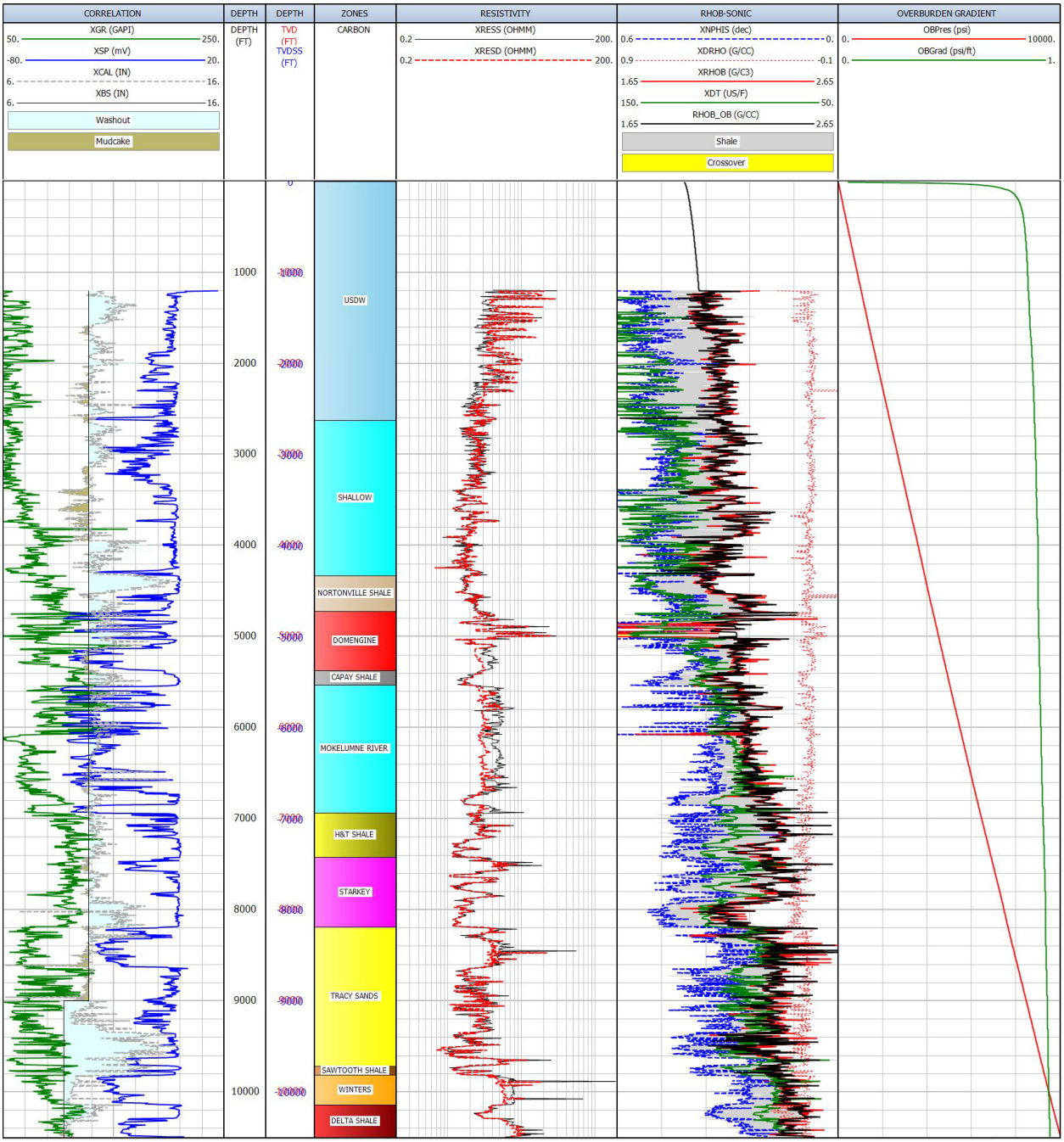

Figure A-38. Overburden gradient calculation for the Ohlendorf_Unit_1_1 (04077203480000). Track 1: Correlation logs and caliper log. Track 2: Measured depth. Track 3: Vertical depth and vertical subsea depth. Track 4: Zones. Track 5: Resistivity. Track 6: Density, neutron, and compressional sonic logs. The black curve shows the merged density curve with the shallow density trend as determined from nearby shallow density logs that was used for the overburden calculation. Track 7: Overburden pressure (red) and overburden gradient (green).

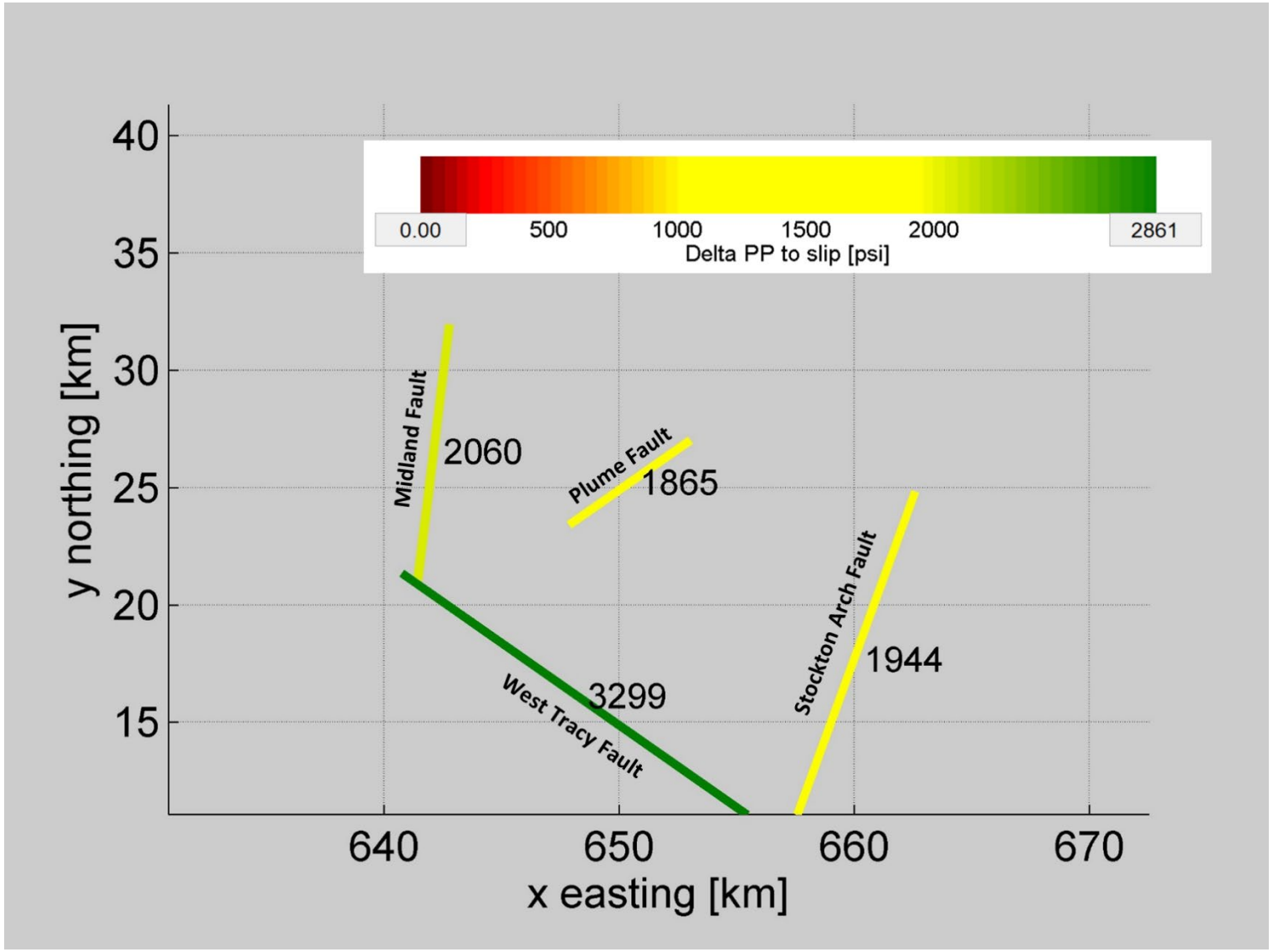

Figure A-39. Map showing the four modeled faults. The numbers on the plot next to each fault represent the necessary increase in pore pressure above present-day conditions to cause failure on that fault segment.

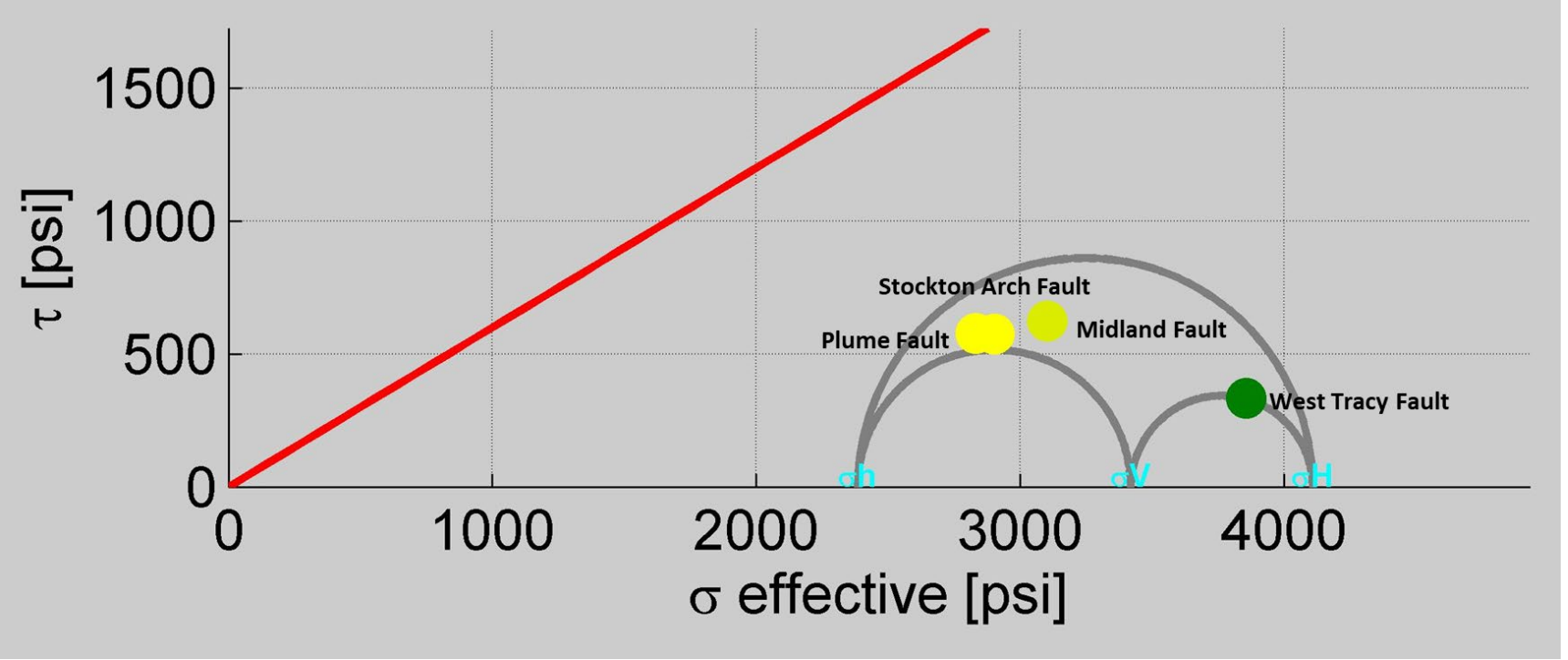

Figure A-40. **Mohr circle of the Mokelumne River Formation at present-day conditions. The effective normal stress (x-axis) and shear stress (y-axis) on the four modeled faults are represented by the yellow and green dots. The red line represents the Mohr coulomb failure surface assuming a coefficient of friction of 0.6 and a fault cohesion of 0 psi.**

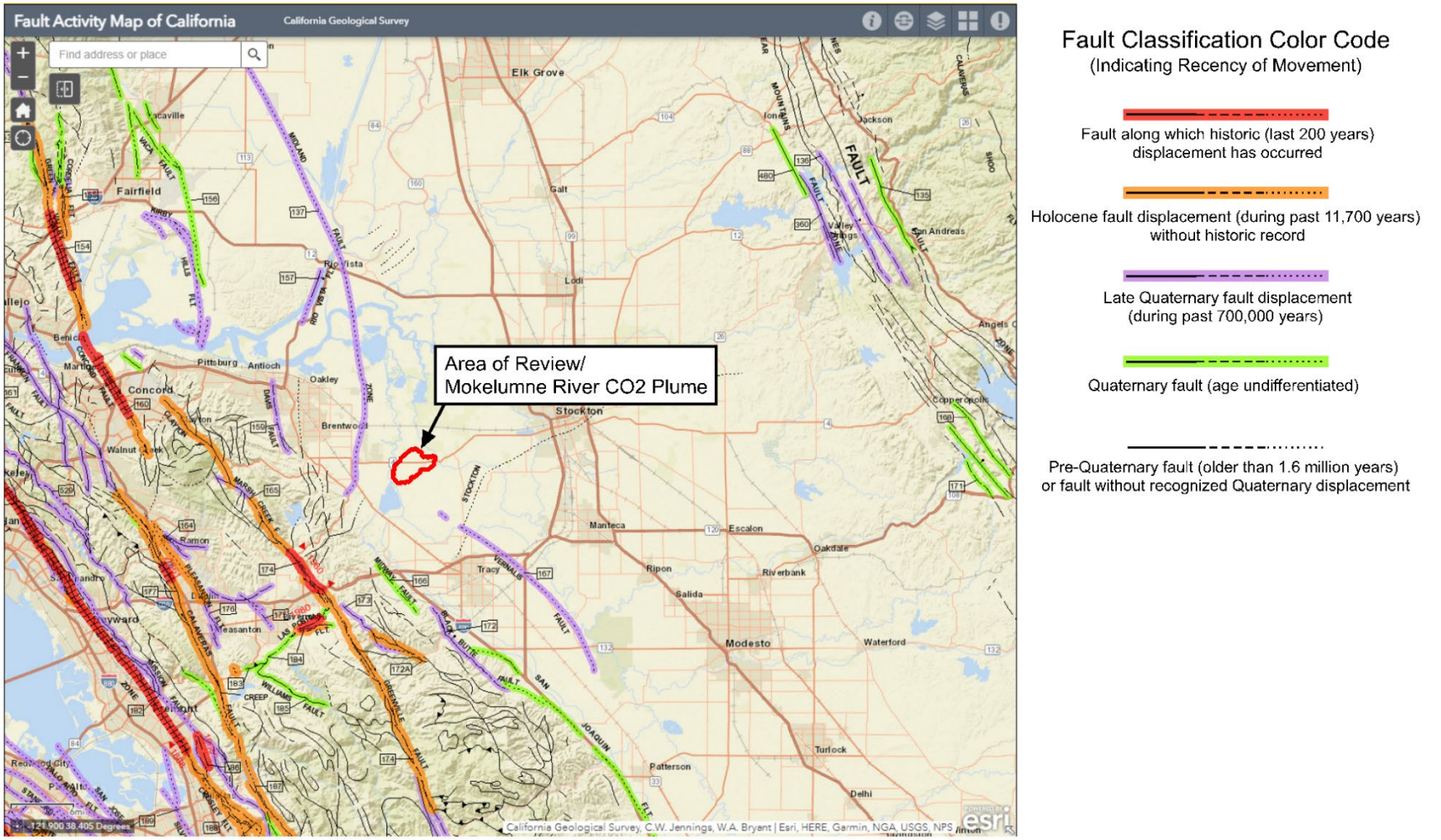

Figure A-41. Fault Activity Map from the California Geologic Survey. Fault traces shown agree with the interpretation of CRC/CTV. The Stockton Arch Fault is considered Pre-Quaternary associated with Post-Eocene/Pre-Miocene movement. The Midland Fault was active in the late Cretaceous-Eocene time; however, the southern end of the Midland fault has been interpreted as reactivated as a reverse fault in the late Cenozoic transpressional tectonic setting.

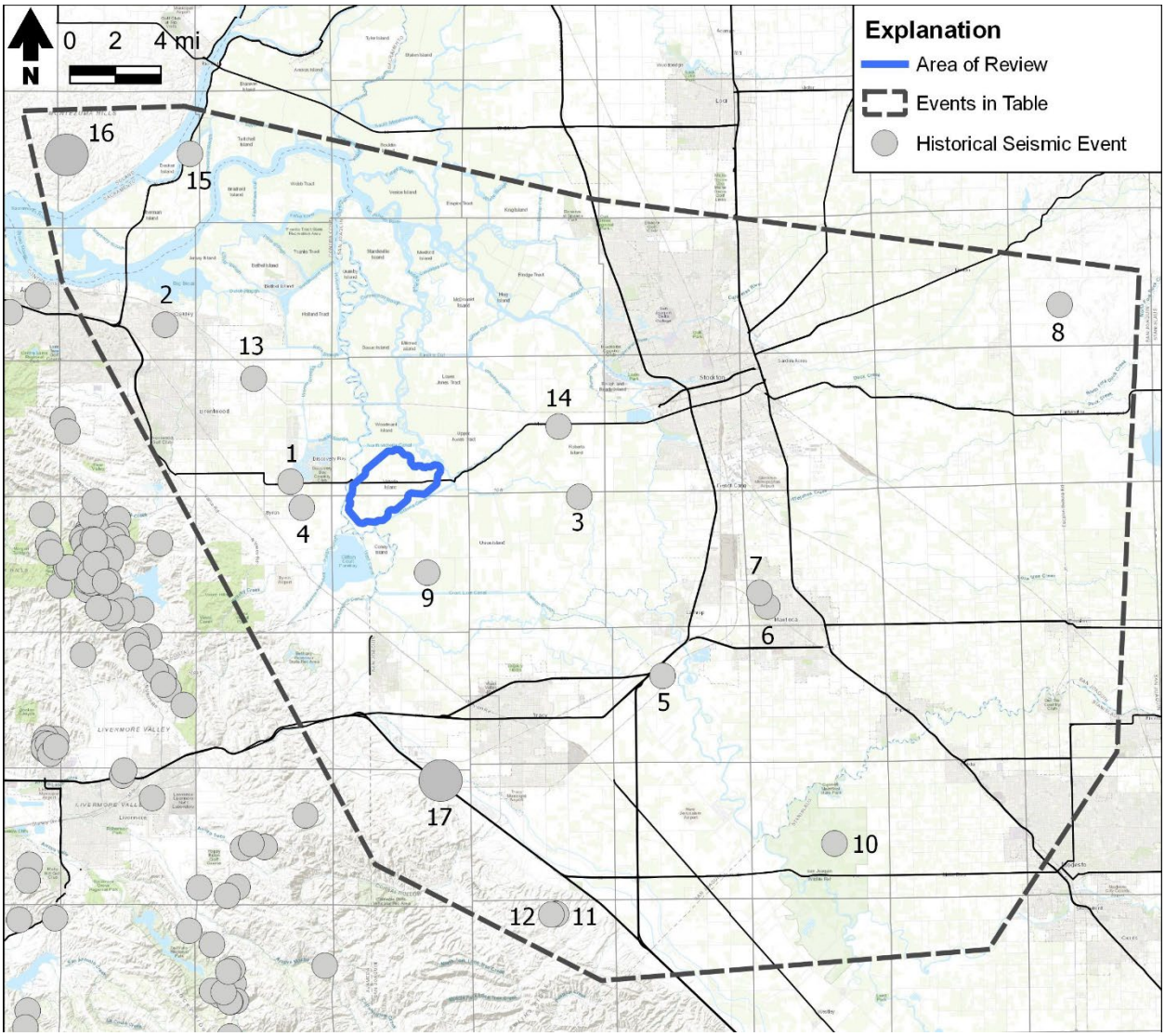

Figure A-42 **Historical earthquakes from the USGS catalog tool for the greater area. Data from these events are compiled in Table A-12 in chronological order associated with events 1 through 16 on the map. Events are sized by magnitude and those to the west are removed due to their association with a different fault trend.**

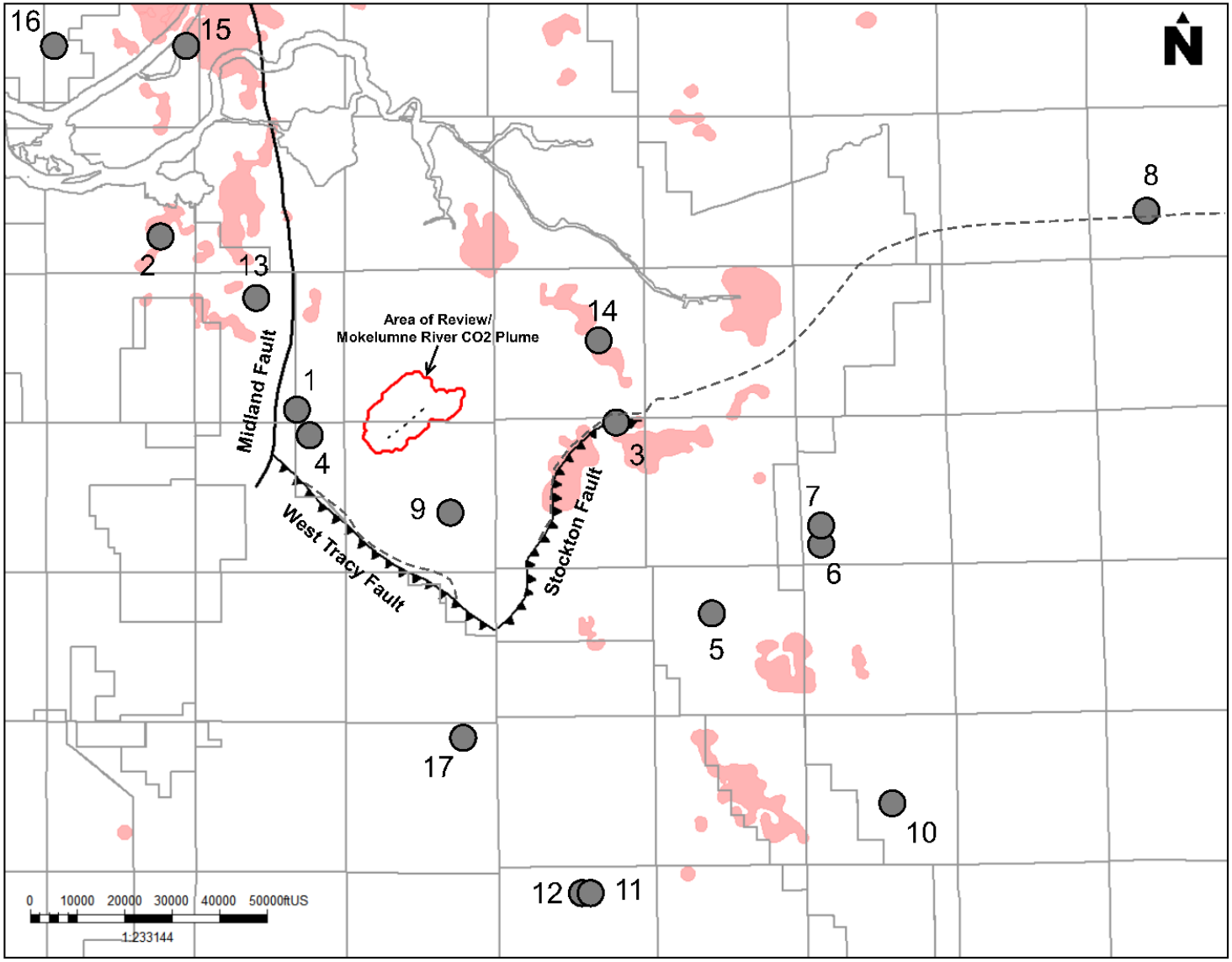

Figure A-43. Summary map of event locations from the USGS catalog relative to the mapped faults near the AoR of CTV III. California Gas Fields are shown in light red for reference.

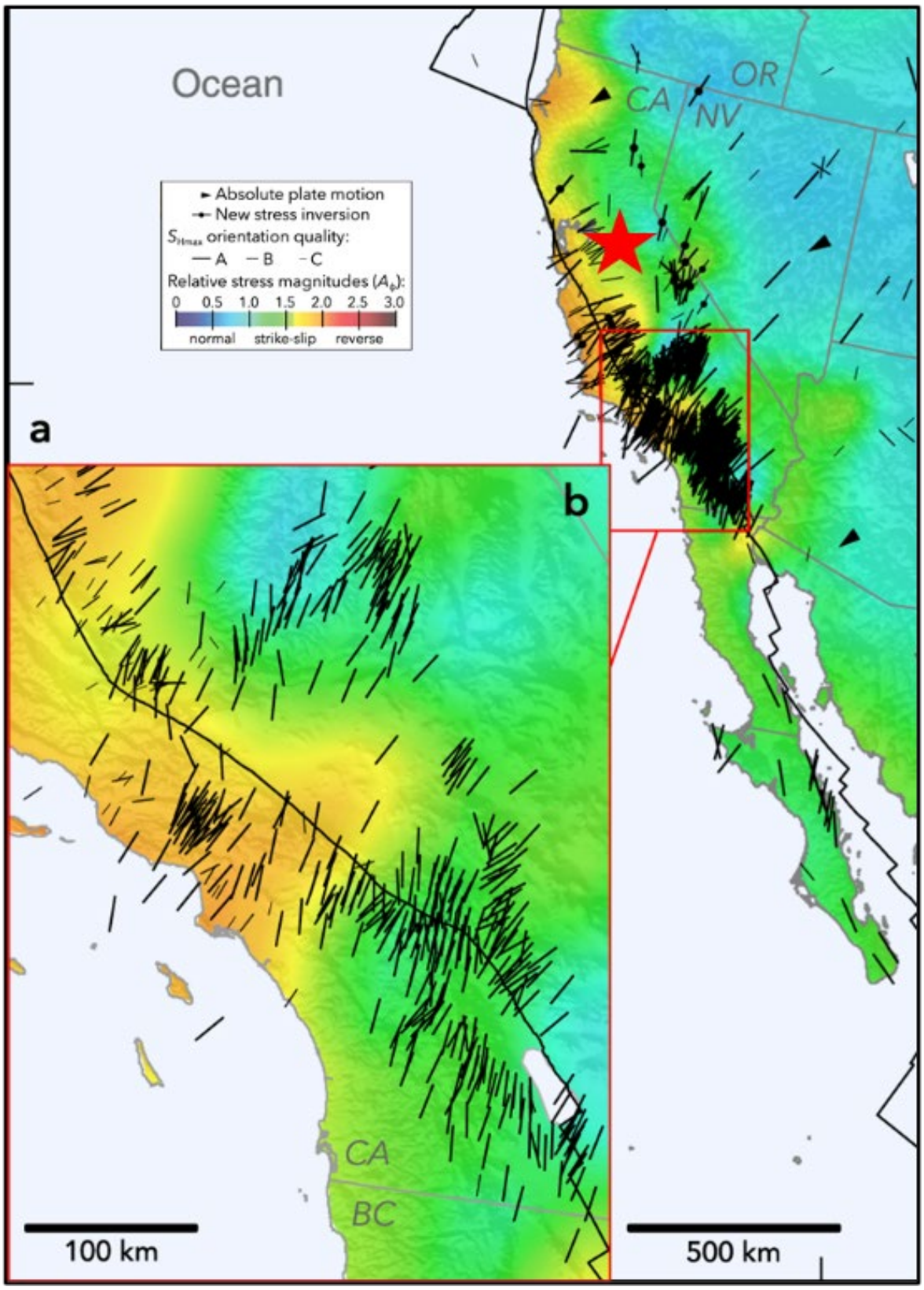

Figure A-44. Image modified from Lund-Snee and Zoback (2020) showing relative stress magnitudes across California. Red star indicates the CTV III site area.

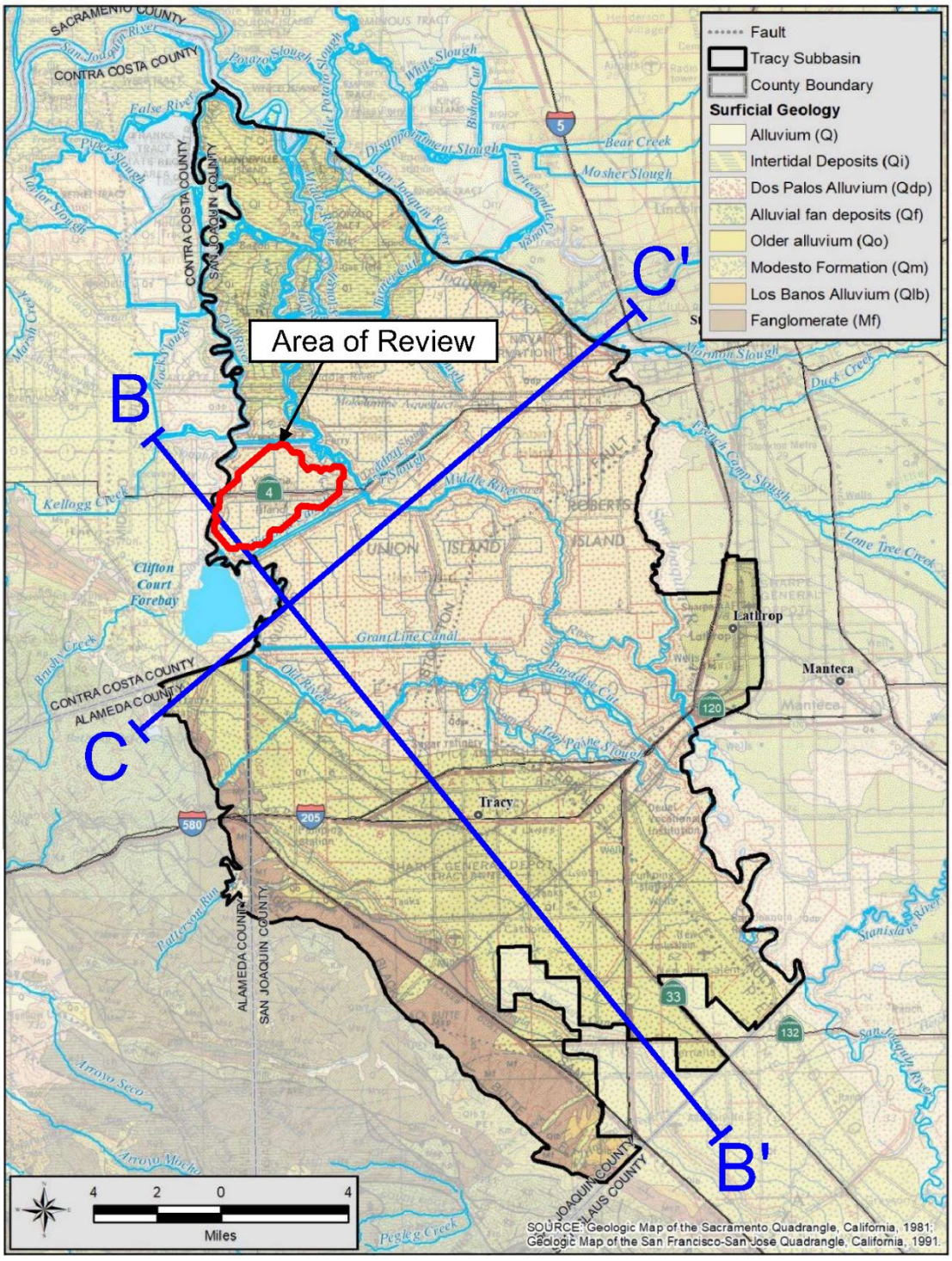

Figure A-45. Tracy Subbasin, surface geology, and cross section index map.

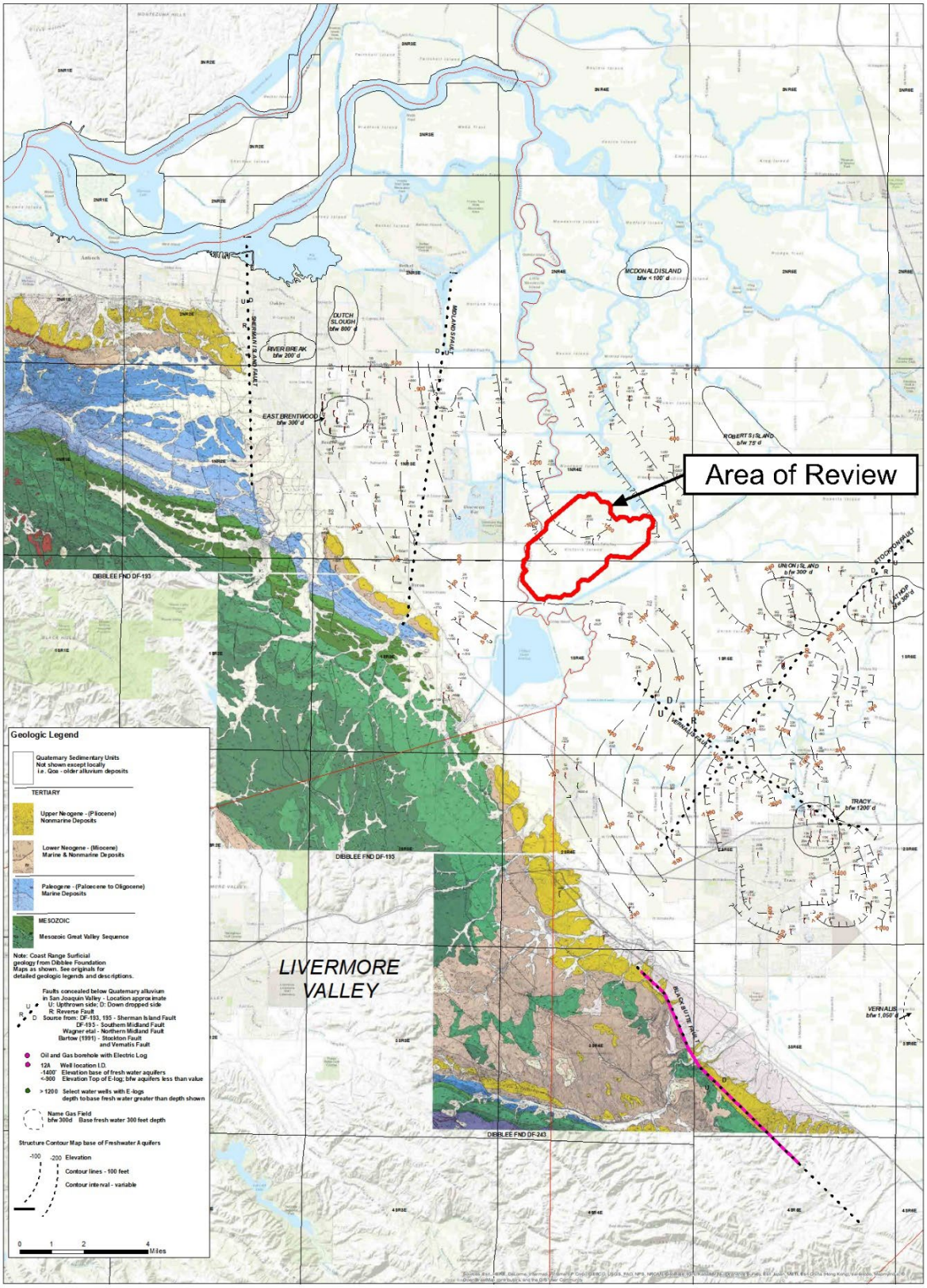

Figure A-46. Geologic map and base of fresh water.

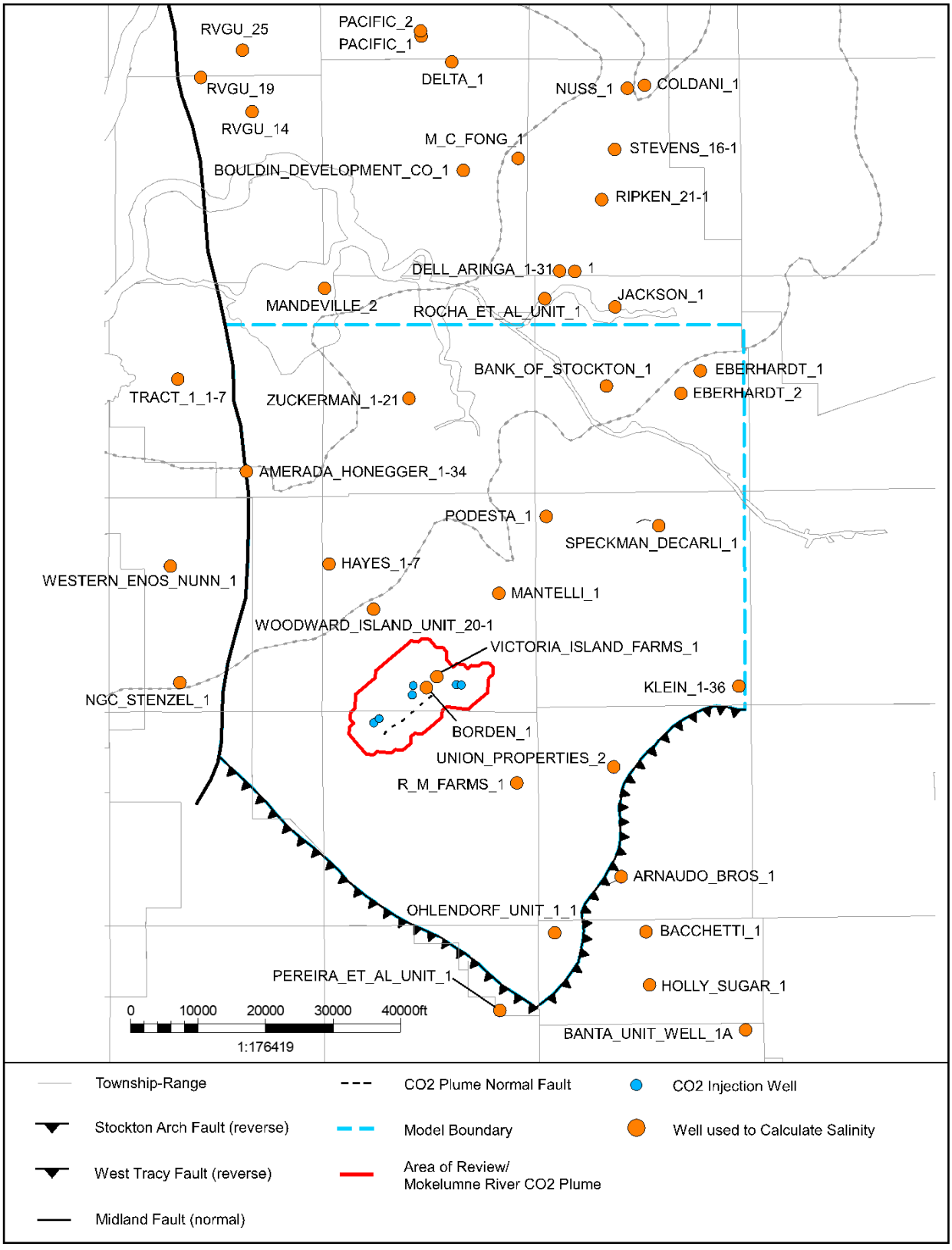

FigureA-47. Map of wells used to calculate salinity.

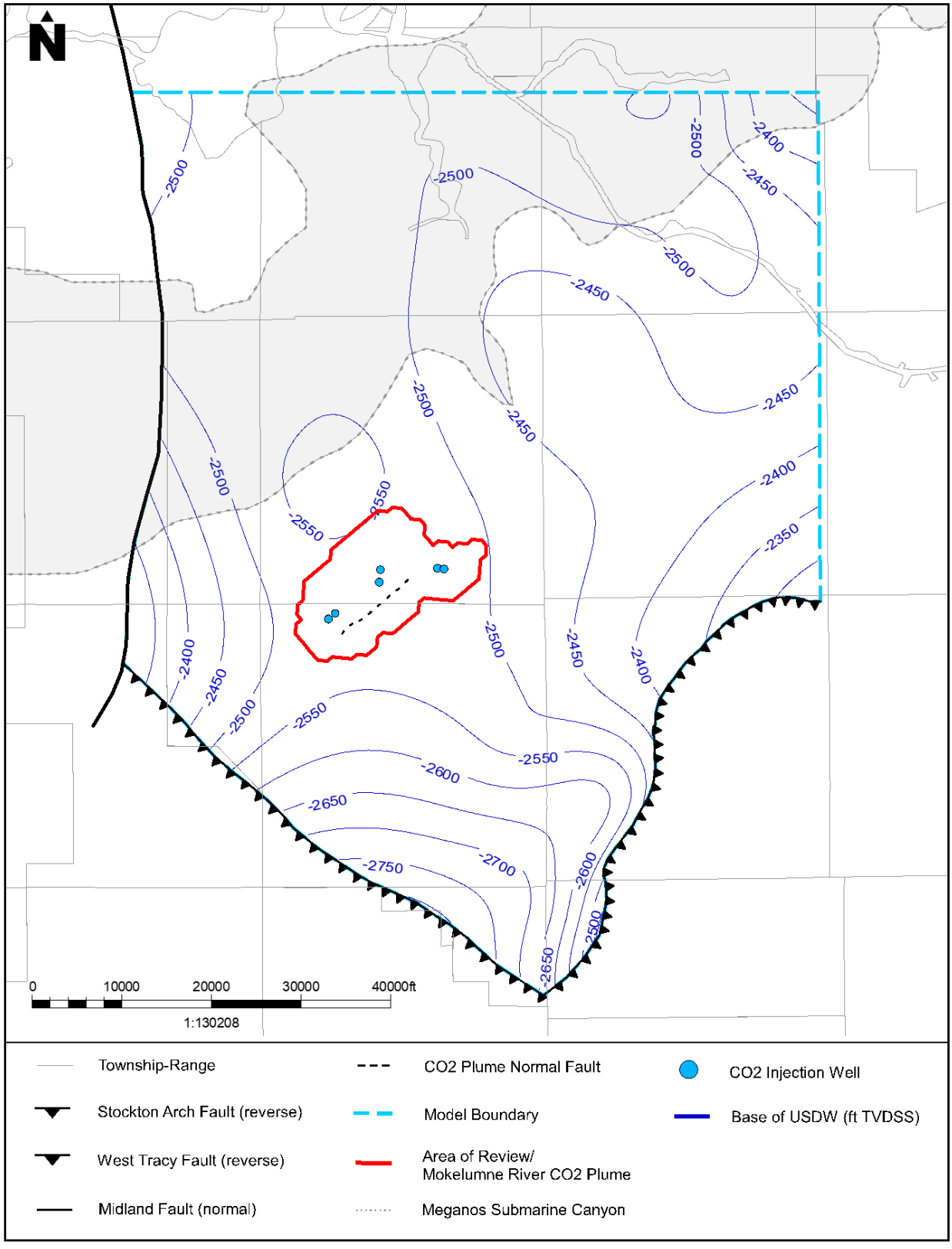

FigureA-48. Base of lowermost USDW map in project vicinity.

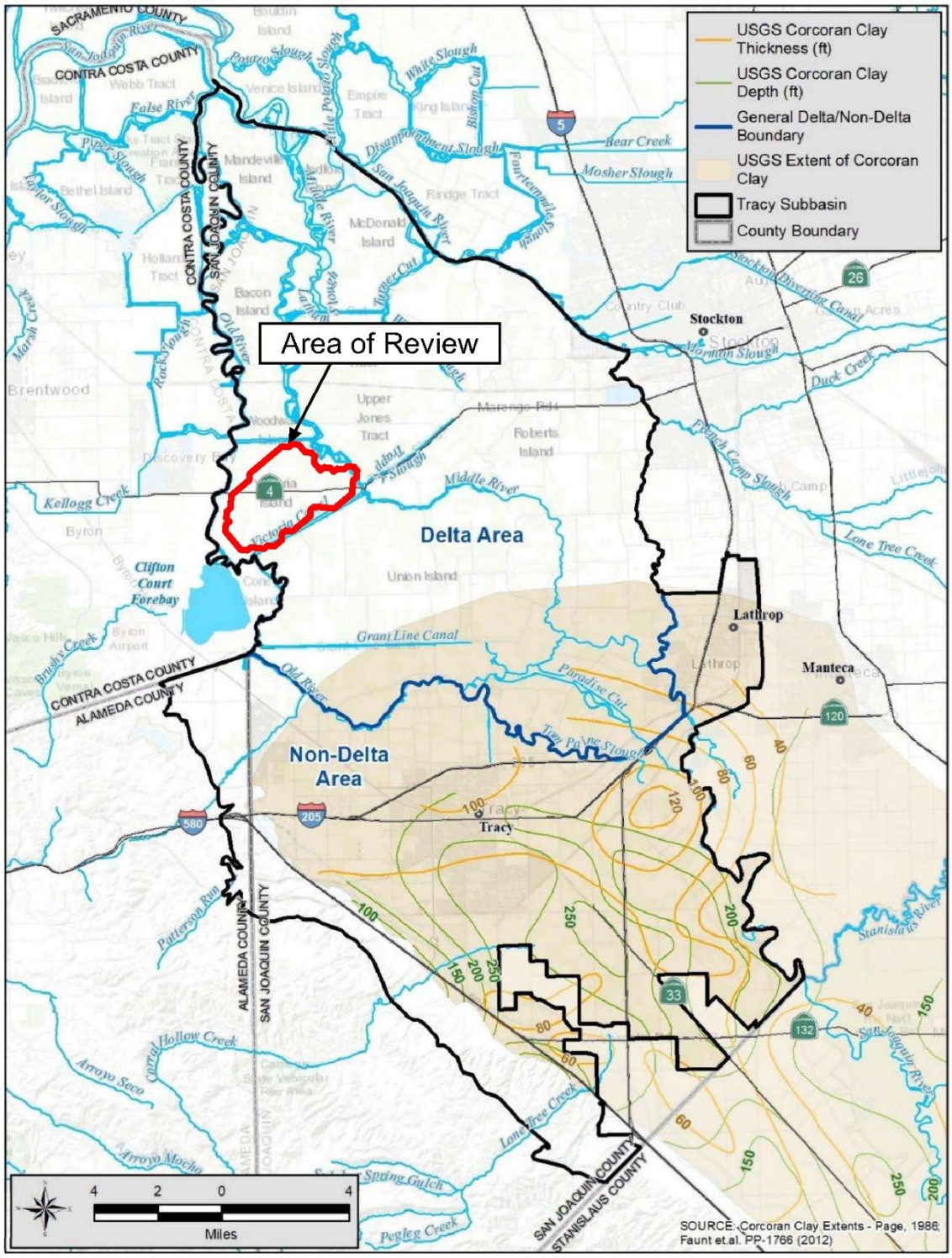

FigureA-49. Estimated Corcoran Clay thickness and extent.

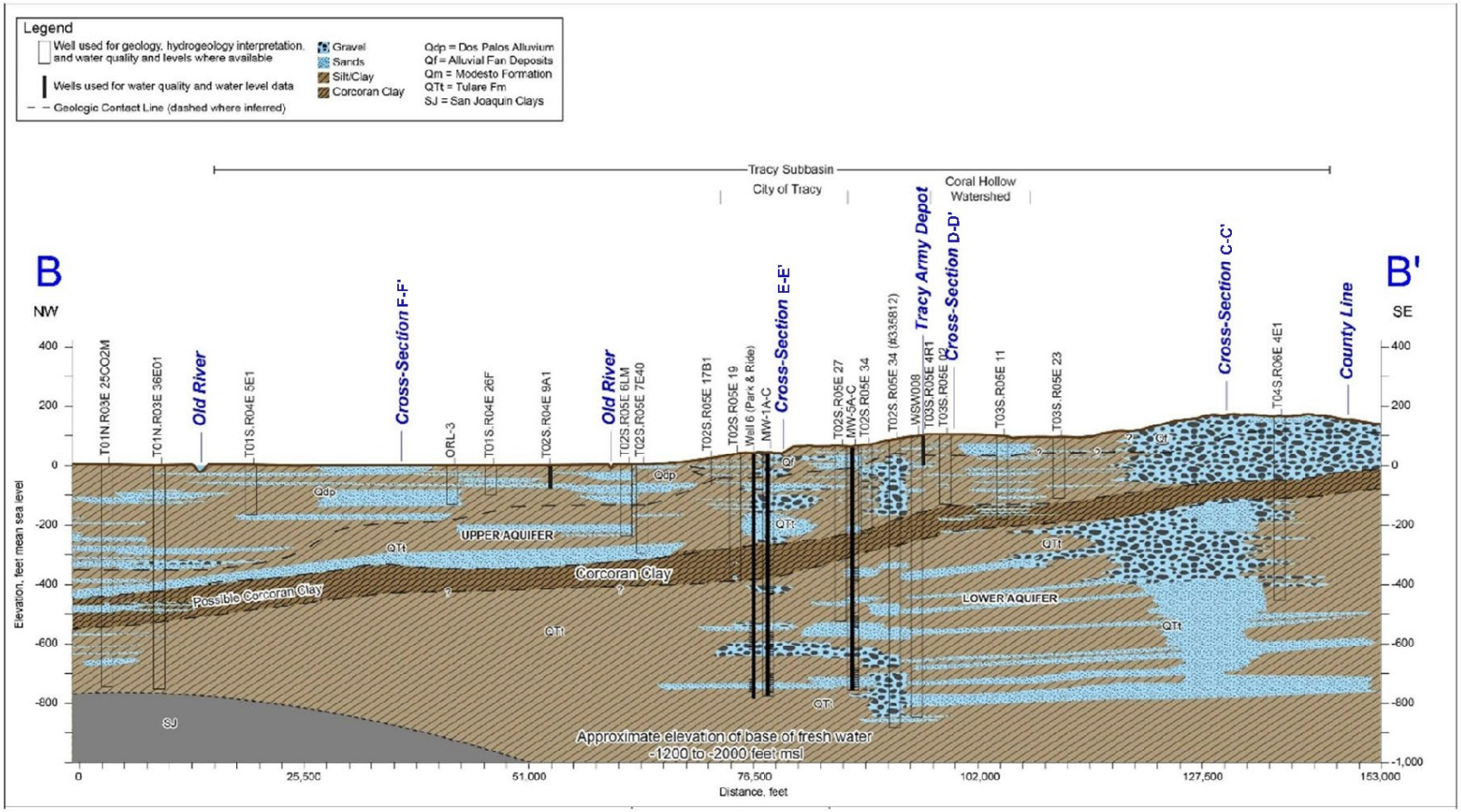

Modified from: GEI Consultants, Inc.; Tracy Subbasin Groundwater Sustainability Plan. November 1, 2021.

Figure A-50. Geologic cross section B-B'.

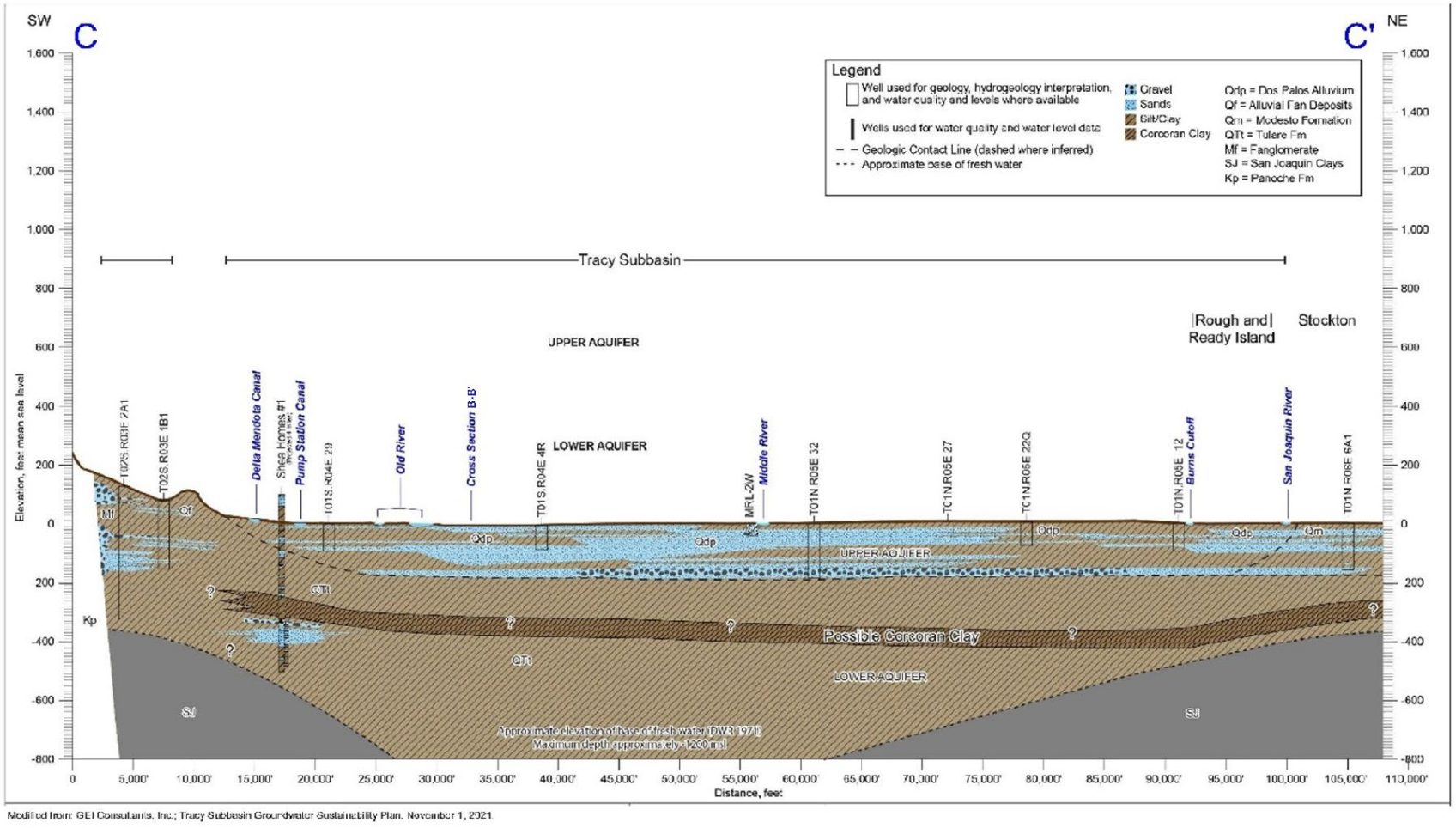

Modified from: GEI Consultants, Inc.; Tracy Subbasin Groundwater Sustainability Plan, November 1, 2021

Figure A-51. Geologic cross section C-C'.

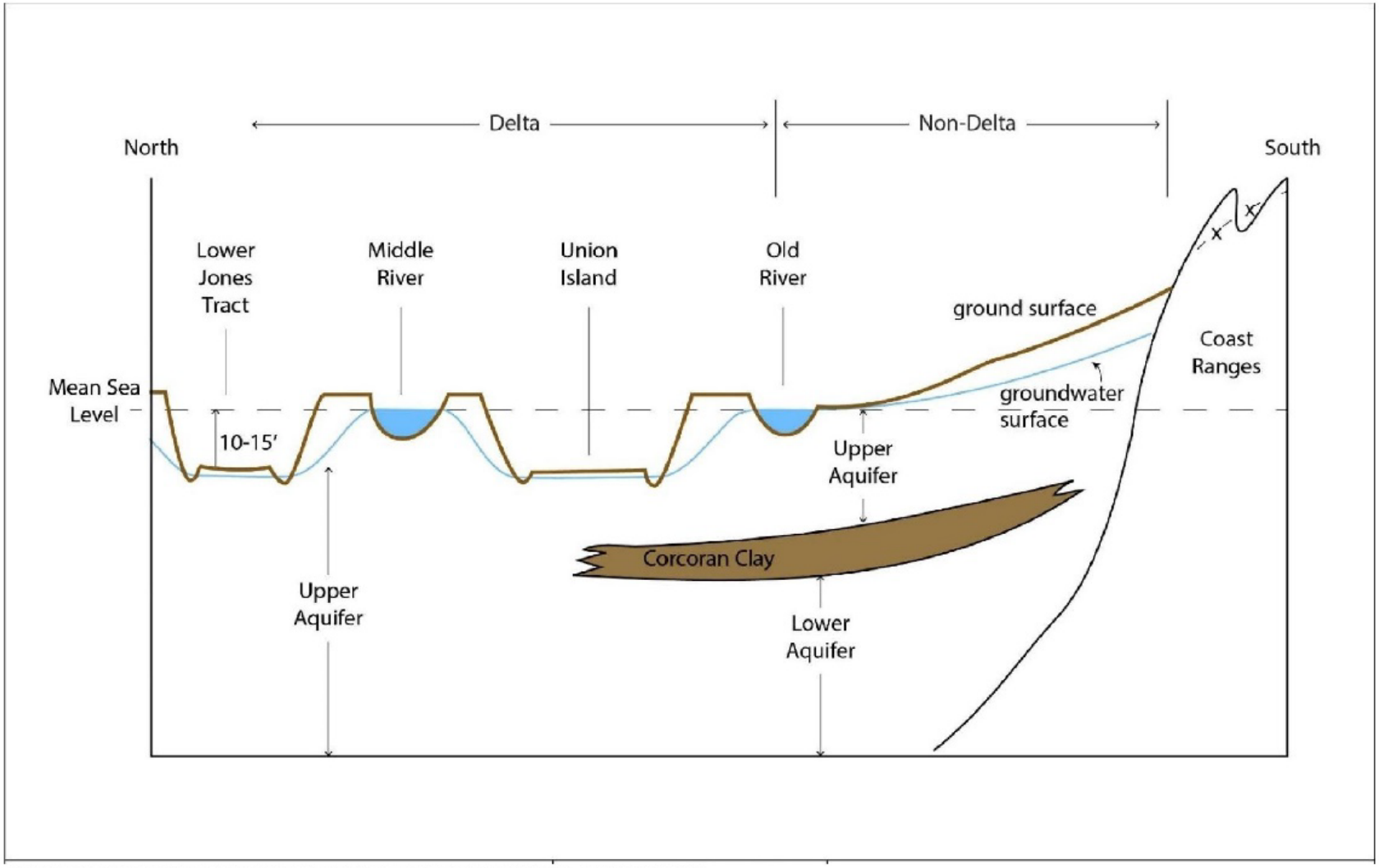

Figure A-52. Principal aquifer schematic profile.

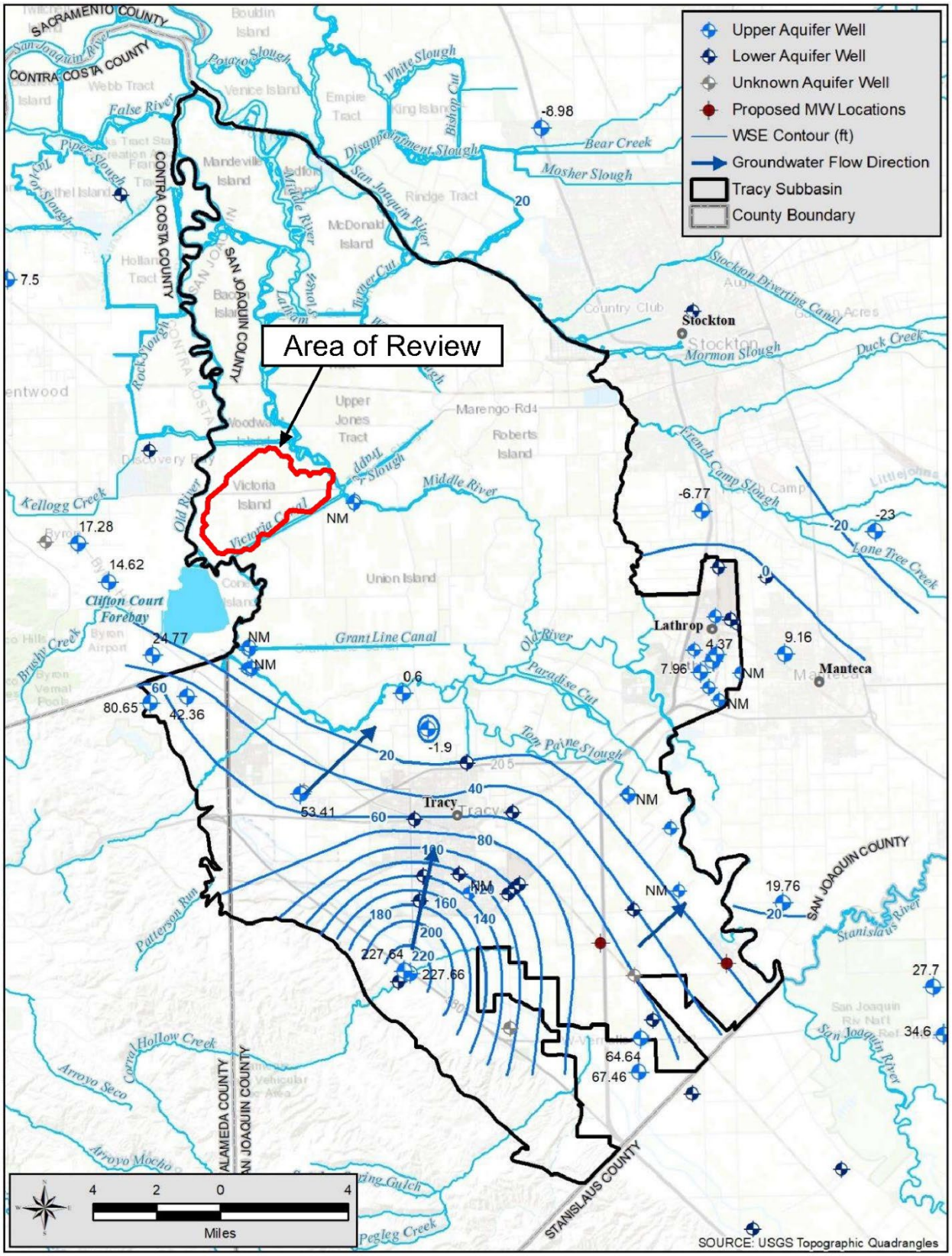

Figure A-53. Upper Aquifer groundwater elevations, fall 2019.

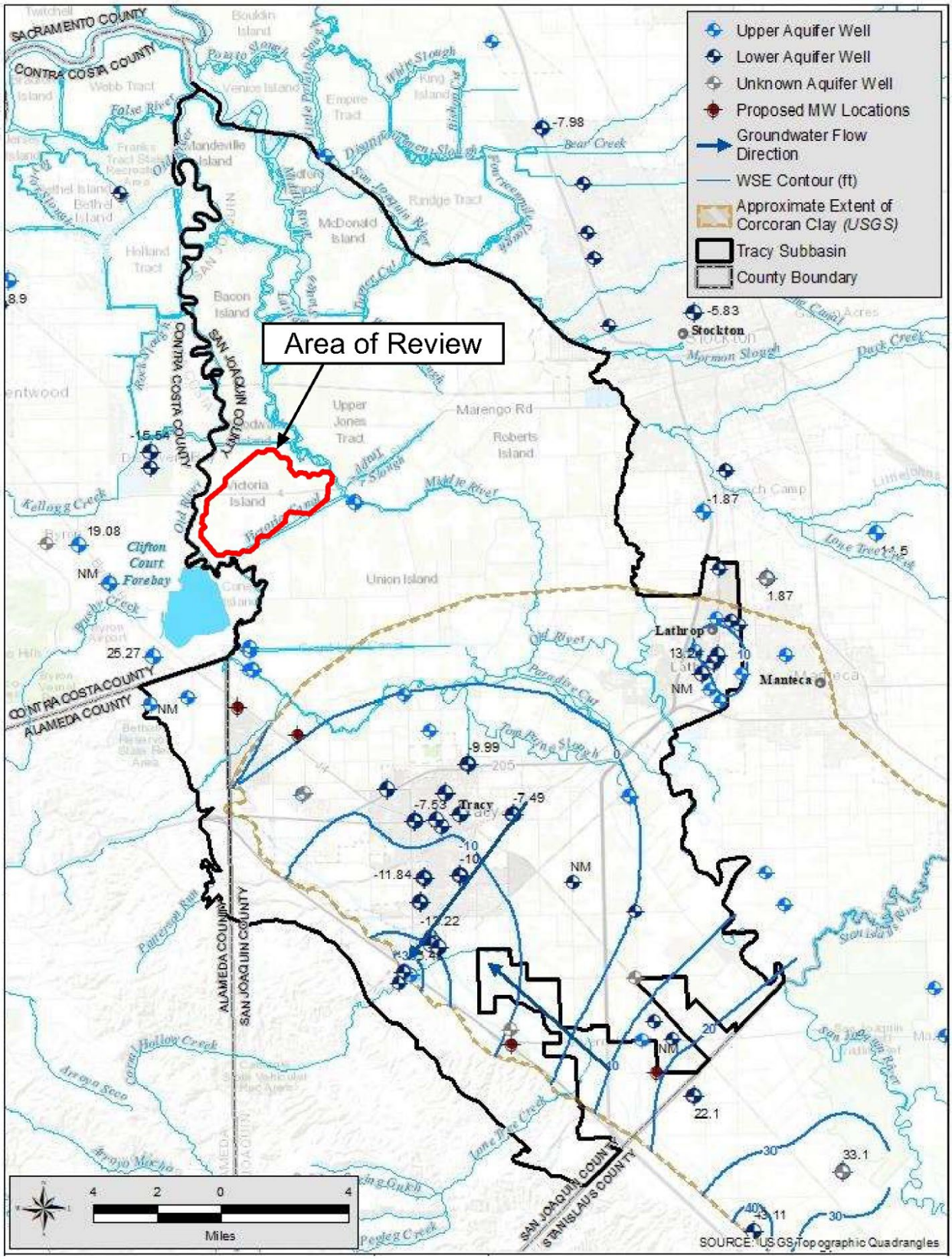

Figure A-54. Lower Aquifer groundwater elevations, spring 2019.

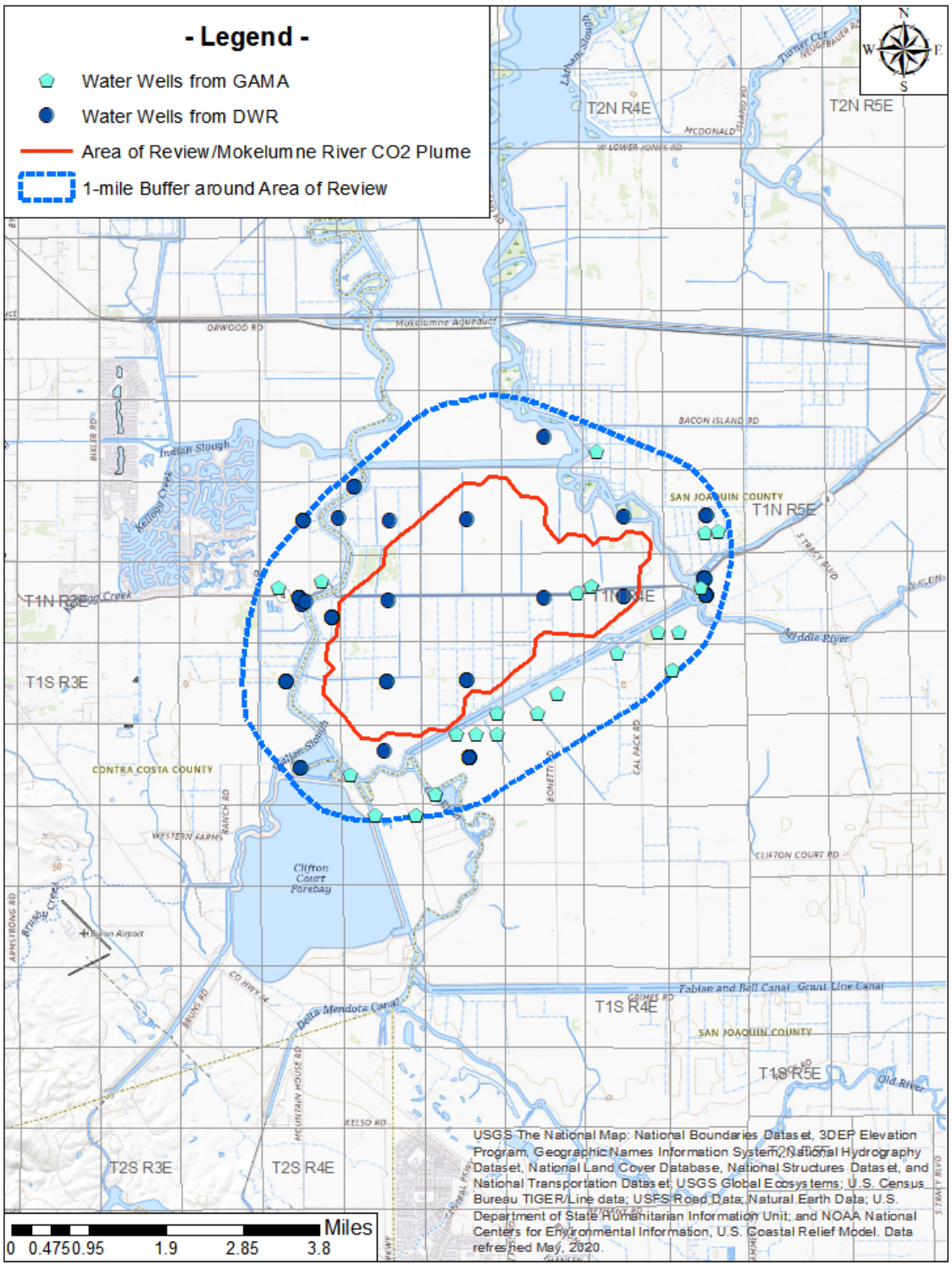

Figure A-55. Water well location map.

GEOCHEM AL ANALYSIS OF WA ER Pro-391

DATE OF REPORT	June 4, 1980	WELL NO.	Midland Fee WI-1, Sec. 3
DATE OF SAMPLING	No date	COMPANY	Chevron USA
SAMPLED BY	Operator	FIELD	Rio Vista, 3N/3E
LABORATORY NO.	32-8N-4E	ZONE	
ANALYST	Yamada	SAMPLE SOURCE	

RADICALS		PARTS PER MILLION MILLIGRAMS PER LITER	REACTING VALUE EQUIVALENTS PER MILLION	REACTING VALUE PERCENT
SODIUM	Na	5053.6	219.82	48.73
CALCIUM	Ca	61.5	3.07	0.68
MAGNESIUM	Mg	8.9	0.73	0.16
BARIUM	Ba			
STRONTIUM	Sr			
POTASSIUM	K	75	1.92	0.43
SULPHATE	SO_4	294.9	6.14	1.36
CHLORIDE	Cl	6867.2	193.70	42.94
CARBONATE	CO_3	58.8	1.96	0.44
BICARBONATE	HCO_3	1448.5	23.74	5.26
HYDROXIDE	OH			
IODIDE	I			
SILICA	SiO_2	12.8		
IRON, ALUMINA	R_2O_3	8.2		
TOTAL		13889.4	451.08	100.00

GROUP	CHEMICAL CHARACTER	MISCELLANEOUS		
ALKALIS	PRIMARY SALINITY	BORON	77.2	PPM
EARTHS	SECONDARY SALINITY	HYDROGEN SULFIDE	Absent	
STRONG ACIDS	PRIMARY ALKALINITY	EQUIVALENT SALT	12000	PPM
WEAK ACIDS	SECONDARY ALKALINITY	RESISTIVITY @ 77°F	0.470	O.M.
Ca/EARTHS		CHLORINITY	11320	PPM
CHLORIDE SALINITY		SPECIFIC GRAVITY	1.0100	
SULPHATE SALINITY	CARBONATE/CHLORIDE	pH	8.32	

REMARKS

D. F. Moran
G. C. Cates
1-C Laboratory

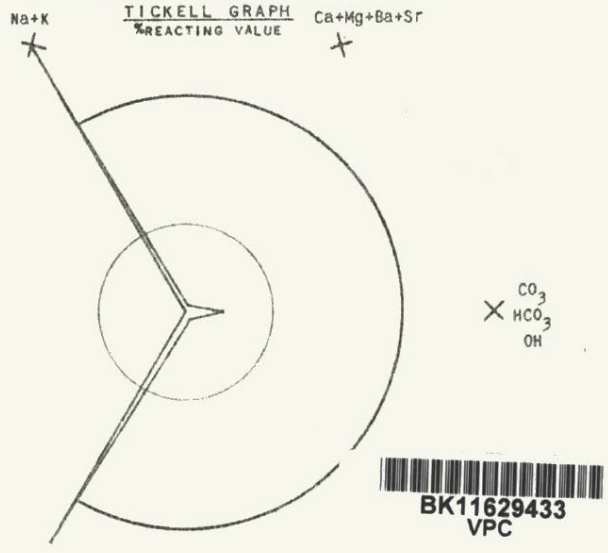

ARC REPRESENTS "CONCENTRATION OF SOLIDS IN NORMAL SEA WATER"

PRO-391 (REV. 7-71)
PRINTED IN U.S.A.

SIGNED: R. M. Yamada

Figure A-56. Water geochemistry for the Midland_Fee_Water_Injection_1 well.

ZALCO LABORATORIES, INC.
Analytical & Consulting Services

4309 Armour Avenue
Bakersfield, California 93308

(661) 395-0539
FAX (661) 395-3069

Core Laboratories
3437 Landco Dr
Bakersfield CA 93308

Laboratory No: 1304060-01
Date Received: 4/5/2013
Date Reported: 4/9/2013

Attention: Larry Kunkel

Sample Identification: Chamber 1507
Sampled by: Date: 3/26/2013 Time:
Report Notes:

COMPLETE GEOCHEM ANALYSIS

pH	7.68	Specific Gravity @ 60 F...	1.009
Electrical Conductivity (EC)	21.3	Resistivity	0.4695
(millimhos/cm @ 25 C)		(ohm meters @ 25 C)	

Constituents	mg/L	meq/L	Reacting %
Calcium, Ca	430	21	4.72
Magnesium, Mg	130	11	2.35
Sodium, Na	4300	190	41.14
Potassium, K	33	0.84	0.19
Iron, Fe (total)	< 1.0	0	0
Alkalinity as:			
Hydroxide, OH	0	0	0
Carbonate, CO3	0	0	0
Bicarbonate, HCO3	150	2.5	0.54
Chloride, Cl	8200	230	50.86
Sulfate, SO4	42	0.87	0.19
Sulfide, S	< 1.0		
Boron, B	9.6		
Barium, Ba	3.2		
Silica, SiO2	< 40		
Strontium, Sr	15		
Totals (Sum)	13200	456	100

Total Dissolved Solids, (Gravimetric)	14000		
Calculated Hardness, CaCO3	1600		
Total Alkalinity, CaCO3	150		
Sodium Chloride, (total)	13000		
		Primary Salinity	82.66
		Secondary Salinity	14.14
		Total Salinity	96.8
Cation/Anion Balance, %	3.0%		
Sodium, Na (Calculated), mg/L	4635.12	Primary Alkalinity	0
Langelier Scale Index	1.13	Secondary Alkalinity	0
Stiff/Davis Stability Index	1.11	Total Alkalinity	0

Laboratory Authorization

Figure A-57. Water geochemistry for the Piacentine_2-27 well.

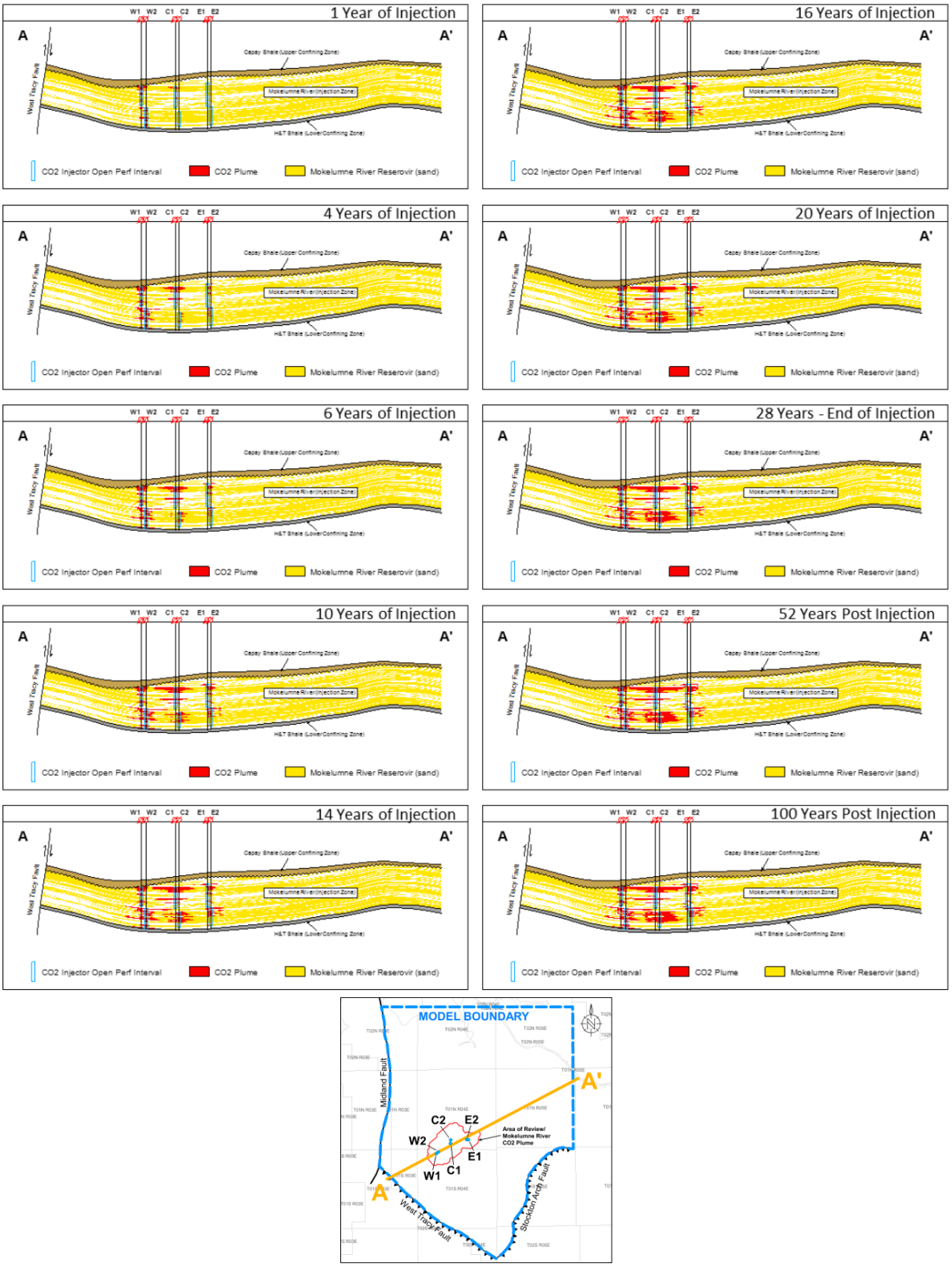

Figure A-58. Proximity of CO_2 to the West Tracy Fault, lateral dispersion of CO_2 throughout time and confinement under the overlying Capay Shale through time.

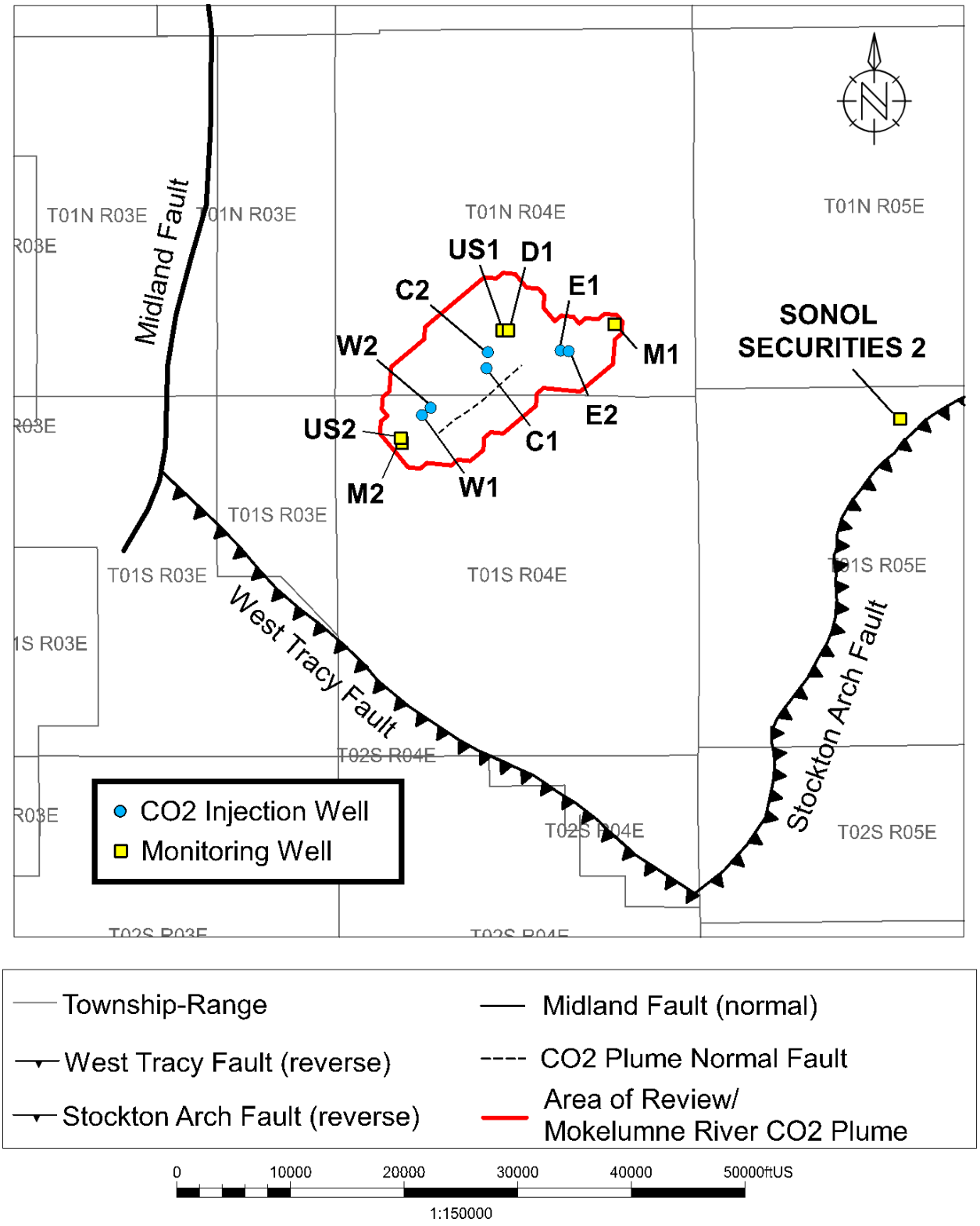

Figure A-59. Map showing the locations of injection wells and monitoring wells.

Tables

Table A-1. Oil and Gas Well Reference List based on CalGEM Data

Number	API	Well Number	Operator Name	Lease Name	Well Status	Well Type	Well Type Label
1	407700425	1	Amerada Hess Corp.	Borden	Plugged	DH	Dry Hole
2	407700423	1	Phillips Petroleum Company	Salyer A	Plugged	DH	Dry Hole
3	407720678	1	ABA Energy Corporation	Victoria Island Farms	Plugged	DG	Dry Gas

Table A-2. Water Well Reference List based on DWR WCR Data

Number	WCR Number	Planned Use
4	WCR0064122	Unknown
5	WCR0134423	Unknown
6	WCR0188052	Unknown
7	WCR0271617	Unknown
8	WCR1954-000752	Water Supply Domestic
9	WCR0118173	Unknown
10	WCR0047146	Unknown
11	WCR1978-001486	Water Supply Domestic
12	WCR2001-001632	Monitoring

Table A-3. Water Well Reference List based on Data from GAMA

Number	Dataset	Well ID
13	DDW	CA3901449_001_001
14	DDW	CA3901430_001_001
15	DWR	01N04E34H001M

Table A-4. Results of Pressures Extracted from Modeling at the Pseudo Well Locations Shown in Figure A-23

Well Location	Depth Range (TVD)	Initial Pressure Average	Max Pressure Average	100 Years Post Injection Pressure Average	Delta Pressure Average (psi)
Normal Fault in Plume	5904’ to 7791’	2871 psi / 0.419 psi/ft	3177 psi / 0.464 psi/ft	2883 psi / 0.421 psi/ft	306
Midland Fault	6285’ to 7955’	2928 psi / 0.411 psi/ft	3182 psi / 0.447 psi/ft	2939 psi / 0.413 psi/ft	254
West Tracy Fault	5622’ to 7122’	2633 psi / 0.413 psi/ft	2868 psi / 0.450 psi/ft	2646 psi / 0.415 psi/ft	235
Stockton Arch Fault	5280’ to 6831’	2490 psi / 0.411 psi/ft	2704 psi / 0.447 psi/ft	2502 psi / 0.413 psi/ft	214

Maximum pressure is 28 years after initial injection starts. Pressure averages are shown in both absolute and gradient formats for the injection zone.

Table A-5. Formation Mineralogy from XRD and FTIR in Four Wells

Well	Zone	Depth (ft)	Quartz	Plagioclase	K-Feldspar	Albite	Andesine	Labradorite	Calcite	Dolomite	Amphibole	Glauconite	Apatite	Pyrite	Kaolinite	Chlorite	Illite & Mica	Smectite	MXL I/S	Total Clay
Wilcox_20	Capay	4622.0	42.2	18.7	10.7				0.0	0.0				0.6	9.4	3.4	4.5		10.5	27.8
Wilcox_20	Capay	4905.0	34.9	20.7	10.2				0.7	0.0				1.1	15.2	5.8	5.8		5.5	32.3
RVGU_209	Capay	4442.5	26.0	25.0	17.0				1.0	0.0					5.0	3.0			23.0	31.0
RVGU_209	Capay	4480.5	26.0	23.0	20.0				0.0	0.0					0.0	6.0			25.0	31.0
RVGU_209	Capay	4476.5	30.0	23.0	18.0				0.0	0.0					5.0	9.0			15.0	29.0
RVGU_209	Capay	4454.5	30.0	29.0	15.0				0.0	0.0					2.0	6.0			18.0	26.0
RVGU_209	Capay	4498.5	34.0	26.0	19.0				0.0	0.0					1.0	2.0			18.0	21.0
RVGU_209	Capay	4500.5	28.0	19.0	19.0				0.0	0.0					0.0	12.0			22.0	34.0
RVGU_248	Capay	4425.5	35.0	25.0	15.0										5.0	5.0	5.0	10.0		25.0
Citizen_Green_1	Mokelumne	5247.0	27.8		16.2	34.0	0.0	0.0			0.0		0.8	0.0	3.6	17.0	0.0	1.1		21.7
Citizen_Green_1	Mokelumne	5249.0	17.0		32.7	6.5	0.0	0.0			0.0			0.0	34.9	0.0	8.4	0.5		43.8
Citizen_Green_1	Mokelumne	6400.0	40.3		17.1	0.0	3.6	29.2			0.2			0.0	5.2	4.0	0.4	0.0		9.6
Citizen_Green_1	Mokelumne	6466.0	36.3		12.6	0.2	0.0	36.6			0.6			0.7	2.7	5.4	5.0	0.0		13.0
Citizen_Green_1	Mokelumne	6532.0	34.2		24.1	0.0	31.0	0.0			1.1			0.5	2.9	2.0	4.2			9.1
Citizen_Green_1	Mokelumne	6598.0	33.9		22.0	0.0	34.5	0.0			0.2			0.2	3.6	5.4	0.1	0.0		9.2
Speckman_Decarli_1	Mokelumne	6987.0	35.0	18.0	17.0				0.0	0.0		3.0		0.0	10.0	4.0			13.0	27.0
Speckman_Decarli_1	Mokelumne	6989.0	26.0	21.0	15.0				0.0	0.0		0.0		0.0	12.0	8.0			18.0	38.0
Speckman_Decarli_1	Mokelumne	6991.0	39.0	25.0	19.0				0.0	0.0		1.0		0.0	3.0	2.0			11.0	16.0
Speckman_Decarli_1	Mokelumne	7000.0	28.0	26.0	17.0				0.0	0.0		2.0		0.0	10.0	4.0			13.0	27.0
Speckman_Decarli_1	Mokelumne	7002.0	20.0	17.0	14.0				0.0	0.0		0.0		0.0	19.0	8.0			22.0	49.0
Speckman_Decarli_1	Mokelumne	7006.0	28.0	30.0	15.0				0.0	0.0		2.0		0.0	8.0	6.0			11.0	25.0
Speckman_Decarli_1	H&T Shale	8828.0	23.0	21.0	9.0				3.0	0.0		0.0		1.0	12.0	5.0			26.0	43.0
Speckman_Decarli_1	H&T Shale	8830.0	30.0	17.0	11.0				0.0	0.0		0.0		4.0	3.4	14.4	6.1	14.1		38.0
Speckman_Decarli_1	H&T Shale	8909.0	20.0	20.0	13.0				0.0	0.0		2.0		2.0	5.0	3.0			35.0	43.0
Speckman_Decarli_1	H&T Shale	8937.0	20.0	12.0	8.0				0.0	0.0		0.0		2.0	14.0	6.0			38.0	58.0
Speckman_Decarli_1	H&T Shale	8939.0	24.0	18.0	11.0				1.0	0.0		0.0		3.0	3.0	15.5	7.7	16.8		43.0
Speckman_Decarli_1	H&T Shale	8940.0	23.0	29.0	12.0				0.0	0.0		0.0		0.0	4.0	5.0			27.0	36.0
Speckman_Decarli_1	H&T Shale	8942.0	23.0	15.0	10.0				0.0	0.0		0.0		2.0	12.0	5.0			33.0	50.0
Speckman_Decarli_1	H&T Shale	9439.0	20.0	14.0	9.0				0.0	0.0		0.0		1.0	0.0	5.0			51.0	56.0
Speckman_Decarli_1	H&T Shale	9441.0	21.0	19.0	12.0				2.0	0.0		0.0		3.0	0.0	0.0			43.0	43.0

Table A-6. Core Samples Within the Mokelumne Formation

UWI	Well	Field	Depth (ft)	Porosity (%)	Permeability Horizontal (mD)	Permeability Vertical (mD)	Grain Density (g/cc)	Description
0407720688	Citizen_Green_1	King Island	6400	33	367.1		2.68	
0407720688	Citizen_Green_1	King Island	6466	31.3	71.9		2.68	
0407720688	Citizen_Green_1	King Island	6532	30.3	54.8		2.7	
0407720688	Citizen_Green_1	King Island	6598	31.3	135.5		2.67	
0407720688	Citizen_Green_1	King Island	6664	30.8	46.4		2.66	
0407720688	Citizen_Green_1	King Island	6800	27.7	4.8		2.65	
0401320269	Enea_Capital_3	Brentwood	4567	26.8	220			
0401320269	Enea_Capital_3	Brentwood	4602	25.1	190			
0401320269	Enea_Capital_3	Brentwood	4620	30	240			
040772073900	PG&E_TEST_INJECTION_WITHDRAWAL_WELL_1	King Island	4713		112			
040772073900	PG&E_TEST_INJECTION_WITHDRAWAL_WELL_1	King Island	4754	8.6	9.2			
040772073900	PG&E_TEST_INJECTION_WITHDRAWAL_WELL_1	King Island	4765	31.4	141.5			
040772073900	PG&E_TEST_INJECTION_WITHDRAWAL_WELL_1	King Island	4771	31.6	42.1			
040772073900	PG&E_TEST_INJECTION_WITHDRAWAL_WELL_1	King Island	4794	32	225.4			
040772073900	PG&E_TEST_INJECTION_WITHDRAWAL_WELL_1	King Island	4810	30.9	159.1			
040772073900	PG&E_TEST_INJECTION_WITHDRAWAL_WELL_1	King Island	4817		118.2			
040772073900	PG&E_TEST_INJECTION_WITHDRAWAL_WELL_1	King Island	4821		31.5			
040772073900	PG&E_TEST_INJECTION_WITHDRAWAL_WELL_1	King Island	4830		119			
040772073900	PG&E_TEST_INJECTION_WITHDRAWAL_WELL_1	King Island	4840		194.6			
040772073900	PG&E_TEST_INJECTION_WITHDRAWAL_WELL_1	King Island	4846		1029.3			
0407720649	Speckman_Decarli_1	Roberts Island	6916	28.5	1159		2.63	Sst gry vf-fgr sslty no stn no flu
0407720649	Speckman_Decarli_1	Roberts Island	6917	30.2	1608		2.62	Sst gry vf-fgr sslty no stn no flu
0407720649	Speckman_Decarli_1	Roberts Island	6918	26.3	375		2.62	Sst gry vf-fgr vslty no stn no flu
0407720649	Speckman_Decarli_1	Roberts Island	6987	28.7	22.7		2.64	Sst gry vf-fgr vslty cly no stn no flu
0407720649	Speckman_Decarli_1	Roberts Island	6989	29.2	21.2		2.63	Sst gry vf-fgr vslty cly incl carb incl no stn no flu
0407720649	Speckman_Decarli_1	Roberts Island	6991	32.2	18.2		2.63	Sst gry vf-fgr slty no stn no flu
0407720649	Speckman_Decarli_1	Roberts Island	6992	29.5	297		2.62	Sst gry vf-fgr slty no stn no flu
0407720649	Speckman_Decarli_1	Roberts Island	6993	28.4	132		2.65	Sst gry vf-fgr vslty cly carb lam no stn no flu
0407720649	Speckman_Decarli_1	Roberts Island	6994	29.9	200		2.65	Sst gry vf-fgr slty scly carb incl no stn no flu
0407720649	Speckman_Decarli_1	Roberts Island	7000	31.6	33.3		2.65	Sst gry vfgr vslty scly carb incl no stn no flu
0407720649	Speckman_Decarli_1	Roberts Island	7001	27.1	16.8		2.63	Sst gry vfgr vslty scly carb incl no stn no flu
0407720649	Speckman_Decarli_1	Roberts Island	7002	28.5	16.2		2.62	Sst gry vfgr vslty vcly carb no stn no flu
0407720649	Speckman_Decarli_1	Roberts Island	7003	29.7	137		2.64	Sst gry vf-fgr slty scly no stn no flu
0407720649	Speckman_Decarli_1	Roberts Island	7004	31	108		2.65	Sst gry vfgr slty no stn no flu
0407720649	Speckman_Decarli_1	Roberts Island	7006	31.1	54.3		2.64	Sst gry vfgr slty carb lam no stn no flu
0407720536	Whiskey_Slough_1A-E	McDonald Island	5442	29.3	16.8	14	2.69	
0407720536	Whiskey_Slough_1A-E	McDonald Island	5446.1	30.3	43.5	24.3	2.69	
0407720536	Whiskey_Slough_1A-E	McDonald Island	5447.6	33.5	799.3	552.4	2.66	
0407720536	Whiskey_Slough_1A-E	McDonald Island	5449.8	34.2	1126.8	1056.8	2.64	

UWI	Well	Field	Depth (ft)	Porosity (%)	Permeability Horizontal (mD)	Permeability Vertical (mD)	Grain Density (g/cc)	Description
0407720536	Whiskey_Slough_1A-E	McDonald Island	5452.7	33.7	1172	990	2.64	
0407720536	Whiskey_Slough_1A-E	McDonald Island	5455.6	34	1765.1	1221.1	2.64	
0407720536	Whiskey_Slough_1A-E	McDonald Island	5457.5	30.3	667.6	380.6	2.66	
0407720536	Whiskey_Slough_1A-E	McDonald Island	5460.2	33.7	1089.2	991.5	2.63	
0407720536	Whiskey_Slough_1A-E	McDonald Island	5463.1	35	1802.4	1925.9	2.64	
0407720536	Whiskey_Slough_1A-E	McDonald Island	5466.1	35.4	1156.5	1125.1	2.63	
0407720536	Whiskey_Slough_1A-E	McDonald Island	5469.1	34.9	1922.9	1212.8	2.64	
0407720536	Whiskey_Slough_1A-E	McDonald Island	5472.1	35.5	1565.9	891.1	2.65	
0407720536	Whiskey_Slough_1A-E	McDonald Island	5474.9	34	1084.7	731.1	2.67	
0407720536	Whiskey_Slough_1A-E	McDonald Island	5476.5	34.5	1397.4	1108.8	2.63	
0407720536	Whiskey_Slough_1A-E	McDonald Island	5543.8	30.6	86.1	23.5	2.69	

Table A-7. Capay Shale and Mokelumne River Formation Gross Thickness and Depth within the AoR

Zone	Property	Low	High	Mean
Upper Confining Zone Capay Shale	Thickness (feet)	100	360	207
	Depth (feet TVD)	4,954	6,164	5,582
Reservoir Mokelumne River Formation	Thickness (feet)	316	1,336	1,024
	Depth (feet TVD)	5,044	10,281	7,395

Table A-8. Wells with Data for Fracture Gradient Determination

UWI	Well	Field	Zone	Date	Test Type	Depth	Frac Grad
04077207390000	PGE Test Inj/withdrawal well 1	King Island	Mokelumne	10/28/2014	SRT	4748	0.822
04077202890000	Yamada_Line_Well_1	Union Island	Mokelumne	10/23/1976	FIT	6042	0.76
04077202780000	Galli_1	Union Island	Mokelumne	5/26/1976	FIT	6207	0.75
04077203600000	Sonol_Securities_8	Union Island	H&T Shale	9/14/1980	LOT	5504	0.809
04077202870000	Galli_2	Union Island	H&T Shale	9/1/1976	FIT	6178	0.76
04077202850000	Pool_B_2	Union Island	H&T Shale	7/29/1976	FIT	6186	0.76

FIT = formation integrity test; SRT = step rate test; LOT = leak off tests

Table A-9. Wells used for Overburden Calculation

Well Name	UWI
L_COCHRAN_20_1	04077204100000
OHLENDORF_UNIT_1_1	04077203480000
GULF_PATTERSON_1_32	04077204480000
OHLENDORF_UNIT_2_1	04077203590000
RIVERVIEW_INV_CO_1	04077204950000
ARNAUDO_18-1	04013203100000
MANTELLI_1	04077201450000

Table A-10. Input Parameters used in Mohr Circle Calculation

Parameter	Present-Day Conditions
Reference Depth (ft TVD)	6900
Pore Pressure (psi)	2860
Overburden Stress Gradient (psi/ft)	0.91
Minimum Horizontal Stress Gradient (psi/ft)	0.76
Maximum Horizontal Stress Gradient (psi/ft)	1.01
Coefficient of Friction	0.6
Fault Cohesion (psi)	0

Table A-11. Modeled Fault Orientations and Expected Pressure Increases

Fault	Strike	Dip (RHR)	Delta Pressure to Slip (psi)	Delta Pressure Average (psi)	Delta Pressure Maximum (psi)
Normal fault in plume	235	55	1865	306	420
Midland Fault	187	47	2060	254	348
West Tracy Fault	125	53	3299	235	279
Stockton Arch Fault	20	50	1944	214	261

Based on simulation modeling compared to the required pressure increase necessary to cause slip on the faults based on Mohr Coulomb analysis. The delta pressure to slip is the calculated pressure increase above present-day conditions from Mohr coulomb analysis that would cause each fault to slip. The delta pressure average and maximum are the actual pressure increases expected to be seen at each fault based on reservoir simulation.

Table A-12. Data from USGS Earthquake Catalog for Faults in the Region of CTV III

#	Date	Latitude	Longitude	Depth (km)	Magnitude	Last Updated	Location
1	3/1/2024	37.89	-121.62	2.2	2.9	3/1/2024	3 km SW of Discovery Bay, California
2	6/22/2018	37.99	-121.72	10.4	3.2	7/9/2021	1 km SW of Oakley, CA
3	10/15/2010	37.88	-121.39	14.6	3.1	1/23/2017	9 km WSW of Taft Mosswood, California
4	9/29/2002	37.87	-121.61	4.3	3.4	2/12/2020	2 km ENE of Byron, California
5	2/10/1992	37.77	-121.32	14.6	3.1	2/9/2016	8 km SSW of Lathrop, California
6	2/4/1991	37.81	-121.24	7.7	3.1	12/18/2016	2 km NW of Manteca, California
7	2/3/1991	37.82	-121.24	9.4	3.1	12/18/2016	2 km E of Lathrop, California
8	1/27/1980	38.00	-121.00	6.0	3.3	4/2/2016	8 km ESE of Linden, California
9	8/6/1979	37.83	-121.51	6.0	4.3	4/1/2016	6 km NNE of Mountain House, California
10	2/2/1979	37.66	-121.19	18.0	3.5	4/1/2016	10 km WSW of Salida, California
11	10/6/1976	37.61	-121.41	2.9	3.3	12/15/2016	13 km S of Tracy, California
12	9/5/1976	37.61	-121.41	6.5	3.5	12/15/2016	13 km S of Tracy, California
13	6/9/1975	37.96	-121.65	15.0	3.1	12/15/2016	2 km SE of knightsen, California
14	2/2/1944	37.93	-121.40	6.0	3.8	1/28/2016	7 km SW of Country Club, California
15	2/14/1909	38.10	-121.70	--	4.5	6/4/2018	7 km S of Rio Vista, California
16	05/19/1889	38.10	-121.80	--	6.0	2/16/2021	North of Antioch, California
17	7/15/1866	37.70	-121.50	--	6.0	1/30/2021	Southwest of Stockton, California

Table A-13. Wells used for Salinity Calculation to Generate USDW Surface

UWI	Name
04077203560000	1
04013000010000	AMERADA_HONEGGER_1-34
04077206240000	ARNAUDO_BROS_1
04077201380000	BACCHETTI_1
04077206270000	BANK_OF_STOCKTON_1
04077203440000	BANTA_UNIT_WELL_1A
04077004250000	BORDEN_1
04077202170000	BOULDIN_DEVELOPMENT_CO_1
04077206660000	COLDANI_1
04077204860000	DELL_ARINGA_1-31
04077202760000	DELTA_1
04077206260000	EBERHARDT_1
04077206450000	EBERHARDT_2
04013202760000	HAYES_1-7
04077206010000	HOLLY_SUGAR_1
04077206300000	JACKSON_1
04077206330000	KLEIN_1-36
04077205070000	M_C_FONG_1
04077205590000	MANDEVILLE_2
04077201450000	MANTELLI_1
04013201780000	NGC_STENZEL_1
04077206650000	NUSS_1
04077203480000	OHLENDORF_UNIT_1_1
04077206440000	PACIFIC_1
04077206960000	PACIFIC_2
04077203710000	PEREIRA_ET_AL_UNIT_1
04077200280000	PODESTA_1
04077206810000	R_M_FARMS_1
04077205660000	RIPKEN_21-1
04077203350000	ROCHA_ET_AL_UNIT_1
04067000510000	RVGU_14
04067000760000	RVGU_19
04067001040000	RVGU_25
04077206490000	SPECKMAN_DECARLI_1
04077205120000	STEVENS_16-1
04013200820000	TRACT_1_1-7
04077203220000	UNION_PROPERTIES_2
04077206780000	VICTORIA_ISLAND_FARMS_1
04013201560000	WESTERN_ENOS_NUNN_1
04013002740000	WOODWARD_ISLAND_UNIT_20-1
04077201570000	ZUCKERMAN_1-21

Table A-14. Water Supply Well Information

Data Source	WCR Number	Wells from GAMA	Legacy Log Number	Planned Use or Former Use	LAT (DWR)	LONG (DWR)	LAT & LONG Accuracy (DWR)	LAT (GAMA)	LONG (GAMA)	T	R	S	APN	Date Work Ended	Total Completed Depth	Top of Perforated Interval	Bottom of Perforated Interval	Static Water Level
DWR	WCR2022-005532	NA	NA	Monitoring	37.88847	-121.57797	Unknown	NA	NA	01N	04E	31	8340036	11/4/2021	30	20	30	NA
DWR	WCR1993-005494	NA	496700	Cathodic Protection	37.888889	-121.57722	NA	NA	NA	01N	04E	31	NA	6/29/1993	100	50	100	NA
DWR	WCR1953-000335	NA	39-995	Water Supply Domestic	37.904	-121.4867	Centroid of Section	NA	NA	01N	04E	25	NA	NA	93	NA	NA	NA
DWR	WCR2008-000925	NA	942083	Water Supply Public	37.8622	-121.55952	Centroid of Section	NA	NA	01S	04E	8	NA	3/24/2008	160	50	80	30
DWR	WCR0047146	NA	NA	NA	37.90369	-121.54086	Centroid of Section	NA	NA	01N	04E	28	NA	NA	NA	NA	NA	NA
DWR	WCR1954-000752	NA	39-1171	Water Supply Domestic	37.87451	-121.55893	Centroid of Section	NA	NA	01S	04E	5	NA	5/3/1954	170	NA	NA	NA
DWR	WCR0316801	NA	NA	NA	37.90393	-121.56984	Centroid of Section	NA	NA	01N	04E	30	NA	NA	NA	NA	NA	NA
DWR	WCR1997-007106	NA	e068440	Monitoring	37.87463	-121.58162	Centroid of Section	NA	NA	01S	04E	6	NA	8/7/1997	20	7	18	NA
DWR	WCR1999-007606	NA	e068421	Monitoring	37.90945	-121.5661	Centroid of Section	NA	NA	01N	04E	29	NA	5/11/1999	20	10	NA	NA
DWR	WCR2009-000027	NA	927013	Monitoring	37.86083	-121.54049	Centroid of Section	NA	NA	01S	04E	9	129-190-24	1/11/2009	53	48	53	NA
DWR	WCR0188052	NA	NA	NA	37.88944	-121.52333	Centroid of Section	NA	NA	01N	04E	34	NA	NA	NA	NA	NA	NA
DWR	WCR0108952	NA	NA	NA	37.90348	-121.55819	Centroid of Section	NA	NA	01N	04E	29	NA	NA	NA	NA	NA	NA
DWR	WCR0296936	NA	NA	NA	37.91827	-121.5233	Centroid of Section	NA	NA	01N	04E	22	NA	NA	NA	NA	NA	NA
DWR	WCR0134423	NA	NA	NA	37.88903	-121.55869	Centroid of Section	NA	NA	01N	04E	32	NA	NA	NA	NA	NA	NA
DWR	WCR0047145	NA	NA	NA	37.9039	-121.50526	Centroid of Section	NA	NA	01N	04E	26	NA	NA	NA	NA	NA	NA
DWR	WCR1999-007608	NA	e068423	Monitoring	37.90355	-121.57765	Centroid of Section	NA	NA	01N	04E	30	NA	5/11/1999	20	20	NA	NA
DWR	WCR1978-001486	NA	121039	Water Supply Domestic	37.874722	-121.54083	NA	NA	NA	01S	04E	4	NA	2/13/1978	85	65	85	NA
DWR	WCR0213236	NA	E0093953	NA	37.88968	-121.48668	Centroid of Section	NA	NA	01N	04E	36	NA	NA	NA	NA	NA	NA
DWR	WCR2001-001632	NA	726677	Monitoring	37.88956	-121.50521	Centroid of Section	NA	NA	01N	04E	35	129-190-29	8/27/2001	500	NA	NA	NA
DWR	WCR1997-007111	NA	e068445	Monitoring	37.88978	-121.57877	Centroid of Section	NA	NA	01N	04E	31	NA	8/7/1997	20	10	20	NA
DWR	WCR2022-008645	NA	NA	Water Supply Irrigation - Agriculture	37.892789	-121.48707	NA	NA	NA	01N	04E	36	131-120-040	7/12/2022	71	NA	NA	NA
DWR	WCR0079885	NA	NA	NA	37.88622	-121.57134	Centroid of Section	NA	NA	01N	04E	31	NA	NA	NA	NA	NA	NA
DWR	NA	01S04E03P002M	NA	NA	NA	NA	NA	37.8688	-121.525	01S	04E	3	NA	NA	NA	NA	NA	NA
DWR	NA	01S04E09B001M	NA	NA	NA	NA	NA	37.8651	-121.5388	01S	04E	9	NA	NA	NA	NA	NA	NA
DWR	NA	01S04E02C001M	NA	NA	NA	NA	NA	37.8796	-121.5068	01S	04E	0	NA	NA	NA	NA	NA	NA
DWR	NA	01S04E03K001M	NA	NA	NA	NA	NA	37.8724	-121.5205	01S	04E	3	NA	NA	NA	NA	NA	NA
DWR	NA	01S04E04R001M	NA	NA	NA	NA	NA	37.8688	-121.5342	01S	04E	4	NA	NA	NA	NA	NA	NA
DWR	NA	01S04E09A001M	NA	NA	NA	NA	NA	37.8651	-121.534	01S	04E	9	NA	NA	NA	NA	NA	NA
DWR	NA	01S04E09C001M	NA	NA	NA	NA	NA	37.8651	-121.543	01S	04E	9	NA	NA	NA	NA	NA	NA
DWR	NA	01N04E35R001M	NA	NA	NA	NA	NA	37.8832	-121.4976	01S	04E	35	NA	NA	NA	NA	NA	NA
DWR	NA	01N04E36A001M	NA	NA	NA	NA	NA	37.894	-121.4793	01S	04E	36	NA	NA	NA	NA	NA	NA
DWR	NA	01N04E23M001M	NA	NA	NA	NA	NA	37.9157	-121.5114	01S	04E	23	NA	NA	NA	NA	NA	NA
DWR	NA	01N04E25K001M	NA	NA	NA	NA	NA	37.9013	-121.4839	01S	04E	25	NA	NA	NA	NA	NA	NA
DWR	NA	01N04E36K003M	NA	NA	NA	NA	NA	37.8868	-121.4839	01S	04E	36	NA	NA	NA	NA	NA	NA
DWR	NA	01N04E36N001M	NA	NA	NA	NA	NA	37.8832	-121.4931	01S	04E	36	NA	NA	NA	NA	NA	NA
DWR	NA	01N04E34H001M	NA	NA	NA	NA	NA	37.8904	-121.5159	01S	04E	34	NA	NA	NA	NA	NA	NA
NA	NA	NA	NA	NA	NA	NA	NA	NA	NA	NA	NA	NA	NA	NA	NA	NA	NA	NA
NA	NA	NA	NA	NA	NA	NA	NA	NA	NA	NA	NA	NA	NA	NA	NA	NA	NA	NA
NA	NA	NA	NA	NA	NA	NA	NA	NA	NA	NA	NA	NA	NA	NA	NA	NA	NA	NA
NA	NA	NA	NA	NA	NA	NA	NA	NA	NA	NA	NA	NA	NA	NA	NA	NA	NA	NA

Data Source	WCR Number	Wells from GAMA	Legacy Log Number	Planned Use or Former Use	LAT (DWR)	LONG (DWR)	LAT & LONG Accuracy (DWR)	LAT (GAMA)	LONG (GAMA)	T	R	S	APN	Date Work Ended	Total Completed Depth	Top of Perforated Interval	Bottom of Perforated Interval	Static Water Level
NA	NA	NA	NA	NA	NA	NA	NA	NA	NA	NA	NA	NA	NA	NA	NA	NA	NA	NA
NA	NA	NA	NA	NA	NA	NA	NA	NA	NA	NA	NA	NA	NA	NA	NA	NA	NA	NA
NA	NA	NA	NA	NA	NA	NA	NA	NA	NA	NA	NA	NA	NA	NA	NA	NA	NA	NA
NA	NA	NA	NA	NA	NA	NA	NA	NA	NA	NA	NA	NA	NA	NA	NA	NA	NA	NA
NA	NA	NA	NA	NA	NA	NA	NA	NA	NA	NA	NA	NA	NA	NA	NA	NA	NA	NA
NA	NA	NA	NA	NA	NA	NA	NA	NA	NA	NA	NA	NA	NA	NA	NA	NA	NA	NA
NA	NA	NA	NA	NA	NA	NA	NA	NA	NA	NA	NA	NA	NA	NA	NA	NA	NA	NA
NA	NA	NA	NA	NA	NA	NA	NA	NA	NA	NA	NA	NA	NA	NA	NA	NA	NA	NA
NA	NA	NA	NA	NA	NA	NA	NA	NA	NA	NA	NA	NA	NA	NA	NA	NA	NA	NA
NA	NA	NA	NA	NA	NA	NA	NA	NA	NA	NA	NA	NA	NA	NA	NA	NA	NA	NA
NA	NA	NA	NA	NA	NA	NA	NA	NA	NA	NA	NA	NA	NA	NA	NA	NA	NA	NA
NA	NA	NA	NA	NA	NA	NA	NA	NA	NA	NA	NA	NA	NA	NA	NA	NA	NA	NA
NA	NA	NA	NA	NA	NA	NA	NA	NA	NA	NA	NA	NA	NA	NA	NA	NA	NA	NA
NA	NA	NA	NA	NA	NA	NA	NA	NA	NA	NA	NA	NA	NA	NA	NA	NA	NA	NA
NA	NA	NA	NA	NA	NA	NA	NA	NA	NA	NA	NA	NA	NA	NA	NA	NA	NA	NA

Notes:
1= All depths are based on feet below ground surface
WCR= Department of Water Resources Well Completion Report LAT= Latitude
LONG= Longitude T= Township
R= Range S= Section
APN= Assessor Parcel Number
NA= Data is not available or not applicable GAMA= State Water Board's GAMA website

Table A-15. Injection Zone Formation Fluid Properties at Reservoir Conditions

Formation Fluid Property	Estimated Value/Range
Density, g/cm^3	0.99981
Viscosity, cp	0.486
TDS, ppm	~14,000-16,000

Table A-16. Injectate Compositions

	Injectate 1	Injectate 2
Component	Mass%	Mass%
CO_2	99.213%	99.884%
H_2	0.051%	0.006%
N_2	0.643%	0.001%
H_2O	0.021%	0.000%
CO	0.029%	0.001%
Ar	0.031%	0.000%
O_2	0.004%	0.000%
SO_2+SO_3	0.003%	0.000%
H_2S	0.001%	0.014%
CH_4	0.004%	0.039%
NO_x	0.002%	0.000%
NH_3	0.000%	0.000%
C_2H_6	0.000%	0.053%
Ethylene	0.000%	0.002%
Total	**100.00%**	**100.00%**

Table A-17. Simplified 4-Component Composition for Injectate 1 and Injectate 2

Injectate 1	
Component	Mass%
CO_2	99.213%
N_2	0.643%
SO_2+SO_3	0.003%
H_2S	0.001%

Injectate 2	
Component	Mass%
CO_2	99.884%
CH_4	0.039%
C_2H_6	0.053%
H_2S	0.014%

Table A-18. Injectate Properties Range over Project Life at Downhole Conditions for Injectate 1 and Injectate 2

Injectate Property at Downhole Conditions	Injectate 1	Injectate 2
Viscosity, cp	0.054	0.056
Density, lb/ft^3	41.39	42.56
Compressibility factor, Z	0.464	0.453